UNIVERSITA' DEGLI STUDI DI PERUGIA

DOTTORATO DI RICERCA
IN INGEGNERIA INDUSTRIALE XX CICLO

INCLUDING HUMAN PERFORMANCE IN THE DYNAMIC MODEL OF A SAILING YACHT: A COMBINED SHIP SCIENCE – BEHAVIOURAL SCIENCE APPROACH TOWARDS A WINNING YACHT-SAILOR COMBINATION

MATTEO SCARPONI

RELATORI
Prof. PAOLO CONTI[1]
Prof. R AJIT SHENOI[2]
Dr. STEPHEN R TURNOCK[2]

COORDINATORE
Prof. CLAUDIO BRACCESI[1]

A.A. 2006/07

[1] Dip. di Ingegneria Industriale, Università degli Studi di Perugia, Italia
[2] Ship Science, University of Southampton, United Kingdom

TABLE OF CONTENTS

CHAPTER 4

DECISION MAKING MODELS AND YACHT RACING

CHAPTER 5

ROBO-RACE: A SIMULINK-BASED TOOL FOR THE SIMULATION OF INTERACTIVE FLEET RACES

LIST OF FIGURES

CHAPTER 1

INTRODUCTION

CHAPTER 2

DEVELOPMENT OF A DYNAMIC MODEL FOR SAILING YACHTS

CHAPTER 3

ROBO-YACHT: A MATLAB-BASED IMPLEMENTATION OF A YACHT-CREW SYSTEM

CHAPTER 4

DECISION MAKING MODELS AND YACHT RACING

CHAPTER 5

ROBO-RACE: A SIMULINK-BASED TOOL FOR THE SIMULATION OF INTERACTIVE FLEET RACES

APPENDIX 1

EVALUATION OF ADDED MASSES AND ADDED MOMENTS OF INERTIA FOR THE IACC YACHT 'M566'

APPENDIX 2

3D MODELLING TECHNIQUES FOR VIRTUAL REALITY ANIMATIONS BASED ON VRML

LIST OF TABLES

CHAPTER 2

DEVELOPMENT OF A DYNAMIC MODEL FOR SAILING YACHTS

CHAPTER 3

ROBO-YACHT: A MATLAB-BASED IMPLEMENTATION OF A YACHT-CREW SYSTEM

CHAPTER 4

DECISION MAKING MODELS AND YACHT RACING

CHAPTER 5

ROBO-RACE: A SIMULINK-BASED TOOL FOR THE SIMULATION OF INTERACTIVE FLEET RACES

APPENDIX 1

EVALUATION OF ADDED MASSES AND ADDED MOMENTS OF INERTIA FOR THE IACC YACHT 'M566'

ABSTRACT

The steady-state, equilibrium performance of a sailing yacht can be predicted with reasonable accuracy and, to some extent, manoeuvering performances can be modelled as well. However, the inclusion of the abilities and skills of the sailors and the assessment of human performance have not been investigated so far.

Within the Sport Psychology domain, the use of computer simulated regattas is reported to clarify the behaviour of expert sailors. Furthermore, non-interactive racing simulators are occasionally used in the Naval Architecture domain, either to evaluate prototypical racing yacht designs and to improve existing ones. The present work aims at partially bridging the gap between the two fields, by incorporating human behavioural models and a 'decision-making engine' into an in-house sailing simulator based on the physics of an International America's Cup Class (IACC) yacht. In particular, the present Thesis describes the design, development, implementation and application of two tools for the investigation of yacht-crew systems.

Initially, the MATLAB-based model 'Robo-Yacht' was developed, in order to simulate solo races and drag races. The benchmark yacht used was the IACC design 'M566', whose resistance and manoeuvering properties have been extensively investigated at the University of Southampton, UK. A model with four degrees of freedom is used as a 'physics engine', whose equations of motion are solved stepwise through a 4^{th} order Runge-Kutta method. The automatic crew is modelled in terms of helmsman, sail tailers and a navigator/tactician. A 'decision-making engine' is modelled in terms of rules-of-thumb derived by questionnaires submitted to skilled sailors. The model predictions are in good agreement with those of a commercial Velocity Prediction Program. Several test cases are illustrated in the Thesis, which highlight the potential of 'Robo-Yacht'. For example, the tool was used to investigate a decision-making problem frequently encountered in sailing: a possible course change (a 'tack') due to a change in the wind direction. Tacking on a windshift can give the crew an advantage, provided that the shift is sufficiently large and stable to compensate the speed lost due to the maneuver. This case was investigated through a decision matrix where three possible decisions and four

possible weather scenarios are considered. The decision strategy is based on the maximization of expected payoff (decision-making under uncertainty) or expected utility (decision-making under risk); in the latter case, the crew's attitude towards risk is modelled. Results are consistent with widely accepted principles of racing strategy.

Then, the Simulink-based tool 'Robo-Race' was developed for the simulation of fleet races. The tool can perform entirely automatic simulations or run in interactive mode. This approach allows the simulation of different degrees of expertise, either in terms of man-machine interaction (e.g. steering and manoeuvering styles, sail trim) and crew-scenario interaction (race strategy and tactics). Such a tool includes automatic yacht-crew models already designed for 'Robo-Yacht', as well as user-controlled yachts. In the latter case, a user is given the control of a yacht (i.e. rudder adjustments, sail trimming) and real-time routing decisions can be made. Simultaneously, a Virtual Reality model embedded in 'Robo-Race' provides a real time visual feedback on the race and on the boat's performance. 'Robo-Race' can be used to estimate human-in-the-loop effects, to assess the performance of existing yachts and to predict the impact of design variations. As far as the human factor is concerned, the tool proved to be useful to investigate the information pick-up and processing, as well as behavioural patterns for beginners and experts. Building on this, the modelling of automatic crews can be further refined and tailored to different levels of expertise. Case studies are presented, where small fleet races in a stochastic wind pattern are simulated. Although the yacht features are a constant for the whole fleet, remarkable differences in the overall performance can be observed due to the skills of the crews and the individual judgment of the navigators. Therefore, the overall quality of the crew technique can be assessed, as well as the quality of the race strategy.

SOMMARIO

Le prestazioni di una imbarcazione a vela in condizioni di equilibrio possono essere previste con sufficiente accuratezza e, in una certa misura, anche le caratteristiche di manovrabilità sono modellabili. Ad oggi però, non sono disponibili modelli che tengano conto delle abilità dell'equipaggio, né modelli che permettano di studiare e quantificare l'impatto del fattore umano sulla prestazione del sistema equipaggio-imbarcazione.

Nel campo della Psicologia dello Sport esistono studi che si avvalgono di simulatori di regata per indagare il comportamento di equipaggi esperti. Inoltre, nel campo dell'Architettura Navale, è riportato l'uso di simulatori di regata sia per valutare prototipi di yacht che per migliorare le prestazioni di imbarcazioni esistenti. Scopo di questa Tesi è contribuire a colmare il divario tra le due discipline, incorporando modelli per il comportamento umano ed una 'logica decisionale' in un simulatore di regata appositamente sviluppato e basato sulla fisica di un'imbarcazione di Coppa America. In particolare, nella presente Tesi vengono descritti la progettazione, lo sviluppo, l'implementazione e l'applicazione di due programmi per lo studio di sistemi equipaggio-imbarcazione.

Il programma 'Robo-Yacht', realizzato nell'ambiente di sviluppo MATLAB®, ha come obiettivo la simulazione di regate in solitario e di 'drag races'. La barca di riferimento è il progetto IACC 'M566', le cui caratteristiche di resistenza e manovrabilità sono state dettagliatamente studiate presso l'Università di Southampton, UK. Il simulatore si avvale di un modello dinamico a 4 gradi di libertà, le cui equazioni del moto vengono risolte ad ogni passo della simulazione grazie ad un solutore basato sul metodo Runge-Kutta di 4° ordine. Il modello di equipaggio automatico è composto da un timoniere, due sail tailers ed un tattico/navigatore. La 'logica decisionale' si avvale di un insieme di regole ottenute da questionari sottoposti a velisti esperti. Il modello permette di ottenere risultati in linea con quelli offerti da un ben noto programma commerciale per la previsione delle prestazioni di imbarcazioni a vela. In questa Tesi vengono illustrati dei cas-studio per evidenziare il potenziale di 'Robo-Yacht'. Ad esempio, il programma è stato usato per indagare una situazione comunemente incontrata nel corso di una

regata: un possibile cambiamento di rotta (‘virata’) in conseguenza di un cambio della direzione del vento. Virare in risposta ad un ‘salto di vento’ può dare all’equipaggio un vantaggio di carattere strategico, qualora il salto sia sufficientemente ampio e stabile da compensare la perdita di velocità dovuta alla manovra. Questo caso è stato studiato con il supporto di una matrice delle decisioni, caratterizzata da tre possibili scelte e quattro possibili scenari meteo attesi. Il criterio di scelta considerato è la massimizzazione del guadagno atteso (decisione in regime di incertezza) o dell’utilità attesa (decisione in regime di rischio). Nel secondo caso, è stato proposto un modello per l’attitudine al rischio del navigatore. I risultati ottenuti sono coerenti con principi di strategia di regata ampiamente condivisi.

Un secondo programma, denominato ‘Robo-Race’ e implementato in ambiente Simulink®, è stato sviluppato per la simulazione di regate di flotta. Il programma si presta sia a simulazioni interamente automatiche che interattive. Tale approccio permette la simulazione di diversi gradi di abilità, sia in termini di interazione uomo-macchina (es. conduzione dell’imbarcazione, manovra, regolazione delle vele) che uomo-ambiente (strategia e tattica di regata). Tale programma comprende sia imbarcazioni automatiche già sviluppate per ‘Robo-Yacht’ che imbarcazioni controllate da utenti. In quest’ultimo caso, l’utente ha sia il compito di controllare lo yacht sia quello di prendere decisioni in tempo reale riguardanti la navigazione. Contemporaneamente, un’animazione realizzata in un ambiente di Realtà Virtuale offre all’utente un riscontro in tempo reale sulla propria condotta di gara e sul rendimento dell’imbarcazione. ‘Robo-Race’ può essere usato per modellare le prestazioni di yachts esistenti, prevedere l’effetto di variazioni progettuali e stimare l’impatto del fattore umano sulla prestazione del sistema barca-equipaggio. In riferimento a quest’ultimo aspetto, il programma si è rivelato utile per indagare sia la raccolta e l’elaborazione di informazioni, sia per valutare modelli comportamentali ricorrenti per principianti ed esperti. Grazie a ciò, la modellazione di equipaggi automatici può essere ulteriormente migliorata ed adattata a diversi livelli di abilità.

Vengono inoltre presentati casi-studio riguardanti regate di flotta in un regime di vento casuale. Nonostante le caratteristiche delle imbarcazioni siano mantenute costanti, si possono notare notevoli differenze di prestazione dovute alle diverse abilità degli equipaggi e alla condotta di gara decisa dal navigatore. Pertanto, la

‘qualità’ complessiva di un equipaggio può essere valutata, unitamente alla qualità della strategia e della tattica di regata.

ACKNOWLEDGMENTS

First of all, I would like to thank my Supervisors, Prof. Conti at the DII in Perugia, Prof. Shenoi and Dr. Turnock at Ship Science, Southampton, for their consistent support and advice throughout this Project. We drew this route together and turned out to be a good crew, despite the distance of the crossing. Also, I gratefully acknowledge the support offered by Prof. Terry McMorris: his guidance has helped me to navigate rough seas, unfamiliar to engineers. I am grateful to Francesco and Marco, my good friends and officemates in Perugia: I have really enjoyed the miles we have done together and have learnt a lot from you. I would also like to thank the friends and colleagues at Ship Science, who supported this work in a variety of ways. Among those, a special mention goes to the espresso appreciation society: our daily meetings in the upstairs galley really brightened up the day! This journey would not have started without the passion for sailing I share with Giancarlo, my first sailing instructor, and all my sailing mates at the CVC. Finally, I would like to thank the colleagues at the Wolfson Unit MTIA for welcoming me onboard and for allowing me time to complete this Thesis.

Un grazie particolare va alla mia famiglia, che mi ha insegnato a poter raggiungere qualsiasi obiettivo senza scendere a compromessi, ma contando solo sulle mie forze e sul loro appoggio incondizionato.

Non sarei riuscito ad arrivare qui senza l'amore, l'entusiasmo ed il continuo incoraggiamento di Michela, che ha condiviso le mie scelte e si é lasciata coinvolgere in questa avventura. Non ho mai ricevuto un regalo piú bello di questo!

to Michela:

‘Mais, si tu m'apprivoises, nous aurons besoin l'un de l'autre.
Tu seras pour moi unique au monde. Je serai pour toi unique au monde.
(…) Alors ce sera merveilleux quand tu m'auras apprivoisé!
Le blé, qui est doré, me fera souvenir de toi.
Et j'aimerai le bruit du vent dans le blé…’

CHAPTER 1

INTRODUCTION

1.1 Background

The naval architecture domain is still a rather conservative field, where improvements to reliable and well established designs are often preferred to dramatic breakthroughs. However, the use of innovative materials and technologies is expanding, sailing yachts and powerboats in the superyacht segment being just two examples. Unusual design specifications, often required by the owner, the yacht stylist or the interior designer pose a challenge that engineers would not have set themselves in the first place. Experimental tests and numerical simulations may assist the design team willing to explore new avenues, although the high costs involved are often beyond the budget allocated to small or medium sized projects.

A further market niche where innovation is paramount is that of high performance sailing yachts. In contexts such as the International America's Cup Class (IACC) or the Volvo 70' Class, small gains in performance are likely to make the difference. For example, the weight breakdown of a typical IACC yacht shows that the 85% of the overall weight is placed in the bulb, in order to maximize the righting moment. The crew is part of such an optimization process and therefore sailors undergo a constant physical and mental training, according to their role onboard. However, the influence of the human factor during sailing races has been neglected in the evaluation of high performance designs. For the 32nd edition of the IACC budgets in excess of €50m were available to many Challengers, and the Swiss Defender Alinghi had declared investments in excess of €100m. Large shares of these resources are usually invested in research and development. In analogy with Formula One racing and Grand Prix motorbike racing, these efforts have a positive impact on the boating industry so that technologies, materials, software and design techniques initially developed for high-end yachts can now be found in the marketplace. For example, innovative materials, performance prediction techniques

and numerical simulations originally developed for America's Cup racing can now be considered as well established in the maritime domain. It is common for high performance yacht design projects to use these methods at an early stage, when screening possible design candidates. Later on in the development, tools such as Velocity Prediction Programmes (VPPs) and Race Modelling Programmes (RMPs) can advantageously be used to estimate the global performance of the yacht and to investigate the handicap the yacht will be given according to Rules such as the International Measurement System (IMS).

While these tools and techniques can be further refined and the accuracy of predictions improved, there is also a need to assess the impact of the human factor on a design. In fact, when one-design yacht racing is considered or well-policed rules are in force, the performance is so leveled that a successful yacht-crew interaction becomes key to winning races.

1.2 Performance prediction of yacht-crew systems

As mentioned in Section 1.1, the global performance of a sailing yacht can be predicted experimentally, through model-scale tests in towing tanks (canoe body, keel and rudder) or wind tunnels (keels and sail plans). Once the aero and hydrodynamic coefficients are derived experimentally, they are usually supplied to VPPs (Claughton and Oliver, 2003) in order to estimate the speed and heel of the full-sized yacht in the desired range of wind speeds and at all points of sails. VPPs were initially developed for rating purposes: the Irving Pratt Project (Kerwin and Newman, 1979) indeed provided the foundations for the International Measurement System VPP (or IMS-VPP). In recent times, Authors such as (Keuning *et al.*, 2005) assert that dynamic performances (e.g. manoeuvering ability, speed loss when tacking) should also be included in handicapping systems. This has not been done so far, despite numerical models for the manoeuvering yacht are available (Masuyama *et al.*, 1995) and optimal tacking and gybing procedures have been investigated to some extent.

When weather databases are used in conjunction with VPPs, simulated races between design candidates can provide insight into the quality of a design. These

methods are known as RMPs (Todter *et al.*, 1993) and their features will be examined in the following Chapter. Setting up an RMP involves modeling the crew, although basic models for the yacht steering and navigation may suffice. For example, the use of a navigation model based on penalty factors is reported in (Philpott *et al.*, 2004) and the use of a proportional-derivative controller to mimic helmsman actions on an upwind course is recommended in (Harris, 2005).

1.3 The human factor: facts and figures

Several papers in the Sport Sciences domain underpin human factor issues in sailing, a discipline rich in uncertainty due to the weather and to the behaviour of the opponents. For example, recent studies by Araùjo claim that a strong correlation exists between sailors' performance and decision-making skills. Indeed, interactive race simulations have shown that 'best sailors function as better decision-makers' (Araùjo *et al.*, 2005).

Figure 1-1 is referred to the 32nd edition of the America's Cup, where the Swiss defender 'Alinghi' and the challenger 'Emirates Team New Zealand' (ETNZ) sailed seven races between June 23rd and July 3rd 2007. The average racing time required to complete the upwind-downwind course was 1h 32m 38s. Finishing deltas below 35 seconds were observed, with a minimum delta of 1 second for the crucial Race 7. The performances of the two yachts were extremely close, so that tactical choices, strategical decisions and manoeuvering skills proved to be crucial for victory.

Further conclusions can be drawn when considering the performance of the Challengers across the races of the Louis Vuitton Cup. For example, ETNZ sailed 50 upwind-downwind races in a wide range of weather conditions. Data for ETNZ show an average winning delta of 77 seconds and an average losing delta of 35 seconds. Although races were occasionally won owing to superior boat performance or to mechanical failure of an opponent, most of the key races (i.e. semi-finals and final) were won through winning tactical decisions and a successful strategical plan. Therefore, it is believed that decision-making (DM) models need to be used to study yacht-crew systems interacting with a complex weather scenario (e.g. oscillating wind regimes). DM theory is widely applied in many disciplines: management

sciences, warfare, medicine, politics, only to mention a few. Many of the models proposed in literature, such as (Payne *et al.*, 1996) make use of decision-making matrices and take into account the effect of time pressure, which is deemed appropriate in sport contexts.

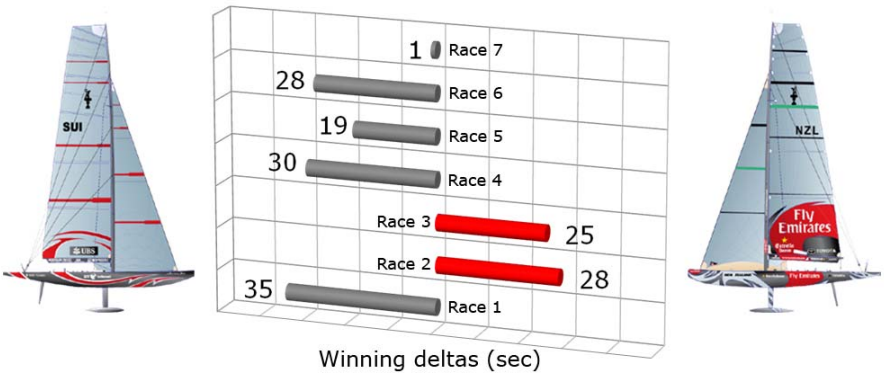

Figure 1-1: 32nd America's Cup, Valencia 2007: winning deltas.

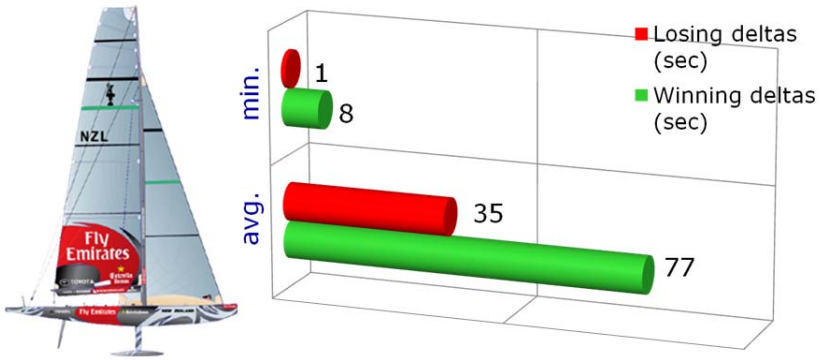

Figure 1-2: Louis Vuitton Cup, Valencia 2007, deltas for Team New Zealand

1.4 Overview of the Thesis

In the light of the above considerations, the inclusion of human behavioural models and man-machine interaction models in the dynamics of a sailing yacht is being addressed in this Thesis, in order to derive a general model for yacht-crew

systems. Two race simulators were developed in MATLAB-Simulink® in order to provide insight into yacht-crew and yacht-fleet interaction issues. The use of MATLAB-Simulink is not uncommon in the maritime field: for example, a Marine Systems Simulator (MSS) has been developed at the University of Trondheim for the simulation of control systems onboard ships and floating structures (Perez *et al.*, 2005). Recent industrial projects have also used MATLAB-Simulink to address programming, simulation and control issues. One example is the Talisman unmanned underwater vehicle developed by BAE Systems (UK) and launched in 2006, where Simulink was used to implement onboard control systems. A further example is provided by the raising of the Kursk submarine, a large-scale salvage operation carried out in 2001. A Model-Based Design approach was chosen and the whole salvage system was modelled in Simulink by the German company IgH, in order to predict the critical stages of the rescue operation for a range of possible sea states.

In Chapter 2, a dynamic model suitable for high performance sailing yachts will be described. The above model necessarily represents a trade-off between accuracy and computational effort, in order to carry out sensitivity studies based on large test matrices and systematic investigations of yacht-crew systems. In Chapter 3, the inclusion of human-in-the loop models is addressed. An automatic crew is designed, developed and implemented in order to carry out a number of onboard tasks: from steering to sail trimming, from navigation to race strategy. Furthermore, the MATLAB® implementation of simulated match-races between automatic yacht-crew systems is described. In Chapter 4 an overview of decision-making models is provided and their application to simulated yacht races is presented in the form of test cases. The decision-making models adopted herein, often used in management sciences, are shown to be consistent with race strategies adopted for yacht racing. In Chapter 5, the development of an improved version of the simulator in MATLAB-Simulink® is described, which can be used for real-time, interactive fleet races in a virtual reality environment. The use of such a tool for educational purposes can be envisaged: extensive post-match analyses can be carried out, the impact of

strategical and tactical decisions can be assessed and the global performance of the boat as a yacht-crew system can eventually be estimated.

1.5 References

Araùjo, D., Davids, K., Serpa, S. 'An Ecological Approach to Expertise Effects in Decision-Making in a Simulated Sailing Regatta'. Psychology of Sport and Exercise, 6, pp. 671-692, 2005.

Claughton, A.R., Oliver, J.C. III., 'Developments in hydrodynamic force models for velocity prediction programs'. Proc. of RINA Conference 'The Modern Yacht', Southampton (UK), pp. 67-77, 2003.

Harris, D.H., 'Time Domain Simulation of a Yacht Sailing Upwind in Waves', Proc. of the 17th CSYS, pp. 13-32, 2005.

Kerwin, J.E., Newman, J.N., 'A summary of the H. Irving Pratt Ocean Race Handicapping Project', Proc. of the 4th CSYS, 1979.

Keuning, J.A., Vermeulen, K.J., de Ridder, E.J., 'A generic mathematical model for the manoeuvering and tacking of a sailing yacht', Proc. of the 17th CSYS, pp. 143-163, 2005.

Masuyama, Y., Fukasawa, T., Sasagawa, H., 'Tacking simulations of sailing yachts - numerical integration of equations of motions and application of neural network technique', Proc. of the 12th CSYS, pp. 117-131, 1995.

Payne, J.W., and Bettman, J.R., 'When time is money: decision behaviour under opportunity-cost time pressure', Organizational Behaviour and Human Decision Processes, Vol.66 (2), pp.131-152, 1996.

Perez, T., Smogeli, Ø.N., Fossen, T.I., Sørensen, A.J., 'An overview of the Marine Systems Simulator (MSS): a Simulink Toolbox for marine control systems', Proc. of SIMS2005 – Scandinavian Conference on Simulation and Modeling, Trondheim, 2005.

Philpott, A., Henderson S.G., Teirney, D.P., 'A simulation model for predicting yacht match-race outcomes', Operations Research, Vol.52(1), pp. 1-16, 2004.

Todter, C., Pedrick, D., Calderon, A., Nelson, B., Debord, F., Dillon, D., '*Stars and Stripes* Design Program for the 1992 America's Cup', Proc. of the 11th CSYS, pp. 207-222, 1993.

CHAPTER 2

DEVELOPMENT OF A DYNAMIC MODEL FOR SAILING YACHTS

Nomenclature

[Symbol]	[Definition]
x, y	yacht's centre of gravity in earthbound frame
L	waterline length
D	draught
φ	roll angle
ψ	yaw (heading) angle
U	surge velocity
V	sway velocity
V_B	boat velocity
ρ	density of water
x_G	longitudinal position of added mass center for the hull
Δ	displacement
X_0	upright resistance
X_H, Y_H, K_H, N_H	hydrodynamic forces and moments on canoe body and keel
X_R, Y_R, K_R, N_R	hydrodynamic forces and moments on rudder
X_S, Y_S, K_S, N_S	aerodynamic forces and moments
m	mass of the yacht
m_x, m_y, m_z	added masses, body axes
I_{xx}, I_{yy}, I_{zz}	moments of inertia, body axes
J_{xx}, J_{yy}, J_{zz}	added mass moments of inertia, body axes
$\overline{\mathrm{GM}}$	metacentric height
β	leeway angle
δ	geometric rudder angle
δ_0	rudder angle for zero lateral force
l_R	effective distance between yacht's CG and rudder
α_R	effective angle of attack, rudder
γ_R	inflow angle of attack, rudder
P	mainsail hoist
E	longitudinal dimension of mainsail triangle
BAD	vertical distance from HBI to bottom of P
I	foresail hoist
J	longitudinal dimension of foretriangle
LP	foresail luff perpendicular
HBI	height of base of I above waterplane

SPL	spinnaker pole length
SMW	spinnaker mid width
SLU	spinnaker luff length
SLE	spinnaker leech length
ISP	height of spinnaker halyard sheave

2.1 Background on yacht performance prediction

The need to predict the performance of sailing yachts initially arose for handicapping purposes in the context of offshore racing. The H. Irving Pratt Project, carried out at the Massachusetts Institute of Technology, USA in the late 1970s, aimed at deriving the equilibrium speed of a yacht, at any given point of sail and wind speed, based on a limited number of design parameters (Kerwin and Newmann, 1979). One of the deliverables of the Project was a Velocity Prediction Program (VPP) that represents the foundation of modern race handicapping systems such as the well known International Measurement System (IMS). The underlying principle of modern VPPs is unchanged: to calculate the yacht's equilibrium conditions by balancing the hydrodynamic forces on the hull and the aerodynamic forces on the sails and the rig, at every wind speed and angle.

In order to do so, data on hull hydrostatics, stability, resistance, keel sideforce generation and sail propulsion must be supplied to VPPs. Such data can be derived experimentally, numerically or by interpolation of existing databases. In the latter case, the use of the Delft Systematic Yacht Hull Series (DSYHS) can be considered as well-established. It can be concluded that the quality of a VPP is that of the underlying aero-hydrodynamic models and databases. To quote Todter: 'the VPP is the glue that ties all the analysis and test data together' (Todter *et al.*, 1993).

The VPP developed for the IMS Rule (or IMS-VPP) underwent several revisions: improved models for hull resistance such as those described in (Claughton, 1999) were adopted and a closer prediction of downwind sails aerodynamics has been achieved. Readers are referred to (Claughton and Oliver, 2003) for an overview on recent improvements to the IMS-VPP.

Owing to the progress of Computational Fluid Dynamics (CFD), results of numerical simulations can now be used within VPPs with a reasonable degree of confidence (Rosen *et al.*, 2000). The development of entirely numerical VPPs, as proposed in (Roux *et al.*, 2002) is an alternative to conventional, experiment-based approaches. For example, a tool based on a Reynolds-Averaged Navier Stokes solver for aerodynamic and hydrodynamic forces is described in (Korpus, 2007) and, having been validated over three America's Cup cycles, represents the most refined tool to date. As pointed out in the above paper, a RANS-based VPP would offer clear advantages, particularly in the early design stages, when a large number of design candidates have to be evaluated. However, the complexity of fluid dynamics phenomena involved (fluid-structure interaction, surface effects of hull and appendages, flow separation and reattachment for offwind sails and so forth) require advanced turbulence models, large computational resources and further validation efforts.

Despite the valuable insight provided by VPPs, it was pointed out since the late 1980s that realistic predictions can be derived only by taking into account the many non-deterministic variables affecting yacht racing, such as possible variation of the weather conditions and the sea state during a race. As a consequence, a judgement that is solely based on VPP results is likely to be 'inconclusive and possibly misleading for determining the order of merit of two candidate yachts over a series of races' (Lechter *et al.*, 1987). Based on the above considerations, weather probabilistic models coupled with VPPs have been developed, which are referred to as Race Modelling Programs (RMPs). For the 1992 America's Cup, the *Stars and Stripes* design team used a RMP in conjunction with weather and sea state data gathered for over ten years and relative to the AC race venue in San Diego, USA (Todter *et al.*, 1993). Aim of the RMP was to estimate win/loss percentages for a pair of boats engaged in a match-race. Indeed, the RMP results helped in the selection of the best design candidate.

The use of fixed-time increment simulations for comparative evaluation of yacht designs is addressed in (Philpott *et al.*, 2004). The Authors used an 'approximate

dynamic model' based on a constant time step and three state variables: the boat's position, speed and heel angle. The 'approximate' nature of the model consists in the use of a VPP to evaluate the yacht state at every time step, rather than solving the equations of motion. Stepwise values of the wind speed and wind angle were provided by a model tuned on the weather conditions encountered in the Hauraki Gulf, New Zealand. With the aid of the above RMP, win/loss probabilities for design candidates in a variety of weather conditions could be evaluated.

The studies mentioned above demonstrate that the quality of a design should not be assessed based on steady state, equilibrium performance only. Factors like a yacht's manoeuverability and the ability to recover speed and ground after tacking have a considerable impact on the time around the course and should therefore be included in race simulations. Examples of maneuvering models in the time domain can be found in recent literature. Some Authors have focused on the evaluation of the optimal tacking procedure (Keuning *et al.*, 2005), while others have simulated a yacht racing on an upwind leg, taking into account its motion in a seaway (Harris, 2005) or its interactions with an opponent (Roncin, 2002). A great part of the Authors concentrate on solving simultaneously the set of unsteady, non-linear equations of motions. The use of system identification, based on neural networks, has been investigated as well.

Although models with six degrees of freedom (DOFs) have been devised, four DOFs (surge, sway, yaw and roll) models proved to perform well for tacking simulations in calm water and yielded results whose agreement with full scale trials is reasonable (Masuyama *et al.*, 1995). Therefore, the latter approach has been followed in this work. The set of non-linear equations of motion adopted here is also that proposed by (Masuyama *et al.*, 1995) and will be described in Section 2.3.

2.2 Requirements and scope of the dynamic model

Keeping in mind the scope of the PhD project, the choice of a dynamic model was driven by the following set of requirements:

1. The selected mathematical model must be able to capture the dynamic behaviour of a yacht in the time domain, including manoeuvers (that is tacks and gybes), response to gusts and wind shifts.
2. The model must be sensitive to the behaviour of a crew. In particular, different steering styles, manoeuvering styles and sail trimming styles that effect performance as it would happen in real-life racing.
3. The yacht dynamics must be based on the solution of the equations of motion, as opposed to quasi-static approaches based on VPPs.
4. The model adopted must have been validated by means of full-scale sea trials and/or numerical simulations.
5. The features of an actual racing yacht must be implemented for dynamic simulations.
6. A comparison between the performance of the benchmark yacht as predicted by commercial VPPs and by the dynamic model should be possible.
7. The dynamic model should simulate solo races, drag races and fleet races. Such simulations should run faster than real time on conventional workstations.
8. Race simulations must give users the possibility of interacting with the software in real time.
9. The simulations must provide a real-time visual feedback of the race in the form of virtual reality animations.

Published evidence exists that a four DoF approach taking into account surge, sway, heel and yaw is appropriate for the scope of this Thesis. In particular, the approach devised in (Masuyama *et al.*, 1995) fulfills requirements 1 to 4; these issues are being expanded later on in the present Chapter. As far as requirement 3 is concerned, in the light of the computational resources available to date, quasi-steady models relying on VPPs are considered obsolete and therefore not appropriate.

2.3 Features of Masuyama's dynamic model

The research reviewed in the present Section has been carried out at the Kanazawa Institute of Technology, Ishikawa, Japan by the research group led by Professor Y. Masuyama. Insight into these studies is offered by (Masuyama *et al.*, 1993), (Masuyama *et al.*, 1995) and (Masuyama *et al.*, 2007) where improvements based on the use of CFD techniques have been included. The former paper laid the groundwork for the numerical modeling of sailing yachts, by presenting a dynamic model based on four simultaneous differential equations, as well as its validation through sea trials. The second paper shows a further refinement to the model, in order to predict more closely the full-scale behaviour of manoeuvering yachts. In particular, the dynamics of tacking is investigated in order to highlight the optimal tacking procedure. The possibility of modelling a tacking yacht with the aid of neural networks is also discussed, as an alternative to the use of equations of motion. The model used for the present Thesis is based on the simultaneous set of equations of motion reported in (Masuyama *et al.*, 1995). Four degrees of freedom are investigated, namely surge, sway, yaw and heel. A 'horizontal body axes', CG-centred reference frame is being used, that was firstly adopted in (Hamamoto and Akiyoshi, 1980) to investigate the motion of a ship in a seaway. The reference sailing yacht for the numerical and experimental analyses described in (Masuyama *et al.*, 1993) is a one-off 34ft cruiser, built in 1988 and fitted with sensors for the simultaneous measurement of boat position, boat speed, leeway, heel and rudder angle, as well as the apparent wind speed and direction. Weight control procedures were used during the construction of the hull, to achieve the designed CG location and inertial properties.

Two dynamic models have been proposed by Masuyama. The first one is based on the use of a neural network whose training dataset is provided by full-scale tacking trials. The approach shows several shortcomings, mainly due to the intrinsic complications of sea trials which, in turn, limited the amount of training data available. The second model is based on four partial differential equations of

motion, addressing the surge, sway, heel and yaw equilibrium for the yacht in the horizontal body reference frame. Manoeuvering simulations were carried out, so that full-scale tacking trajectories could be compared with those predicted numerically. A close prediction of the actual trajectories and surge speed loss could be achieved through the 4 DoF dynamic model. Moreover, the model proved to be particularly sensitive to the rudder's rate of turn. In particular, numerical tacking trials showed that successful tacks could be carried out by using a gradually increasing rudder angle. Since Masuyama's model represents the starting point for this research, a detailed analysis of its features is reported below; variations to the force models are proposed and will be highlighted as well.

2.3.1 Equations of motion

The four differential equations below express the equilibrium condition for the yacht in surge (2.1), sway (2.2), heel (2.3) and yaw (2.4) as devised in (Masuyama *et al.*, 1995). As mentioned earlier, the four equations of motion are referred to the CG-centered, 'horizontal body axes' system. Its *x* axis lies on the yacht's centerline and is orientated stern to bow, the *y* axis is positive to port while the *z* axis is perpendicular to the sea surface and orientated downwards, i.e. towards the seabed. Due to the chosen reference frame, the upright added masses and added moments of inertia have to be corrected for heel angle φ.

$$\begin{aligned}(m+m_x)\dot{U} - (m+m_y\cos^2\varphi + m_z\sin^2\varphi)V\dot{\psi} \\ -(m_y\cos^2\varphi + m_z\sin^2\varphi)x_G\dot{\psi}^2 \\ = X_0 + X_H + X_{V\dot{\psi}}V\dot{\psi} + X_R + X_S\end{aligned} \tag{2.1}$$

$$\begin{aligned}(m+m_y\cos^2\varphi + m_z\sin^2\varphi)\dot{V} + (m+m_x)U\dot{\psi} \\ + 2\left(m_z - m_y\right)\sin\varphi\cos\varphi\left(V + x_G\dot{\psi}\right)\dot{\varphi} \\ + (m_y\cos^2\varphi + m_z\sin^2\varphi)x_G\ddot{\psi} \\ = Y_H + Y_{\dot{\varphi}}\dot{\varphi} + Y_{\dot{\psi}}\dot{\psi} + Y_R + Y_S\end{aligned} \tag{2.2}$$

$$(I_{xx} + J_{xx})\ddot{\varphi} - \{(I_{yy} + J_{yy}) - (I_{zz} + J_{zz})\} \sin\varphi \cos\varphi \, \dot{\psi}^2 + 2(m_y - m_z) \sin\varphi \cos\varphi \, x_G V \dot{\psi} = K_H + K_{\dot{\varphi}}\dot{\varphi} + K_R + K_S + \Delta\overline{GM} \sin\varphi \tag{2.3}$$

$$\{(I_{yy} + J_{yy}) \sin^2\varphi + (I_{zz} + J_{zz}) \cos^2\varphi\}\ddot{\psi} + 2\{(I_{yy} + J_{yy}) - (I_{zz} + J_{zz})\} \sin\varphi \cos\varphi \, \dot{\psi}\dot{\varphi} - 2(m_y - m_z) \sin\varphi \cos\varphi \, x_G V \dot{\varphi} + (m_y \cos^2\varphi + m_z \sin^2\varphi)(\dot{V} + U\dot{\psi})x_G = N_H + N_{\dot{\psi}}\dot{\psi} + N_R + N_S \tag{2.4}$$

Forces and moments exerted on the yacht have been grouped together on the right-hand side of Eqns. (2.1) to (2.4). Details on the breakdown of forces are provided in the following Sections.

2.3.2 Hydrodynamic forces

The force model used in Masuyama's model takes into account the contributions of the upright resistance component X_0, the forces and moments acting on the appended hull X_H, Y_H, K_H and N_H, the rudder forces and moments X_R, Y_R, K_R and N_R and the unsteady components $X_{V\dot{\psi}}V\dot{\psi}$, $Y_{\dot{\varphi}}\dot{\varphi} + Y_{\dot{\psi}}\dot{\psi}$, $K_{\dot{\varphi}}\dot{\varphi}$, $N_{\dot{\psi}}\dot{\psi}$. Further unsteady effects are included in the aerodynamic forces X_S, Y_S, K_S and N_S and will be accounted for in Section 2.3.3

In (Masuyama *et al.*, 1993), the upright resistance X_0 of the reference yacht was evaluated in the towing tank at 1/4.275 scale and at 1/8 scale. An attempt to use full scale towing tests was made, obtaining a good agreement with tank data for Fn<0.5. The forces on the appended hull X_H, Y_H, K_H and N_H were evaluated through Eqns. (2.5) to (2.8) below, expressed in terms of hydrodynamic derivatives.

$$X_H = X_{VV}V^2 + X_{V\varphi}V\varphi + X_{\varphi\varphi}\varphi^2 + X_{VVVV}V^2 \tag{2.5}$$

$$Y_H = Y_V V + Y_\varphi \varphi + Y_{VVV}V^3 + Y_{VV\varphi}V^2\varphi + Y_{V\varphi\varphi}V\varphi^2 + Y_{\varphi\varphi\varphi}\varphi^3 \tag{2.6}$$

$$K_H = K_V V + K_\varphi \varphi + K_{VVV}V^3 + K_{VV\varphi}V^2\varphi + K_{V\varphi\varphi}V\varphi^2 + K_{\varphi\varphi\varphi}\varphi^3 \tag{2.7}$$

$$N_H = N_V V + N_\varphi \varphi + N_{VVV} V^3 + N_{VV\varphi} V^2 \varphi + N_{V\varphi\varphi} V \varphi^2 + N_{\varphi\varphi\varphi} \varphi^3 \quad (2.8)$$

The hydrodynamic derivatives $X_{V\dot{\psi}}$,$Y_{\dot{\psi}}$,$K_{\dot{\psi}}$ and $N_{\dot{\psi}}$ were obtained through empirical formulae and, in some cases, through full scale trials. For example, $Y_{\dot{\psi}}$ was obtained through roll decrement tests at full scale, both with and without sails. However, due to the impossibility of performing such tests on the IACC model used as a benchmark, the results of CFD tests performed at the University of Southampton were used as a starting point for the analysis (see Section 2.4.3).

The rudder forces and moments X_R, Y_R, K_R and N_R are based on the experimental coefficients $C_{X\delta}$, $C_{Y\delta}$, $C_{K\delta}$ and $C_{N\delta}$ obtained through rudder angle tests.

$$X_R = \left(\frac{1}{2}\rho V_B^2 LD\right) X_R' = \left(\frac{1}{2}\rho V_B^2 LD\right) C_{X\delta} \sin\alpha_R \sin\delta \quad (2.9)$$

$$Y_R = \left(\frac{1}{2}\rho V_B^2 LD\right) Y_R' = \left(\frac{1}{2}\rho V_B^2 LD\right) C_{Y\delta} \sin\alpha_R \cos\delta \cos\varphi \quad (2.10)$$

$$K_R = \left(\frac{1}{2}\rho V_B^2 LD^2\right) K_R' = \left(\frac{1}{2}\rho V_B^2 LD^2\right) C_{K\delta} \sin\alpha_R \cos\delta \quad (2.11)$$

$$N_R = \left(\frac{1}{2}\rho V_B^2 L^2 D\right) N_R' = \left(\frac{1}{2}\rho V_B^2 L^2 D\right) C_{N\delta} \sin\alpha_R \cos\delta \cos\varphi \quad (2.12)$$

where L is the waterline length, D is the draught, V_B is the boat speed and δ is the geometric rudder angle (i.e. between the rudder blade and the yacht's centreline). Although a CFD-based approach to rudder modelling will be used for the sailing simulator, the evaluation of the effective angle of attack for the rudder α_R follows Masuyama's formulation:

$$\alpha_R = \delta - \gamma_R \tan^{-1}\left(-\frac{V + l_R\dot{\psi}}{U}\right) \quad (2.13)$$

Eqn. (2.13) takes into account both the leeway and the angular velocity experienced by the rudder when turning at a yaw rate $\dot{\psi}$ about the yacht's CG.

The coefficient γ_R is referred to as 'inflow angle of attack' and was derived experimentally, based on Eqn. (2.14).

$$\gamma_R = \frac{\delta_0}{\beta} \tag{2.14}$$

where δ_0 is the geometric rudder angle yielding a null turning moment (i.e. a $\delta=\delta_0$ the hydrodynamic rudder force is parallel to the centerline of the yacht). Being δ_0 a function of the leeway angle β, towing tank tests were carried out for leeway angles in the range $\beta=[0,30]$, to evaluate $\delta_0(\beta)$ by regression. The upper end of the range was included in order to be able to model sharp turns such as tacks. Experimental results relative to the function $\gamma_R(\beta)$ can be found in (Masuyama *et al.*, 1995): the trend is almost linear at leeway angles below 14°, while $\gamma_R$is found to independent of β above 14° owing to the stall of the fin keel.

The added masses and added moments of inertia of the canoe body and those of the appendages (keel plus rudder) were calculated individually. In order to do so, four main assumptions were originally formulated by Masuyama and co-authors:

- low frequencies for the swaying and yawing motion: this allowed to formulate m_y and J_{zz} for the canoe body based on the Lewis form factors C_1 and C_3;
- the added mass in surge m_x is assumed to be that of an equivalent spheroid: this yielded $m_x=0.037$ for the case of a 34ft yacht;
- the measured value of the natural frequency for the pitch-heave motion was 0.53Hz, which allowed a simplified calculation of m_y and $J_{zz,}$ also based on the Lewis form factors;
- the appendages were approximated by ellipsoid planforms and mirrored about the waterline;
- the natural period of rolling, calculated through the roll decrement tests mentioned above, was used to obtain J_{xx}.

The above added masses and moments of inertia were evaluated in body axes and therefore need to be adjusted based on heel angle φ.

2.3.3 Aerodynamic forces

A classical formulation in terms of sail coefficients was adopted by Masuyama. Lift and drag coefficients were derived experimentally, based on wind

tunnel tests of scaled sailplans of the Flying Fifteen class. Approximated formulae for the calculation of aerodynamic inertia forces can be found in the paper. These are based on the assumption of triangular sail shapes.

It is believed that this section of the model should be considerably improved in order to be used in a race modeling program including the human factor. For example:

i. the possibility of trimming the mainsail and the headsail independently should be included;
ii. sail trim parameters adopted for VPPs like reef, flat and twist should be introduced, accounting for human judgement;
iii. unsteady effects on the sail plan should also be introduced, such as the boat's accelerations and angular velocity.

In Masuyama's paper, an approximation is being used to model the variation of sail forces across a tack. In particular, both the aerodynamic lift and drag are supposed to vary linearly with the apparent wind angle. When head to wind, the sails are modelled as pure windage elements, i.e. sources of drag.

2.3.4 Model validation

As pointed out in the previous Sections, Masuyama's model has been validated through full-scale trials, reported for example in (Masuyama *et al.*, 1993). Although part of the model is based on semi-empirical formulae (e.g. for the calculation of hydrodynamic derivatives, added masses and moments of inertia), its predictions are shown to be consistent with straight-line speed tests and manoeuvering trials.

A first set of sea tests carried out by Masuyama and co-authors consisted in well-established trials for ships as described in (Lewis, 1988): these were performed under power and consisted in turning circles and zig-zag manoeuvers. The dynamic model approximated well the full-scale trajectories and the trace of surge speed in response to pre-defined rudder actions. Also, an accurate prediction of the delay between rudder actions and vessel's response was observed: a sign change for the rate of turn of the rudder did not yield an immediate change of heading for the yacht. This behaviour is known as 'heading overshoot'. The delay in the response and the

amount of overshoot depend on the inertial properties of the yacht and its manoeuvering ability.

Tacking trials were also simulated in order to investigate the best tacking procedure. These tests have shown the sensitivity of the model to subtle changes to the commanded rudder angle across a tack. The model highlighted that better performance in terms of speed recovery could be achieved by gradually increasing the rudder angle while tacking. This result is reported to be consistent with tacking trials carried out at sea. Due to its sound validation, the present methodology is deemed to be appropriate to model the impact of human factor on the steering (and therefore on performance), one of the key issues addressed in the present Thesis.

2.4 The benchmark yacht: IACC 'M566'

2.4.1 Design overview

The reference yacht for the dynamic simulations is the International America's Cup Class (IACC) design 'M566' based on Version 5 of the IACC Rule. The 'M566' lines, design parameters, displacement and arrangement of appendages are representative of actual IACC designs for the 2000 America's Cup. The yacht underwent extensive towing tank testing at the University of Southampton (UK), mostly for educational purposes. In particular, a family of canoe body forms was evaluated, as well as several appendage configurations; this resulted in more than 15 candidate designs tested in the tank. A general overview of the design is provided in Table 2-1. A combination of the 'M566' canoe body, a standard fin-bulb keel and a high-aspect rudder will be considered for the simulations.

A sail inventory consisting in one mainsail, one genoa, one jib and one spinnaker was used for this Thesis. Sail areas and headsails' overlaps are based on educated guesses for typical IACC designs for the year 2000. A standard set of sail coefficients will be used herein, whose trend is shown in Figure 2-1. These sail coefficients are part of the 'Aerolib' library, provided as a default choice by the commercial Velocity Prediction Program WinDesign. These coefficients were derived experimentally and are used worldwide for comparative analyses of sailing

yachts. Therefore, they are deemed to provide a sensible estimate of sail performance for upwind-downwind race courses.

Table 2-1: General design parameters for the 'M566' (Hull) and typical design values for IACC yachts, Rule version 4.0 (Sails and Rig)

Hull		*Rig and Sail Inventory (m)*			
Δ (kg)	26448	*Main triangle*		*Fore triangle*	
LOA (m)	23.880	P	30.5	IG	25.6
LWL (m)	18.894	E	8.0	J	8.0
BWL (m)	3.324	BAD	2.0	LP	7.6
HBI (m)	1.362	*Spinnaker dimensions*			
Sail areas (sqm)		SPL	10.80		
Mainsail	196.10	SMW	16.85		
Genoa	134.80	SLU	29.36		
Jib	102.00	SLE	29.36		
Spinnaker	447.75	ISP	31.50		

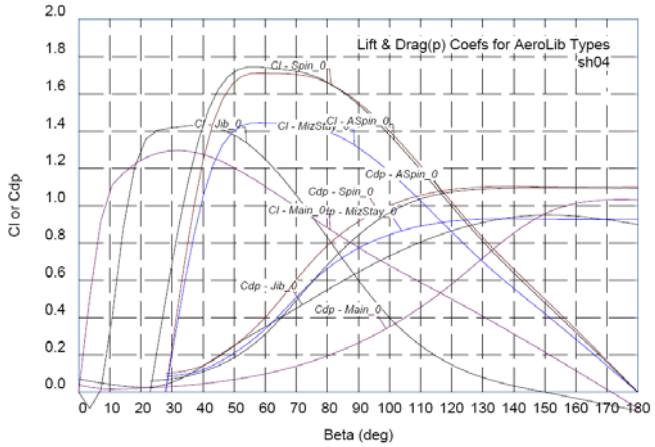

Figure 2-1: Aerolib sail coefficients, 'WinDesign' VPP

2.4.2 Steady hydrodynamic forces and moments

As mentioned earlier, both experimental and CFD-based data are available for the 'M566' hullform. Towing tank results were used to derive the upright resistance X_0 (Eqn. 2.1), whose trend is shown in Figure 2-2 below.

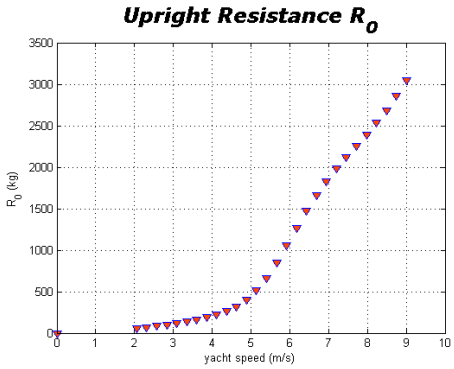

Figure 2-2: Upright resistance for the IACC 'M566'

As mentioned in Section 2.3.2, the hydrodynamic forces exerted on the appended hull of the benchmark yacht were expressed as a function of hydrodynamic derivatives. Several investigations such as that of (Rousselon, 2005) were carried out at the University of Southampton on the manoeuvering properties of the 'M566'. These studies involved the use of a Planar Motion Mechanism (PMM) and Palisupan (PArallel LIfting SUrface PANel code), a CFD code to solve potential, three dimensional flow with the aid of panel method analyses (Turnock, 1997). The shortcomings of the above analyses are clear: for example, acceleration derivatives cannot be calculated through Palisupan and PMM results only must be relied upon. Also, the hypothesis of potential flow can yield unsatisfactory predictions of keel-rudder interaction. A closer modeling could be achieved with the help of Reynolds-Averaged Navier Stokes (RANS) codes.

Although the prediction of hydrodynamic derivatives could be refined, a good approximation of the performance of IACC yachts can still be achieved and therefore the values in Table 2-2 are used in this Thesis. In fact, the steady hydrodynamic forces predicted by the simulator match closely those predicted by

VPPs such as WinDesign, provided that the same aerodynamic model is being used. Moreover, a reasonable agreement can be achieved between simulated and full-scale tacking trials for IACC yachts. Indeed, the time histories for Velocity Made Good (VMG) and surge speed across a tack are representative of those of IACC yachts. This is a key feature in race modeling, since high speed losses yield great disadvantages in tacking duels and/or oscillating wind regimes, where windshifts normally require yachts to tack.

Table 2-2: Hydrodynamic derivatives (dimensions have been omitted)

X_{VV}	-2.8E-1	Y_V	-1.2	K_V	-2.0	N_V	9.3E-2
$X_{V\varphi}$	1.6E-2	Y_φ	-2.9E-4	K_φ	8.2E-3	N_φ	-4.6E-4
$X_{\varphi\varphi}$	3.0E-4	Y_{VVV}	-4.2	K_{VVV}	-3.4	N_{VVV}	-3.2E-2
X_{VVVV}	7.8E-3	$Y_{VV\varphi}$	-1.9	$K_{VV\varphi}$	-2.3E+1	$N_{VV\varphi}$	-2.6E-1
		$Y_{V\varphi\varphi}$	0.5	$K_{V\varphi\varphi}$	4.7E-1	$N_{V\varphi\varphi}$	4.3E-3
		$Y_{\varphi\varphi\varphi}$	-3.7E-3	$K_{\varphi\varphi\varphi}$	2.9E-2	$N_{\varphi\varphi\varphi}$	3.1E-4
		$Y_{\dot{\varphi}}$	-2.078	$K_{\dot{\varphi}}$	-3.97	$N_{\dot{\varphi}}$	2.385

2.4.3 Unsteady hydrodynamic forces and moments

Based on (Masuyama *et al.*, 1993) and considerations by (Rousselon, 2005) the following formulations were used to model unsteady hydrodynamic forces and moments:

$$X_{dyn} = {X_{\dot{\varphi}}}^2\dot{\varphi}^2 + {X_{\dot{\psi}}}^2\dot{\psi}^2 = \left({Y_{\dot{\varphi}}}^2/C'\right)\dot{\varphi}^2 + \left({Y_{\dot{\psi}}}^2/C''\right)\dot{\psi}^2 \quad (2.15)$$

$$Y_{dyn} = Y_{\dot{\varphi}}\dot{\varphi} + Y_{\dot{\psi}}\dot{\psi} \quad (2.16)$$

$$K_{dyn} = K_{\dot{\varphi}}\dot{\varphi} \quad (2.17)$$

$$N_{dyn} = N_{\dot{\psi}}\dot{\psi} \quad (2.18)$$

As far as Eqn. (2.15) is concerned, the resistance component ${X_{\dot{\varphi}}}^2\dot{\varphi}^2$ dependent on heel rate was added to the dynamic forces acting along the X axis. This has been done to achieve a closer modelling of tacking, a manoeuvre where variations of heel in excess of 50 degrees across a time span of 15 seconds are common. The efficiency parameters C' and C'' were derived from CFD analyses for a surge speed

U = 3.0 m/s. A weak correlation with the heel angle φ was observed, so that it was deemed reasonable to consider them as constants. The values used herein are C'=1.31 and C''=-0.40.

The derivatives of Eqns. (2.16) to (2.18) are also based on systematic CFD studies carried out with PALISUPAN (Turnock, 1997). In particular, it is demonstrated in (Rousselon, 2005) that CFD analyses and regression techniques can advantageously be used to derive response surfaces $Y = f(\dot{\varphi}, \dot{\psi})$, $K = g(\dot{\varphi}, \dot{\psi})$, $N = h(\dot{\varphi}, \dot{\psi})$, whose local slopes yield the partial derivatives required.

2.4.4 Added masses and added moments of inertia

First attempt values for the added masses and added moments of inertia were obtained by scaling Masuyama's results, in the light of considerations by (Rousselon, 2005). However, it was believed that some of the assumptions highlighted in Section 2.3.2, particularly the Lewis form approximation, were unsuitable for a correct modelling of the M566 and accurate calculations became necessary.

A detailed account on the calculation of added masses and added moments of inertia for the 'M566' is provided in Appendix 1. In particular, the calculation of added masses and moments of inertia in sway and heave are based on (Keuning and Vermeulen, 2002). Under the assumption of linear superposition of responses, the yacht's added masses in sway and heave was calculated by summing the individual contributions of a discrete set of underwater stations or 'strips'. This approach is usually referred to as 'strip theory' and has been implemented in commercial packages such as 'Ship Motions' by the Wolfson Unit MTIA, whose use for manoeuverability and seakeeping assessment is common practice.

2.5 References

Araùjo, D., Davids, K., Serpa, S. 'An Ecological Approach to Expertise Effects in Decision-Making in a Simulated Sailing Regatta'. Psychology of Sport and Exercise, 6, 671-692, 2005.

Claughton, A.R., 'Developments in the IMS VPP Formulations'. Proc. of The 14th CSYS, pp. 1-20., 1999.

Claughton, A.R., Oliver III, J.C., 'Developments in hydrodynamic force models for velocity prediction programs. Proc. of RINA Conference 'The Modern Yacht', pp. 67-77, Southampton, United Kingdom, 2003.

Harris, D.H., 'Time Domain Simulation of a Yacht Sailing Upwind in Waves', Proc. of The 17th CSYS, pp. 13-32, 2005.

Kerwin, J.E., Newman, J.N., 'A summary of the H. Irving Pratt Ocean Race Handicapping Project', Proc. of the 4th CSYS, 1979.

Keuning, J.A., Vermeulen, K.J., de Ridder, E.J., 'A generic mathematical model for the manoeuvering and tacking of a sailing yacht', Proc. of The 17th CSYS, pp. 143-163, 2005.

Lechter, J.S., Jr., Marshall, J.K., Oliver III, J.C., Salvesen, N., 'Stars and Stripes', Scientific American, 257(2), pp. 34-40, 1987.

Lewis, E.W., 'Principles of Naval Architecture', SNAME, 1988.

Masuyama, Y., Fukasawa, T., Sasagawa, H., 'Tacking simulations of sailing yachts - numerical integration of equations of motions and application of neural network technique', Proc. of The 12th CSYS, pp. 117-131.

Masuyama, Y., Nakamura, I., Tatano, H., and Takagi, K., 'Dynamic performance of a sailing cruiser by full scale sea tests', Proc. of The 11th CSYS.

Philpott, A., Henderson S.G., Teirney, D.P., 'A simulation model for predicting yacht match-race outcomes', Operations Research, 52(1), pp. 1-16, 2004.

Rosen, B.S., Laiosa, J.P., Davis, W.H., Jr., 'CFD design studies for the America's Cup 2000', AIAA Paper 2000-4339, Proc. of the 18th Applied Aerodynamics Conference, Denver, USA, 2000.

Roncin, K., ‘Simulation dynamique de la navigation de deux voiliers en interaction’, PhD Thesis, Laboratoire de mécanique des fluides, ECN, 2002.

Rousselon, N., ‘Prediction of hydrodynamic and aerodynamic forces and moments for use in a 4 DoF simulation tool, using a lifting surface panel code’, MSc Thesis, Ship Science, University of Southampton, 2005.

Roux, Y., Huberson, S., Hauville, F., Boin, J.P., Guilbaud, M., Ba, M., ‘Yacht performance prediction: towards a numerical VPP’, Proc. of High Performance Yacht Design Conference, Auckland, NZ, 2002

Todter, C., Pedrick, D., Calderon, A., Nelson, B., Debord, F., Dillon, D., ‘*Stars and Stripes* Design Program for the 1992 America’s Cup’, Proc. of The 11th CSYS, pp. 207-222.

Turnock, S.R., ‘Technical manual and user guide for the surface panel code Palisupan’, Ship Science Report no. 100, University of Southampton, 1997.

CHAPTER 3

ROBO-YACHT: A MATLAB®-BASED IMPLEMENTATION OF A YACHT-CREW SYSTEM

3.1 Overview of MATLAB

MATLAB® is a high level programming language marketed and maintained by The Mathworks Inc. The first, Fortran-based version of MATLAB was released in the late 1970s by Cleve Moler, mathematician and Professor of Computer Science at Stanford. At that time the standard programming language for numerical analysis was Fortran, whose capabilities were extended by EISPACK and, subsequently, by LINPACK. The latter was, effectively, a collection of Fortran routines for solving linear equations co-authored by Prof. Moler himself. Although satisfactory for mathematicians, the Fortran-based environment was inappropriate for solving engineering-related problems. In particular, a higher level language was required, that could handle large matrices efficiently and perform operations on whole arrays and matrices with only a few lines of code.

In order to fill this gap, a first academic version of MATLAB was released. Initially, it consisted of 80 functions only and the only available data type was 'matrix' hence the name, short for 'MATrix LABoratory'. Later on, a few commercial packages based on MATLAB were developed by Stanford graduates, addressing issues in signal processing and control analysis. As the commercial potential of MATLAB became clear, the code was rewritten in C by Jack Little and Steve Bangert, who also added dedicated libraries (or 'toolboxes') and enhanced the graphics. Moler, Little and Bangert founded The MathWorks in 1984.

Nowadays, MATLAB includes a large number of toolboxes spanning many disciplines: image processing, system identification, optimization, neural networks being just a few examples. Since the early 1990s the graphical programming language Simulink has been developed alongside MATLAB, mainly in support of

the design of control systems. At present, Simulink is the standard for the modelling, simulation and analysis of linear and non-linear dynamic systems, with an active community of engineers and academics driving its development, sharing a number of open-source projects and contributing to the enhancement of its capabilities.

3.2 Simulator requirements

The framework of the sailing simulator was already defined in Section 2.2 through a list of general requirements (replicated below for the readers' convenience).

1. The selected mathematical model must be able to capture the dynamic behaviour of a yacht in the time domain, including manoeuvers (that is tacks and gybes), response to gusts and wind shifts.
2. The model must be sensitive to the behaviour of a crew. In particular, different steering styles, manoeuvering styles and sail trimming styles should affect performance as it would happen in real-life racing.
3. The yacht dynamics must be based on the solution of the equations of motion, as opposed to quasi-static approaches based on VPPs.
4. The model adopted must have been validated by means of full-scale sea trials and/or numerical simulations.
5. The features of an actual racing yacht must be implemented for dynamic simulations.
6. A comparison between the performance of the benchmark yacht as predicted by commercial VPPs and by the dynamic model should be possible.
7. The dynamic model should simulate solo races, drag races and fleet races. Such simulations should run faster than real time on conventional workstations.
8. Race simulations must give users the possibility of interacting with the software in real time.
9. The simulations must provide a real-time visual feedback of the race in the form of virtual reality animations.

While Requirements 1, 3, 4 and 5 were expanded on in Chapter 2, the following Sections will focus on Requirements 2, 6 and 7, as well as providing insight into the choice of the programming language adopted. The implementation of the yacht-crew model will be described, as well as its partial validation. The latter has been carried out by comparing the steady-state performance of the IACC-M566 as calculated via the simulator, with the predictions of the well-established VPP.

3.3 Architecture of the MATLAB-based simulator

3.3.1 Generalities

The MATLAB version of the simulator, or 'Robo-Yacht', will be presented in the following Sections. Based on a physics engine already used by (Rousselon, 2005), and on crew models developed from scratch, this version was intended to:

- simulate solo races and investigate decision-making patterns for race strategy. This is to say that routing decisions are made based on the race scenario only (marks, wind and weather) without the influence of other yachts.
- investigate the steady-state and the manoeuvering performance of the benchmark yacht, as described in Chapter 2 and validate the model with the aid of a commercial VPP.
- devise an appropriate model to simulate the behaviour of a virtual crew. The implementation of sub-models and controls supervising the yacht steering, the sail trimming and the navigation will be presented.

The MATLAB version of the software can run in 'SingSim' mode, for the simulation of a solo-race with fixed parameters for the yacht, the crew and the weather scenario. If the 'SingSim' mode is used, a Graphical User Interface (GUI) is made available to define the simulation parameters; an overview of the GUI is provided in Section 3.3.4. Alternatively, a 'MultiSim' mode can be chosen, to carry out systematic analyses driven by appropriate test matrices. For example, a test

matrix can be set up in order to explore variations to a base crew (e.g. different tacking styles or race strategies) given a fixed yacht or vice versa.

3.3.2 The 'Yacht' module

The default dataset for the 'Yacht' module is relative to the IACC 'M566'. Such data include, for example, the general design parameters for the hull, the rig and the sails outlined in Table 2-1, as well as the hydrodynamic derivatives of Table 2-2. However, such a dataset can be partially or entirely modified by users, for example to assess how variations to a base design would affect performance. Both a graphic user interface (GUI) and MATLAB '.mat' data files can be used for this purpose. The latter are organized as multi-level structures, to facilitate the navigation within the dataset. This option has been added specifically for the purpose of 'MultiSim' analyses mentioned in the previous Section.

While a simulation is running, a solution of the four simultaneous equations of motion is calculated at each time step. A standard 4^{th} order Runge-Kutta solver was deemed appropriate for this purpose and therefore an ad-hoc routine was implemented, no such function being available in the MATLAB library. This well known numerical method requires four evaluations of the equations of motion per time step. As MATLAB is an interpreted programming language, this may slow the simulation down; however, a satisfactory compromise between accuracy and computational effort could be achieved by using a discrete time step of 0.2 seconds. Such time step is normally adopted by other yacht manoeuvering models referred to in this Thesis and is shown to be adequate for tacking simulation purposes.

Based on these considerations, the average CPU time required to simulate a one mile upwind leg in an arbitrary true wind pattern is 60 seconds on conventional workstations with 1Gb RAM. This performance could be further improved by using the MATLAB compiler, which automatically generates low-level code (FORTRAN or C) out of the existing set of m-files. However this avenue has only been partially explored, due to the later use of a compiled, Simulink-based approach for fleet race simulations.

3.3.3 The 'Scenario' module

The term 'scenario' is referred to the environment of a solo race, therefore including the racecourse and the weather conditions for the race.

As far as the racecourse is concerned, the scenario includes the position of the race marks, the way marks have to be rounded, the finishing line (position and width) and the end-race conditions (e.g. maximum time around the course). As pointed out in Section 3.4, the navigator is in charge to identify the yacht's position within the racecourse and to deal with mark roundings. In order to do so, a mark is identified as 'rounded' as soon as it is seen past amidships.

As far as the weather model is concerned, it was observed in (Philpott and Mason, 2002) that speed and direction of true wind should be considered as independent stochastic variables, whose values vary over time and over the racecourse. In the model devised by Philpott, changes in wind conditions are supposed to propagate downstream according to Taylor's hypothesis of wind engineering: wind eddies travel down the flow field at a given mean wind speed. The model is based on wind measurements on Hauraki Gulf, New Zealand and can model large shifts in wind direction occurring at random intervals.

In the case of the present simulations, a close modelling of the atmospheric wind profile and its propagation over the race area was considered unnecessary. In fact, it is believed that a good insight into the interactions between a yacht-crew system and the race scenario can be achieved with less sophisticated wind models than those presented above. On the other hand, the possibility of simulating elementary patterns for wind speed and angle, according to common classifications found in race strategy manuals such as (Perry, 2000) was of primary importance for the purposes of this Thesis. Examples of such patterns are illustrated in Table 3-1.

Table 3-1: combinations of wind speed and angle

Wind Speed	*steady,* *rising / dropping (slowly, suddenly, occasionally),* *rhythmically oscillating in phase with wind angle,* *rhythmically oscillating out of phase with wind angle*

Wind Angle	*steady,* *veering clockwise,* *veering counterclockwise,* *rhythmically shifting in phase with wind speed,* *rhythmically shifting out of phase with wind speed,*

The above patterns have been implemented in Robo-Yacht, as well as a 'Stochastic Wind' option to simulate noise superimposed to an arbitrary wind trend. The information on wind speed and angle consisted therefore in deterministic parameters (e.g. period, amplitude and phase) and stochastic information, expressed in terms of variance. The stepwise values for wind speed have the form:

$$WS(t) = WS_{base}(t) + WS_{osc}(t) + WS_{noise}(t) \quad (3.1)$$

where $WS_{base}(t)$ is a linear term, $WS_{osc}(t)$ is a periodic term and the superimposed noise $WS_{noise}(t)$ is derived from the variance on wind speed σ_{WS} and a random value *rand* drawn from a uniform distribution over the interval [0,1].

$$WS_{noise}(t) = \sigma_{WS} * rand \quad (3.2)$$

As opposed to the 'Stochastic Wind' mode, simulations can be run in 'Steady Wind' mode i.e. wind speed and angle constant throughout a simulation. This feature is used to derive the yacht's polar curves for VPP comparison purposes. As well as the boat target speeds, the regime heel angles, leeway angles and the amount of weather helm can be calculated.

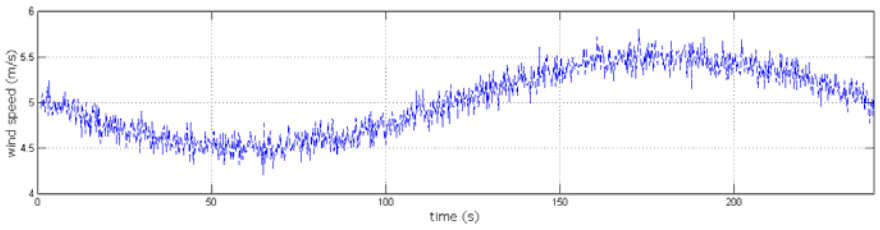

Figure 3-1: wind speed time history; T = 240s, mean=5m/s, σ=0.01

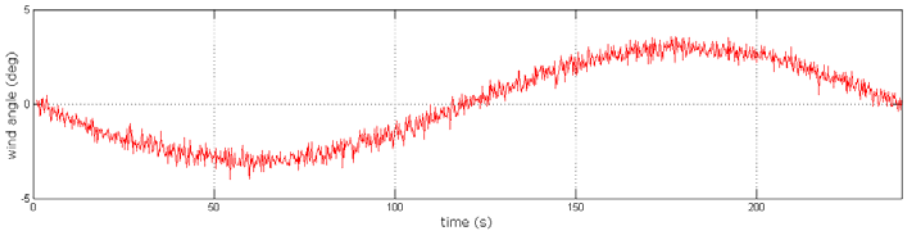

Figure 3-2: wind angle time history; T = 240s, mean=0deg, σ=0.1

3.3.4 The Graphical User Interface (GUI)

A GUI consisting in five consecutive pop-ups is available to the user for setting up and initializing the simulation. The graphical interface was entirely developed in MATLAB, through the dedicated 'GUIDE' tool. The pop-up opening process is driven by the 'PopUpManager' routine and is based on an intuitive breakdown of the simulator's features:

- Step #1: Scenario;
- Step #2: Crew;
- Step #3: Hull, appendages and rudder;
- Step #4: Rig and Sails;
- Step #5: Initialization.

As far as the yacht physics is concerned, the main features of the hull, appendages, rig and sailplan can be defined. Examples are the geometry and resistance of the canoe body, individual sail areas and sail coefficients, rig effective height, rudder lift and drag coefficients. However, due to cross-correlation of design parameters, some of these cannot be changed through the GUI; on the contrary, a major revision of the model would be required. For example, increasing the displacement would cause a gain in waterline length, waterline breadths and sectional area coefficients over the waterline. This would thereby affect the added masses and added moments of inertia of the yacht (see Appendix 1), with a direct influence on the equations of motion. Therefore, a clear picture of the hull hydrostatics must be available and a thorough revision of the yacht's model should be carried out. If not, the simulation results

would be biased and a poor, unrealistic performance prediction would be derived as a consequence.

3.4 Features of the virtual crew

An automatic crew has been implemented that is composed of three sub-systems, organized as shown in Table 3-2. The automatic crew has the task of sailing the yacht on a given racecourse, while minimizing the racing time. A set of basic strategical rules is used, in order to take advantage of any changes to the weather scenario. Details on the three sub-systems are provided in the following paragraphs.

Table 3-2: Virtual crew

Sub-system	*Input*	Output
Helmsman	*yacht state variables* *decisions of navigator*	$\delta, \dot{\delta}$
Sail Tailer		$\gamma, \dot{\gamma}$
Navigator	*yacht state variables* *racecourse* *tws, twa*	*decisions on:* *steering* *routing* *sail trimming*

3.4.1 Helmsman

An attempt to simulate human actions on a yacht rudder can be found in (Harris, 2005), where a proportional-derivative (PD) controller is implemented that controls the error between the actual heading and the target or 'setpoint' heading. Weather helm effect is accounted for by applying an open-loop rudder offset expressed as a predetermined function of true wind angle (*twa*). The PD controller is switched off while manoeuvering, when rudder position is being supplied as a function of time.

Several steering modes have been implemented here, in order to allow the yacht to sail an upwind-downwind racecourse. The '*awa-based*' mode is used for upwind and 'dead downwind' legs, when *beating* is necessary to reach the mark. The '*heading-based*' mode is used for reaching legs, when it is possible to sail to the

next mark without manoeuvering (i.e. tacking or gybing). Both steering techniques are based on Partial Integral Derivative (PID) controllers, whose gains have been adjusted to mimic actual time-histories of rudder angle. The reference formulae are Eqns. (3.3) to (3.6) where *awa* and ψ are the process variables and awa_{ref} and ψ_{ref} are the respective setpoints. The coefficients K_p, K_i and K_d are the controller gains for the proportional, integral and derivative terms. For both PIDs, the output is the commanded rudder angle δ.

$$\delta = K_p\left(awa - awa_{ref}\right) + K_i \int e_{awa}(t)dt + K_d \frac{de_{awa}(t)}{dt} \tag{3.3}$$

$$\delta = K_p\left(\psi - \psi_{ref}\right) + K_i \int e_{\psi}(t)dt + K_d \frac{de_{\psi}(t)}{dt} \tag{3.4}$$

where

$$e_{awa} = awa - awa_{ref} \tag{3.5}$$

and

$$e_{\psi} = \psi - \psi_{ref} \tag{3.6}$$

When used on upwind legs, the '*awa-based*' PID offers a straightforward, yet effective, model for tacking: the sign of target *awa* is changed and the PID lets the yacht tack around without exhibiting unrealistic overshoots.

Studies on the optimization of tacking are reported in the literature. For example, both (Harris, 2005) and (Masuyama *et al.*, 1995) show the considerable influence of the rudder time history on the overall tacking performance. Therefore, it was decided to implement a further option for tacking: switching the PID controller off and supplying the rudder angle δ as a function of *awa* across the tack.

3.4.2 Sail tailer(s)

Details on the sail inventory and the relative sail coefficients have already been provided in Chapter 2. As far as the virtual sail tailers are concerned, three options have been implemented:

Optimal

The sailplan's C_L and C_D are provided as a function of *awa*. Just as in VPPs, the apparent wind angle yielding the higher C_L/C_D ratio at the given windspeed represents the optimal course upwind. Since no human judgement is involved, this can be regarded as the optimal trimming mode.

Controller-based

The sailplan's C_L and C_D are provided as a function of the sheeting angle γ. In order to do so, the sailplan is modelled in terms of an equivalent mainsail, whose only trimming possibility consists in modifying γ, i.e. the boom angle with respect to the yacht's centreline. When the 'controller-based' mode is used, the sail trimming routine takes *awa* as an input and returns a value for the sheeting angle γ. Once γ is known, the sail angle of attack α is calculated out of *awa*, the yacht leeway β and γ through the formula below, based on the notation of Figure 3-3

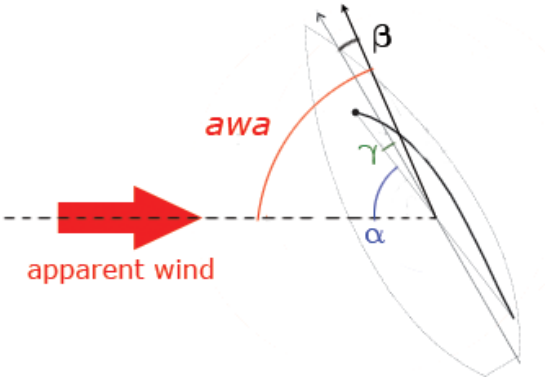

Figure 3-3: schematic of reference angles for the yacht

$$\alpha = awa - (\beta + \gamma) \tag{3.7}$$

$C_L(awa)$ and $C_D(awa)$ can then be calculated through lookup tables. Linear and non-linear monotonic $\gamma(awa)$ trimming 'rules' are adopted here: this is to say that sails are eased off as the apparent wind angle increases, for example when the helmsman bears away. This is consistent with basic sail trim techniques.

A PID for heel control purposes has been implemented alongside the 'controller-based' trimming model. The PID is required to take over in strong breezes, when the yacht is overpowered and sails should be eased off to reduce the sideforce and therefore the heel. A setpoint parameter φ_{ref} is used for the maximum acceptable heeling angle. The choice of such a threshold for the heel angle represents a further aspect open to human judgement.

Dual tailer for mainsail and genoa/jib

A further sail trimming model was implemented to simulate the independent trim of the headsail (jib or genoa) and mainsail on upwind legs. The underlying aerodynamic force model is that of the IMS-VPP, originally developed by Hazen (Hazen, 1980), that after several revisions can now be considered a 'widespread and robust sail model' (Krebber and Hochkirch, 2006). Such a model takes into account sail interaction effects, such as the upwash/downwash of individual sails or the headsail's influence on flow separation over the mainsail, a relevant issue when the flow is guided by the foresail onto the leading edge of the aft sail (Claughton, 2006).

Following the IMS-VPP, a conventional breakdown is used for the sail drag: the total drag coefficient $C_{D,TOTAL}$ is obtained as the sum of parasite drag and induced drag. The parasite drag is composed of a linear component $C_{D,P}$ and a quadratic component, or 'quadratic profile drag'.

Based on the IMS-VPP, the combined effect of two sails can be modelled with a superimposition of the individual sail coefficients of lift and linear parasite drag, as in Eqns. (3.8) and (3.9) below:

$$CL_X = \sum (CL_{Xi} B_i) w_i \tag{3.8}$$

$$CD_P = \sum (CD_{Pi} B_i) w_i \tag{3.9}$$

$$w_i = A_i / A_{REF} = A_i / \sum A_i \tag{3.10}$$

where i = 1,2 for the foresail and the mainsail respectively. B_i is a 'blanketing factor' supposed to be equal to 1 when sailing upwind, that is no blanketing effects are introduced in the model. The height of the aggregate center of effort for the sailplan is, again, derived from those of individual sails. In particular, weighting factors are used which take into account A_i and the individual force coefficients.
The judgement of individual sail tailers is accounted for through the sail trim parameters *reef* (r), *flat* (f) and *twist* (t), whose formulation is also derived from the IMS-VPP. The implications of the three coefficients and their influence on the yacht's performance are well documented in (Campbell, 1998), (Claughton, 1999) and (Krebber and Hochkirch, 2006). Suffice it to say that one advantage of an approach based on trim parameters is that sail forces and explicit features of sail trim are 'cleverly avoided' (Jackson, 1996).

Based on (Kerwin, 1978) and (Hazen, 1980), *reef* accounts for all crew actions aiming at a reduction of lift through a reduction of sail area. Other actions taken by the crew towards the reduction of lift, such as sail sheeting or adjustments to sail camber, are modelled through the *flat* parameter. An addition to the IMS-VPP, based on the *twist* parameter and adopted in 1999, is due to Jackson (Jackson, 1996). The effect of *twist* is a reduction in the heeling moment achieved by twisting off (unloading) the head of a sail at the cost of a higher induced drag. A proposal for the additional sail trim parameter *power* (p) is due to (Fossati, 2006).

$$CL_{TOTAL} = r^2 * f * CL_X \tag{3.11}$$

$$CD_{TOTAL} = r^2 CD_P + K_q (r * f * CL_X)^2 + \frac{A_{REF}(r * f * CL_X)^2}{(\pi {H_E}^2)} \tag{3.12}$$

Due to the hypothesis of linear superposition of forces, the aggregate value of the 'quadratic parasitic drag' coefficient K_q is the sum of those of the individual sails. K_q=0.016 is a good approximation for a mainsail-jib inventory (Poor and Sironi, 1990). The effective rig height H_E is normally taken as 110% of the geometric rig

height (masthead) when sailing upwind, then drops for apparent wind angles wider than 30° until the value of 100% is achieved for beam reach conditions.

According to Jackson's extension of the IMS-VPP, the vertical position of the centre of effort Z_{CE} is influenced by *r* and *t* and can be obtained from:

$$Z_{CE} = Z_{CE}^{opt} * r * (1 - t) \tag{3.13}$$

In the present model, the judgement of the sail tailer is modelled in terms of individual trimming response surfaces i.e. r(*awa*, *aws*), f(*awa*, *aws*), t(*awa*, *aws*) for each sail. These functions and correlations among them can be derived from VPPs and refined by simulations and questionnaires/interviews to sailors in order to identify what action are likely to be taken in response to a change in wind speed or angle (e.g. priority given to boatspeed over pointing ability or vice-versa). Artificial Intelligence-based models for sail tailing could be based on neural networks trained with the datasets above. Simulations based on the Monte-Carlo method or driven by a Design of Experiment test matrix are required, owing to the large number of design factors involved. An example of such investigations is provided in Section 3-7.

3.4.3 Navigator

The navigator module is the core of the control system and, as in real-life sailing, issues decisions that influence both the steering and the sail trim. Firstly, it checks the yacht position at each time-step of the simulation, detecting for example when a layline is hit or a mark has to be rounded. Secondly, it detects changes to the weather conditions and can issue strategical decisions accordingly (e.g. to tack on a windshift, as described below). The navigator sub-system also deals with manoeuvers: for instance, it issues the decision of tacking and detects when the boat has recovered from a tack (through attainment of surge speed target value) and when the next tack needs to take place. A list of the main features implemented by the navigator is provided below:

- To keep the boat within a given distance from the racecourse axis when sailing upwind. When the lateral boundaries of the racecourse are crossed, the situation is identified as too risky and a tack is called for.

- To tack in the event of an unfavourable windshift or 'header'. A 'header' is a windshift that forces the helmsman to bear away in order to keep sailing at a given awa_{ref}. Therefore, sailing on the 'headed' tack is disadvantageous, because the boat would have a lower speed towards the upwind mark.
- To tack onto laylines. A layline is a course leading directly to an upwind mark, for a given wind speed and wind direction.
- To check the boatspeed recovery after tacking, forbidding a further tack before a given percentage of the target speed has been achieved.
- To identify the most advantageous layline (e.g. the port tack layline if marks have to be rounded to port) when approaching an upwind mark. Windshifts would be neglected if they drove the boat away from the chosen layline.
- To sail directly to the upwind mark when the mark itself is within a given distance from the boat. If bearing away is required in order to do so, the '*heading-based*' steering mode is activated and the '*awa-based*'switched off.

Despite the basic set of strategic rules implemented, broad spaces for simulating human behaviour are present. One example is provided below:
Windshifts: when sailing in shifty wind conditions on upwind or dead-downwind legs, a considerable advantage can be obtained by sailing on the 'lifted' tack (i.e. the one that yields the higher boatspeed towards the mark). The decision of tacking when a boat is hit by a windshift is not trivial: the shift should be sufficiently large and stable to be worth the time loss of a tack. Risk-takers are supposed to tack as soon as the boat encounters an advantageous windshift, while running the risk that the wind might shift back soon. On the other hand, risk-averse sailors would sail the unfavoured tack longer, to make sure that the shift is stable.

3.5 VPP-based validation

As mentioned in Chapter 2, an initial validation of the dynamic model used for this Thesis was carried out by running Robo-Yacht alongside a commercial VPP. As reported below, the straight-line, equilibrium state variables predicted by Robo-

Yacht are consistent with those predicted by the well-established VPP code 'WinDesign', marketed and maintained by the Wolfson Unit MTIA.

Polar curves are probably the most significant output of VPP calculations, as they provide an overview of the yacht performance. In order to derive the polar curves of models supplied to 'Robo-Yacht', a dedicated routine has been implemented which is based within the iterative simulation mode 'MultiSim'. This allows the set-up of a three-dimensional test matrix, taking into account the following parameters:

1) windspeed,
2) sail inventory,
3) point of sail.

In order to derive the equilibrium state for a given windspeed, sail inventory and point of sail, (e.g. one point of the graph in Figure 3-4), a PID-based helmsman working in '*fixed heading*' mode has been used. Each Robo-Yacht run yields one experimental point of the 3d test matrix described above. After setting up the test matrix, at any given wind speed and sail inventory the PID is automatically given a setpoint heading. Irrespective of the setpoint heading, five to ten seconds are required to achieve the equilibrium condition, starting from a heading of 35 degrees and a vector of initial conditions for the state variables matching that for the 10 knots condition. A tolerance of ±.1 degree of heading was deemed accurate enough for the purpose.

The straight line, equilibrium speed of a yacht at all windspeeds and all points of sails is usually plotted in the form of polar curves. An example is given in Figure 3-4, where the polar for a true wind speed of 10 knots is plotted, based on simulations carried out with 'Robo-Yacht'. Such predictions are in good agreement with those of 'WinDesign' VPP, particularly for true wind angles below 40°, i.e. points of sail representative of upwind performance. Differences of speed below 1 knot were observed between 'Robo-Yacht' and 'WinDesign' predictions. This is well within the overall accuracy required for the human-in-the-loop simulations presented herein, and therefore no further revisions of the model were carried out for this stage. Larger differences in the surge velocity can be observed over 40 degrees,

but never in excess of 2 knots (approx 18% higher than the velocities predicted by the VPP).

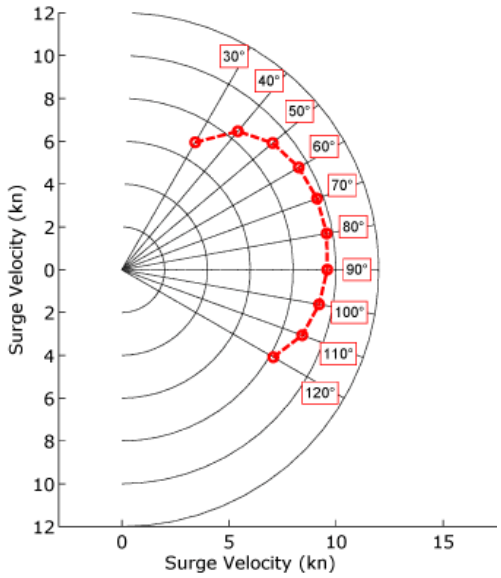

Figure 3-4: yacht polars, mainsail-genoa combination, 10knots true wind

In analogy with ordinary VPPs, the polars derived through 'Robo-Yacht' provide an insight into performance-related matters, such as the optimum upwind angle at any given windspeed, optimum downwind angle, spinnaker vs. gennaker performance and sails' crossover points.

3.6 Virtual Reality offline postprocessing

At every time step, the yacht state variables (yacht velocities, accelerations, leeway, heading, apparent wind speed and angle) are recorded, as well as the hydrodynamic and aerodynamic forces, rudder angle and sail trim parameters.

The above dataset can be supplied to a visualization routine, implemented in Simulink and connected to a Virtual Reality 'sink' in order to generate 'offline' animations. The use of Virtual Reality Modeling Language (VRML) allowed both

the modelling and the animation of the yacht motion within a 3D environment; this issue will be addressed in Appendix 2.

The choice to postprocess results in the form of animations as well as graphs, was made to provide sailors with a visual feedback on the yacht accelerations, heading, heel, rudder movements and sail trim. Also, the Simulink routine was designed to postprocess several solo-races at once and therefore visualize 'drag races' (i.e. relative to a same course and wind pattern, but without mutual interactions between yachts). The use of 'drag races' allows the highlighting of positive and negative aspects of the race strategy implemented by the automatic crew, as the simulation proceeds on (Figure 3-5). 'Drag races' are indeed a powerful training tool for the improvement of technical skills (i.e. driving style, sail trim) and race strategy.

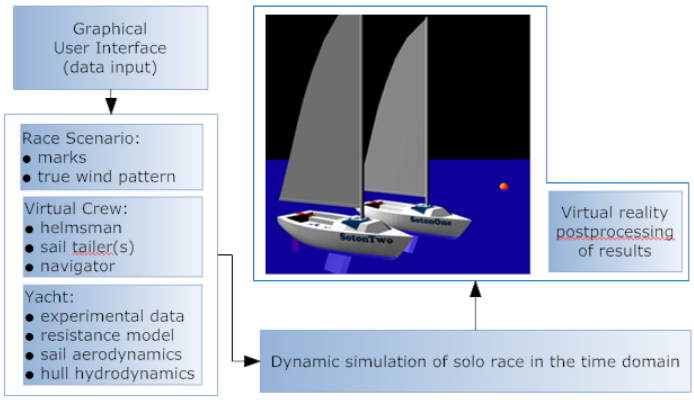

Figure 3-5: flow chart of Robo-Yacht simulations for 'drag-races'.

3.7 Example of Robo-Yacht simulation

A typical Robo-Yacht simulation is presented below, in order to clarify the inputs, stepwise outputs, global outputs and data postprocessing, as well as the settings and behaviour of the automatic crew. The reference yacht for the simulation is the IACC 'M566', whose features are described in Chapter 1 and Appendix A1.

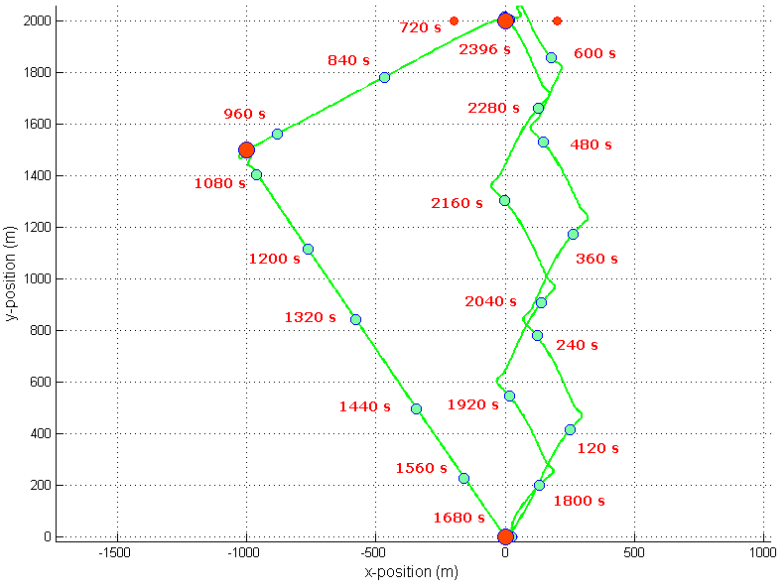

Figure 3-6: yacht track for 3.7Nm solo race

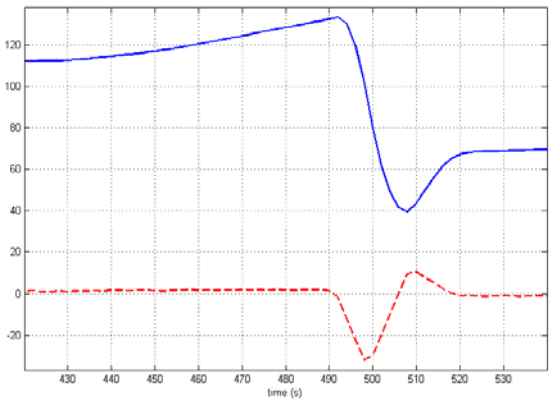

Figure 3-7: upwind leg no.1, tack no.4: tracks for heading angle (solid blue line) and rudder angle (dashed red line)

Racecourse and simulation timing: A course of 3.7Nm is considered, with two upwind legs and two broad reaching legs. All marks have to be rounded on port. The solo-race starts at t_0=0, the Robo-Yacht (RY) being positioned in the origin of the earthbound reference frame Oxy. The finishing line is square to the average wind direction, 400m wide and positioned at the end of the second upwind leg. A time step of 0.2 seconds is used for the simulation.

Initial conditions: The state variables are initialized with the steady state values at 10kn windspeed and a heading ψ_0 = +35°, on port tack. The yacht is initially required to reach a steady state sailing condition, which is based on the stabilization of *awa*(t). In particular, the average absolute deviation of the 20 most recent *awa* observations is calculated and compared to a target angle of (awa_{ref} ± 0.01) degrees. Similar steady-state conditions are applied after tacking, so that further tacks are not allowed unless the boat is sufficiently close to her target speed and target *awa*.

Weather: the oscillating wind conditions of Table 3-3 are used, whose symbols are consistent with Eqns. (3.1) and (3.2).

Table 3-3: wind conditions for demo race

<table>
<tr><td>WS_{mean}</td><td>5m/s</td><td>WA_{mean}</td><td>0°</td></tr>
<tr><td rowspan="3">WS_{osc}</td><td>period = 360s</td><td rowspan="3">WA_{osc}</td><td>period = 240s</td></tr>
<tr><td>ampl = 0.1m/s</td><td>ampl = 15°</td></tr>
<tr><td>phase = 0.0</td><td>phase = 0.0</td></tr>
<tr><td>σ_{WS}</td><td>0.001</td><td>σ_{WA}</td><td>0.01</td></tr>
</table>

Helmsman: an awa_{ref} of 22° is used for both upwind legs. The PID gains for the helmsman in *awa-based* mode (i.e. upwind legs) are K_p = 1; K_i = 0.1; K_d = 0.01. The above gains are also used for the *heading-based* mode (i.e. reaching legs, upwind laylines). Tacks are driven by the *awa-based* PID. The tracks for the yacht's heading angle and the rudder angle are shown in Figure 3-7, between t_1=420 and t_2=540. The interval [t_1, t_2] is relative to tack no.4, upwind leg no.1, onto port. For t_1<t<490s, the heading angle gradually rises as a consequence of the yacht being headed by a

windshift. The rudder track shows a little amount of weather helm, as expected. Then the windshift amplitude becomes 'critical', based on the navigator's settings, the helmsman comes up suddenly ($\delta \sim 28°$), tacks and eventually achieves a new heading of approximately 70°. The PID yields a 35% overshoot on the rudder angle in the second part of the manoeuver: this is due the dominance of the proportional and integral parts on the derivative part. The latter feature can be used to model the behaviour of a helmsman that exceeds in the use of the rudder (in terms of angle and time). Two overshoots can be observed in Figure 3-6 at mark roundings (t~=700s and t~=1000s). In the first case, the reason is the *heading-based* PID taking over for the next reaching leg: a large error is 'seen' between the present heading and the setpoint and therefore large commanded rudder angles are issued. This can either be sorted by limiting further the maximum rudder angle allowed or using anti-wind up PID algorithms. Similar considerations can be made for the overshoot experienced while gybing.

Sail tailers: the sail inventory is composed of a mainsail, a genoa (upwind legs) and a gennaker (downwind legs). Sails are trimmed through the 'dual sail tailing model' described in Section 3.4.2. Sensitivity studies were carried out to investigate the influence of sail trim parameters r,f,t on the upwind performance. Based on results described in Section 3.8, the use of [r,f,t] = [1.0, 1.0, 1.0] was deemed appropriate for a base wind speed of 10kn.

Navigator: the navigator carries out the race strategy based on four rules of thumb. The primary goal for the upwind leg consists in sailing the lifted tack. A threshold of ±5° is used for the wind direction, so that wider windshifts would trigger a tack unless the boat is recovering from a previous tack. Secondly, the navigator is in charge of detecting laylines, and triggering a tack in close proximity of a layline (e.g. t=580s, upwind leg one). Based on past wind observations and the navigator's judgment, a tack onto a layline can be triggered earlier than the crossing (when a header is expected) or delayed (when a lift is expected, to avoid further tacks). Thirdly, in order to minimize risk in the event of a major windshift, the navigator

does not allow excessive lateral separation between the boat and the racecourse axis. A threshold of 500m is used for the present simulation. Lastly, the navigator is in charge of switching between steering modes (*awa-based* or *heading-based*) when the race strategy requires doing so. For example, the *heading-based* mode is activated while sailing directly towards an upwind mark and a windshift allows sailing to the mark at an $|awa| > awa_{ref}$.

Stepwise outputs: a dataset for t=340s, corresponding to a condition of aero-hydrodynamic equilibrium, is reported in Table 3-4 below. The dataset includes the yacht state variables, bundled in the structure 'strYachtState' and local wind observations, bundled in the structure 'strLocalWind'. All routing information is bundled in the structure 'strNavInfos': these are not displayed In Table 3-4 since no strategical decisions were about to be made at the time step considered. This has been done to encapsulate the code appropriately and to simplify the information exchange between the various modules of Robo-Yacht, including the automatic crew.

Table 3-4: stepwise outputs for Robo-Yacht

Tack	Port	*tws*	5.13 m/s
x	184 m	*twa*	37.9°
y	1102 m	*aws*	8.65 m/s
u (surge vel.)	4.14 m/s	*awa*	-22.07°
v (sway vel.)	0.17 m/s		
λ (leeway)	2.32°		
ψ (heading)	59.8°		
φ (heel)	19°		
δ (rudder angle)	-2.1°		
VMG	3.49 m/s		

3.8 Test Case no.1: influence of trim parameters on upwind performance

A test case is set up to evaluate the influence of sail trim parameters *reef* (r), *flat* (f) and *twist* (t) over one upwind leg. The scenario is summarized in Table 3-5.

Table 3-5: scenario and settings for Test Case no.1

Wind	tws = {3,5,7,9} ± 0.5 m/s, T_{tws}=120s, twa = ± 5°, T_{twa}= T_{tws},
Course	*solo race, upwind course,* *two marks 0.5Nm apart, axis North-South*
Helmsman	*'awa-based' PID,* awa_{ref} *= 22°*
Sail Tailer(s)	*'dual', test matrix for r,f,t*
Navigator	*rule-based*

Using the 'MultiSim' option of the sailing simulator, a test matrix was set up where both reef and flat were varied over eleven levels (0.5 to 1.0 with .05 increments) for the four windspeeds of Table 3-5, while the sail twist was kept constant at 1.0. Furthermore, owing to the stochastic nature of the wind speed and angle, a range of variances were explored both for the wind speed and for the wind angle. For each simulation, the initial conditions are the regime values of the yacht state variables for the windspeed concerned, at the heading ψ_0=35°. Each race starts on Mark #1, with the yacht on port, and ends once Mark #2 is about to be rounded on port, that is Mark #2 is seen at amidships by the yacht sailing on the port layline. All results are presented in terms of time around the course.

The response surface of Figure 3-8 shows the Race Time (RT) as a function of *reef* and *flat* for the case tws_{avg} = 7m/s. Although two local minima can be encountered at (r, f) = (0.6, 1.0) and (r, f) = (1.0, 0.8), the settings yielding the minimum values for RT are positioned around (r,f) = (0.9, 0.88). This suggests that a simultaneous reduction of both r and f is the way to minimize RT as the wind picks up.

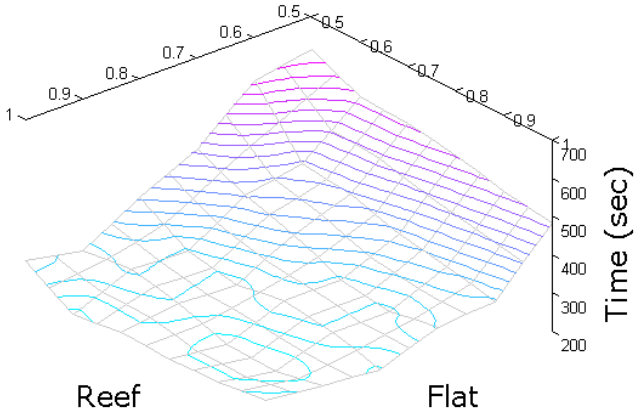

Figure 3-8: response surface for RT(r,f) at t = 1.0, tws_{avg} = 7m/s

Figures 3-9 and 3-10 show the influence of twist on RT for a tws_{avg} of 5m/s; for each case, the optimal (r,f) combination is also highlighted. When t=1.0, a minimum RT of 277s can be achieved when sails are neither reefed not flattened; this is reasonable, given the moderate breeze considered.

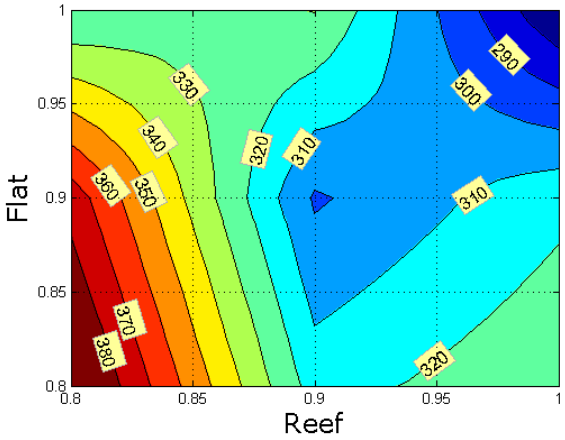

Figure 3-9: contour plots for RT(r,f) at t = 1.0, tws_{avg} = 5m/s

On the other hand, if sails were twisted (t=0.8), higher RTs are to be expected and even for the optimal combination of *reef* and *flat* (r,f) = (0.92, 1.0) a gap in excess of 10 second is predicted between the twisted and the untwisted case.

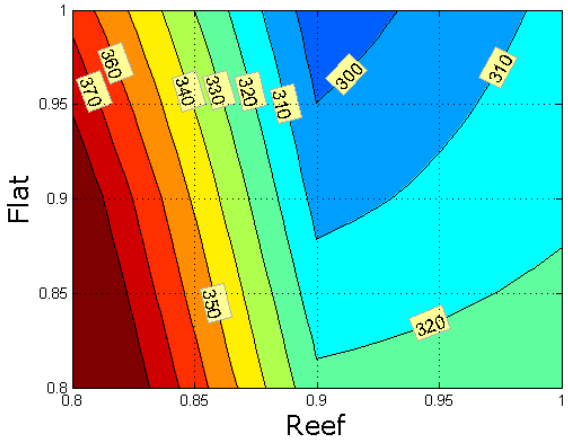

Figure 3-10: response surface for RT(r,f) at t = 0.8, tws_{avg} = 5m/s

It should be borne in mind that, as the wind period T is a constant, the frequency of windshifts is the same at all windspeeds. Therefore, as shown in Figure 3-11a, a larger number of tacks due to headers is expected at low average windspeeds. So, the effect of sub-optimal combinations of trim parameters (i.e. low boatspeeds) is somewhat amplified.

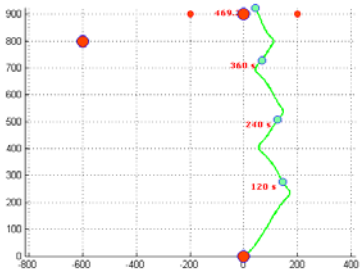

Figure 3-11a: yacht tracks, tws_{avg} 3m/s

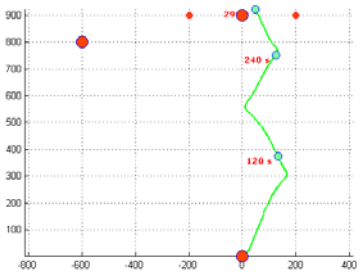

Figure 3-11b: yacht tracks, tws_{avg} 5m/s

3.9 Test Case no.2: sensitivity studies on helmsman models

A systematic analysis was carried out with Robo-Yacht, in order to assess the influence of the rudder angle $\delta(t)$ on tacking performance. The use of an *awa*-based PID controller ('PID-assisted mode') was compared with the use of prescribed time histories for the rudder ('prescribed δ mode'), in a range of wind speeds. It was found that the PID-based rudder control yielded the best performance in terms of speed recovery, as well as limiting the speed loss. When tacking in 'prescribed δ mode', the use of large rudder angles first (that is, when coming up) proved to be beneficial: limited speed losses were observed and a performance close to that of the PID was achieved. When tacking in 'PID-assisted mode', peaks of δ in the region of 60% of the maximum allowed rudder angle were not uncommon. This result is consistent with considerations in (Masuyama *et al.*, 1995), where the use of large rudder angles in the first stages of a tack proved to be advantageous.

Wind speeds of 4, 5 and 6 m/s were considered for the present investigations. The gains used for the *awa-based* PID controller were K_p=1.0, K_i=0.01 and K_d=0.1; these derive from a tuning process focused on tacking performance, as well as on accuracy in achieving the prescribed setpoint. Considerations by (Harris, 2002) on avoiding an 'unrealistic' helmsman modelling (e.g. high frequency oscillations for the rudder angle) were also taken into account. In Figure 3-12, the prescribed rudder angle for the tack is plotted over a [0;1] domain, where '0' is the yacht's heading prior to tacking and '1' is the target heading at the end of the manoeuver (i.e. the heading that corresponds to awa_{ref} for the given wind speed). The tacking simulations were designed so that a switchover between the 'PID-assisted mode' and the 'prescribed δ mode' would occur automatically, within a 15° tolerance from the final heading.

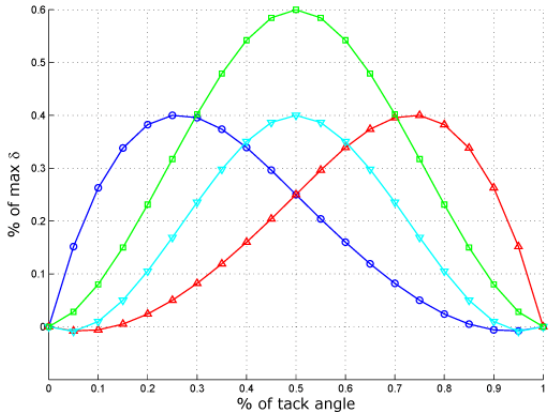

Figure 3-12: rudder angle tracks for 'prescribed δ' mode

The monitored parameters were: u_{start} (surge speed at the beginning of a tack), u_{min} (minimum surge speed across a tack), t_{90} (time interval to recover 90% of u_{start}). Simulation results are plotted in Figure 3-13.

The present sensitivity study shows that the 'PID-assisted mode' generally yields the fastest speed recovery. For the case of *twa* = 4m/sec, the 'PID-assisted' tack is as effective as the one controlled by the 'come up peak' steering style. In the latter case, a close matching is observed between the two time histories $\delta(t)$ for a generic tack. The other three models yield similar results and, all in all, show a poor tacking performance.

In conclusion, this sensitivity study shows that the amount of rudder angle used when tacking has a great impact on the 'quality' of the tack itself. This is a further example that using correct models for crew-yacht interaction is crucial for the estimate of the yacht's overall performance.

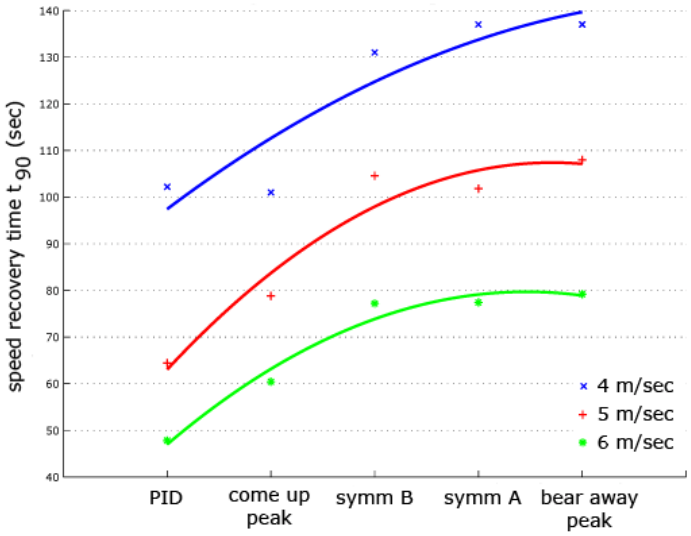

Figure 3-13: t_{90} for a range of steering models and windspeeds

3.10 References

Moler, C., 'The origins of MATLAB', MATLAB News &Notes, December 2004, visited on September 1st, 2007. http://www.mathworks.com/company/newsletters/news_notes/clevescorner/dec04.html

Campbell I.M.C., 'The performance of offwind sails obtained from wind tunnel tests', Proc. of R.I.N.A. International Conference on the Modern Yacht, pp. 89-102, 1998.

Claughton, A.R., 'Developments in the IMS VPP Formulations', Proc. of The 14th CSYS, pp. 1-20, 1999.

Claughton, A.R., Oliver III, J.C., 'Developments in hydrodynamic force models for velocity prediction programs', Proc. of R.I.N.A. International Conference on the Modern Yacht, pp. 67-77, Southampton, UK, 2003.

Claughton, A.R., Wellicome, J.F., Shenoi, R.A., 'Sailing Yacht Design: Theory', University of Southampton, ISBN 0854328297, pp. 40-41, 2006.

Harris, D.H., 'Time Domain Simulation of a Yacht Sailing Upwind in Waves', Proc. of The 17th CSYS, pp. 13-32, 2005.

Harris, D.H., 'Simulation of upwind manoeuvering of a sailing yacht', PhD Thesis, University of Maryland, 2002.

Hansen, H., Jackson, P.S., Hochkirch, K., 'Real-time velocity prediction program for wind tunnel testing of sailing yachts', Proc. of R.I.N.A. International Conference on the Modern Yacht, pp. 67-77, Southampton, UK, 2003.

Hazen, G.S., 'A model of sail aerodynamics for diverse rig types', Proc. of New England Sailing Yacht Symposium, 1980.

Kerwin, J.E., Newman, J.N., 'A summary of the H. Irving Pratt Ocean Race Handicapping Project', Proc. of the 4th CSYS, 1979.

Keuning, J.A., Vermeulen, K.J., de Ridder, E.J., 'A generic mathematical model for the manoeuvering and tacking of a sailing yacht', Proc. of The 17th CSYS, pp. 143-163, 2005.

Krebber, B. and Hochkirch, K., 'Numerical investigation on the effect of trim for a yacht rig', Proc. of the 2nd High Performance Yacht Design Conference, Auckland, 2006.

Lewis, E.W., 'Principles of Naval Architecture', SNAME, 1988.

Masuyama, Y., Fukasawa, T., Sasagawa, H., 'Tacking simulations of sailing yachts - numerical integration of equations of motions and application of neural network technique', Proc. of The 12th CSYS, pp. 117-131, 1995.

Masuyama, Y., Nakamura, I., Tatano, H., and Takagi, K., 'Dynamic performance of a sailing cruiser by full scale sea tests', Proc. of The 11th CSYS, pp. 161-179, 1993.

Perry, D., 'Winning in One-Designs', 3rd ed., US Sailing, ISBN 1-882502-78-7, 2000.

Philpott, A., Henderson S.G., Teirney, D.P., 'A simulation model for predicting yacht match-race outcomes', Operations Research, 52(1), pp. 1-16, 2004.

Poor, C.L. and Sironi, N., 'The International Measurement System', Proc. of the 11th HISWA Symposium on Yacht Design and Yacht Construction, 1990.

Roncin, K., 'Simulation dynamique de la navigation de deux voiliers en interaction', PhD Thesis, Laboratoire de mécanique des fluides, ECN, 2002.

Rousselon, N., 'Prediction of hydrodynamic and aerodynamic forces and moments for use in a 4 DoF simulation tool, using a lifting surface panel code', MSc Thesis, Ship Science, University of Southampton, 2005.

CHAPTER 4

DECISION MAKING MODELS AND YACHT RACING

Nomenclature

[Symbol]	[Definition]
WADD	Weighted Additive rule
EQW	Equal Weights rule
LEX	Lexicographic rule
TTB	Take The Best rule
SAT	Satisficing rule
MCD	Majority of Confirming Dimensions rule
RAND	Random choice rule
EIP	Elementary Information Processing units
EV	Expected Value
DMG	Distance Made Good

4.1 Generalities on decision making

Modern sailors are required to possess a wide spectrum of skills: technical abilities, athletic performance and the 'talent' of making the right decisions at the right time under severe psychological pressure. The latter aspect is emphasized in one-design classes, such as Olympic dinghies and keelboats, where little differences in boat performance are present, yielding close races and tight winning margins. As well as for one-designs, this can also be observed when a mature Rule is in force, such as the ACC Rule Version 5.0: in the 32nd America's Cup well-established design solutions could be observed in terms of hullforms and appendages, presumably with little scope for further optimization.

In the light of the above considerations, the importance of the human factor is emphasized. For example, the development of a good strategic plan before the race start can often make the difference, as well as the ability to modify such a plan when required by race tactics or when changes in the weather scenario occur. Recent studies in the Sport Psychology domain have partially clarified this point. As

reported in (Rulence-Paques *et al.*, 2005), athletes' knowledge base is apparently structured and organized in decision-making schemata, whose 'quality' is likely to affect performance. Further studies emphasize the relationship between sailing expertise and decision-making skills, by pointing out that experimental evidence exists that 'best sailors' function 'as better decision-makers' (Araùjo *et al.*, 2005). For the purposes of the present Chapter, sailors are indeed considered as decision-makers, gambling on the weather scenario, making guesses on payoffs offered by strategical choices and, eventually, deciding by trading off costs and benefits. In addition, it should be considered that regattas are 'high-velocity' environments: scenarios evolve quickly and delaying a decision, either a good or a poor one, can result in a loss. Sailors are therefore pressured by time stress, which can conveniently be modelled in terms of opportunity-cost time pressure: with this purpose, results of past research on effort-accuracy frameworks are referred to in the next Sections.

4.2 Decision Making investigations in Sport Psychology

4.2.1 Cue pick-up and information processing: novices vs. experts

It is claimed by Sport Psychologists that when uncertainty-rich contexts are considered, skilled performers are often characterized by effective decision-making strategies. Studies by Abernethy focused on decision making issues in fast ball sports such as tennis. For example, a well-known paradox is addressed in (Abernethy, 1991): the time required by a successful decision-making process, based on ball flight information and under the temporal constraints defined by the competitive context, can be considerably shorter than tennis players' reaction time (RT). Therefore, a reduction of RT is presumably achieved by decreasing the total amount of information to be processed. These improved strategies are likely to be based on advanced usage of *cues* such as early movements of opponents' arm and racquet. Furthermore, experimental research has shown substantial similarities in the visual search strategies of both expert and novice players, but differences in the information pick-up process for the two groups. As pointed out by Abernethy,

‘looking does not, in itself, guarantee useful information pick-up’; therefore, novices are unlikely to develop decision-making strategies typical of experts by being instructed on which cues to pick up. These theories raise issues on the attentional cost of decision-making**.** Published evidence exists (Bard *et al.*, 1994) that the speed of operation of perceptual system is the same for novices and experts. However, skilled athletes can obtain better performances by relying on memorized schemata rather than being driven by stimuli as novices are. An expert athlete can therefore be regarded as a ‘powerful communication system’ (Bard *et al.*, 1994), able to process efficiently chunks of information picked up from the environment and to trigger movements accordingly.

4.2.2 Information processing: the ‘ideal athlete’.

Definitions:

‘Signal’	any relevant information appearing in the environmental field and requiring either a motor and a non-motor attentional response;
‘Noise’	irrelevant information provided by the environment.
Attentional flexibility	ability to quick disengage, orient and engage attention on various locations in space.

Considerations reported in (Nougier *et al.*, 1991) yield the definition of ‘ideal athlete’, from a psychological standpoint. Expert athletes are able to deal with information either in an ‘attentional processing mode’ or in an ‘automatic processing mode’; the latter is mainly based on athletes’ past experience and skills developed by means of training. According to the complexity of the task, experts can switch from the first mode to the second and vice-versa. Visual attention is compared to a ‘spotlight’, by means of which a selective exploration of the environment can be carried out. In order to provide a definition of ‘ideal athlete’, the definition of ‘ideal observer’ is required. Similarly to a powerful computer, the ‘ideal observer’ has unlimited attentional resources: therefore there are no limits to the amount of information that can be processed. However, since performance is directly related to the quality on information received, a poor level of performance is to be expected

when the information is partial or wrong. Similarly to the ‘ideal observer’, an ‘ideal athlete’ has no attentional limitations and is expected to realize a good performance as long as the information received is meaningful. Conversely, when wrong or incomplete information is provided, the ‘ideal athlete’ can operate as a ‘very efficient decider’ by simultaneously suppressing noise and mobilizing powerful attentional resources.

A classification of athletes is therefore possible, based on the breadth and depth of the information they can collect. However, studies reported in (Ripoll, 1991) highlight that stress and time pressure should also be considered when athletes’ performance is investigated. For this purpose, Ripoll takes into account a ‘semantic visual function’ (identification and interpretation of the situation in which the athlete participates) and a ‘sensorimotor visual function’ (whose task is to carry out the visuo-motor response). Ripoll draws different conclusions for ‘open sports’ (when time pressure or uncertainty or both are imposed externally such as for athletics or gymnastics) and ‘closed sports’ situations (where all the events likely to occur are predictable such as for skiing and on-sight rock climbing). Sailing is explicitly classified as an open, externally-paced sport: according to Ripoll, no elements of uncertainty are conveyed by the opponent, since the decision-making process only deals with the route to be followed and with the quickest way to complete the course itself. Therefore, no further information is added as the subject is actually performing the task: the quantity of uncertainty is referred to as ‘closed’. It is evident that, in the case of modern sailing, the interaction with opponents (race tactics) is just as important as that with the environment (race strategy) and therefore such classification is debatable. When open sports are considered, the semantic and sensorimotor processing seems ‘to be serially organized’; this is to say that an athlete under time pressure, may choose to focus on the semantic function (therefore using the maximum allocated time to identify the situation and selecting the most adequate response) or on the sensorimotor function (processing incomplete information and selecting an inadequate response). In this context, an ‘understanding-acting trade-off’ is likely to occur: this is to say that time pressure calls for a decision-making process that ideally should be either correct (semantic

function) and fast (sensorimotor function). The test case of Section 4-5 is indeed focused of measuring the effectiveness of this trade-off process.

4.2.3 Decision making schemata.

The skills of professional batsmen are investigated in (McLeod & Jenkins, 1991). These athletes are capable of hitting a fast ball in a time which is less than 200 msec (average reaction time of normal subjects, according to laboratory tests) and to achieve timing accuracies in the region of 2 msec. The reasons for such a paradox can be summarized as follows: on the one hand, extensive training can help athletes to develop extremely precise motor patterns while on the other hand, practice helps players to develop 'game-related schemata' where the background of experience relative to a given game context can allow a prediction of 'likely outcomes in similar situations in the future'. So, extensive practice at a given sport can help players to develop 'perceptual schemata' that, in turn, allow players themselves in understanding, remembering and predicting the outcome of specific game situations.

It was mentioned in Section 4-1 that athletes' behaviour relies on decision-making schemata whose quality depends on expertise. In particular, recent research by (Rulence-Paques *et al.*, 2005) on footballers highlight that players' decisions appear to be driven by informational cues (e.g. current score or team status) combined through simple algebraic rules. It is also suggested that a rule-based approach to decisions is extremely likely to be used under stress and time pressure. For example, a test is reported in the paper where players were asked to judge the outcome of a quick restart of play in different situations, that is for various sets of factor combinations (e.g. numerical superiority/equality/inferiority or when losing/tie/winning). The analysis of variance allowed the identification of the most influential factors, relatively to three different sports (soccer, basketball and handball) and, also, the identification of combination rules between such factors. It was concluded that simple algebraic rules (i.e. combination of cues) can model conveniently the decision-making schemata driving players' actions.

4.2.4 Adaptive behaviour.

A further distinctive behaviour of many top-range athletes, either in individual and team sports, is the largely stable level of performance they exhibit whatever the opponent. It is unclear whether such stability is due to a constant style of playing, irrespective of the opponent, or to the experts' ability of adapting the athletic response to given competitive contexts. Research by (Mc Garry and Franks, 1995) is focused on squash competitions, with the purpose of identifying players' profiles and persistent playing patterns at different levels of expertise. Statistical tools are being used to demonstrate that a player's profile (e.g. shot response against the same opponent or different opponents) is likely to change within a match in order to adapt to the competitive environment. Mc Garry and Franks claim that a game-theoretic approach could clarify the adaptive response of players, which often aim at minimizing the opponent's gains while maximizing their own score.

Other sport psychologists support the hypothesis that adaptive behaviour can be considered a 'trademark' of experts. For example, it is claimed in (Saury and Durand, 1988) that sailing coaches behave adaptively when facing complex situations: these individuals are likely to recall decisional patterns when highly uncertain situations occur. The tasks and the constraints of a sailing coach are highlighted, focusing on the methods and the strategies adopted to minimize the impact of uncertainty due to unpredictable changes of environmental conditions. Data were gathered by the Authors during five training sessions and by interviewing coaches. When dealing with ever-changing weather conditions, the main issue is setting a correct task timing: any reactions based on a past state of the environment is likely to have negative consequences, since it could be no longer suitable for the present state. Expert coaches, instead, make use of both standard routines and flexible training plans, which is presumably the best strategy for dealing with the 'dynamic nature' of the context. Another interesting feature of coaches' decision-making strategies is the capability of reacting quickly, after a 'superficial analysis of the events', in order to avoid the risk of reacting too late (e.g. to a major windshift). Presumably, this is due to the fact that coaches involved in the present study had all been top athletes themselves: their wide practical experience can therefore support

them in making complex decisions quickly. According to the Authors, such knowledge may be 'stored in the form of contextualized directories of diagnostics and operational acts'.

The above findings are particularly relevant for this Thesis, as they support the possibility of implementing behavioural models for sailors in terms of rule-based choices and decision-making trees. Computer simulations based on the above models could therefore take into account factors such as individual judgment and expertise.

4.3 Formulation of a decision making problem

A well-established method to formulate and investigate a decision-making problem is the use of a decision matrix. As shown in Table 4-1, such a matrix is composed of *m* rows, the alternatives A_1, A_2,…, A_m and *n* columns, the scenarios S_1, S_2,..., S_n. In addition, a probability distribution P_1, P_2,..., P_n can be associated with S_1, S_2,..., S_n, P_j being the probability that outcome S_j occurs. The matrix is arranged in a way that, when A_i is the selected alternative and scenario S_j occurs, the decision maker is 'rewarded' with a payoff $C_{i,j}$.

If a 'normative' decision-making strategy is considered, the most rewarding alternative is the one yielding the largest expected payoff E_i, whose formulation is that of Eqn. (4.1). It is supposed that the alternative showing the higher expected payoff will be preferred by the decision maker and, therefore, chosen.

Table 4-1: General formulation of a decision making problem

	S_1	S_2	…	S_j	…	S_n
	P_1	P_2	…	P_j	…	P_n
A_1						
A_2						
…						
A_i				$C_{i,j}$		
…						
A_m						

$$E_i = \sum_{j=1}^{n} P_j C_{i,j} \tag{4.1}$$

The above results refer to a linear relationship between payoff and utility, in the sense that an alternative yielding twice the payoff is also twice as 'desirable'. However, experience shows that doubling an expected payoff (i.e. a sum of money) does not necessarily result in doubling the attractiveness of the payoff itself. As an example, D. Bernoulli (1738) asserted that a plausible relationship between a sum of money and its expected utility is a logarithmic function, which involves a quickly decreasing marginal utility. In particular, when the individual attitude towards risk is taken into account, such a relationship may be of a non-linear nature and choices are likely to be driven by the maximization of expected utility (Kelly, 2003).

Following the classical von Neumann-Morgenstern formulation, the expected utility value U_i of a choice A_i can be defined as:

$$U_i = u(A_i) = \sum_{j=1}^{n} P_j u(C_{i,j}) \tag{4.2}$$

where $u(C_{i,j})$ represents the utility value associated with the payoff $C_{i,j}$.

It is important to note that the exact relationship between the generic payoff $C_{i,j}$ and the corresponding utility $u(C_{i,j})$ is debatable. However, it is widely accepted that different models should be chosen, according to a decision maker's own 'attitude' towards risk. Three prototypical attitudes are usually modelled in literature: neutral, risk-averse/conservative and risk-taking/adventurous; these correspond to Eqns. (4.3.a), (4.3.b) and (4.3.c) respectively.

$$u(C_{i,j}) \propto C_{i,j} \tag{4.3.a}$$

$$u(C_{i,j}) \propto \sqrt[n]{C_{i,j}} \tag{4.3.b}$$

$$u(C_{i,j}) \propto \left(C_{i,j}\right)^n \tag{4.3.c}$$

Readers are referred to (Kelly, 2003) for an insight into concepts and implications of the expected utility theory.

4.4 Implementation of a decision making model under weather uncertainty

Sailing races present many dilemmas of a strategical and a tactical nature. This is particularly so for upwind legs, open-outcome contexts where considerable gains and losses often result from one or two key decisions only. The skills of the strategist and the insight of the navigator are crucial for a successful upwind performance.

Due to the physics of sailing, a yacht cannot sail to an upwind mark in a straight line: its course must be at an angle top the local wind direction and must necessarily include manoeuvres or ‘tacks’. Tacks may involve a considerable speed loss, since sails do not generate lift at small angles of attack. When racing in oscillating wind conditions, the timing of tacks is often synchronized with the timing of shifts of the wind direction. In fact, when the wind direction and the racecourse axis are not parallel, sailing on the lifted tack yields higher boatspeed towards the mark. The effects of a windshift on two yachts sailing upwind is shown in Figure 4-1.

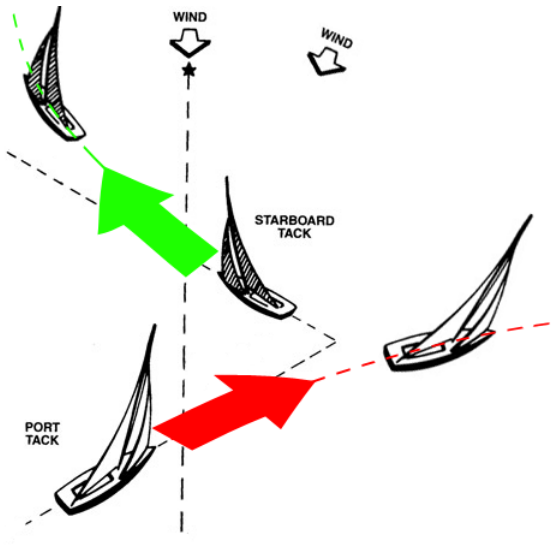

Figure 4-1: Effect of a windshift on two yachts beating upwind

A dilemma often encountered when sailing upwind is indeed related to a correct estimate of windshifts: only if the shift is sufficiently large and stable enough, does the expected rewards of tacking overcome the time loss. A decision-making problem is investigated below where the risks and rewards of tacking are addressed in the case of four different wind patterns.

4.4.1 Description of test case and decision matrix

A test case is investigated where an IACC yacht is racing solo against the clock. Its dynamic model is based on the 'M566' design, already described in Chapter 1. The environmental conditions are characterized by flat water, variable wind direction and a constant wind speed of 4 m/s. The course is a two miles upwind leg with two marks: No.1 and No.2. The race starts at Mark No.1 at time t_0 = 0 and boats are required to 'beat' up to Mark No.2 (the 'upwind' Mark) while minimizing the racing time by taking advantage of wind shifts. The maximum time allowed for the race is t_{end} = 800s. The boat handling models (e.g. PID controller gains for the helmsman) and the tacking technique are constant throughout the race, in order to reduce the number of simulation parameters.

Between t_0 = 0 and t_1 = 120s, the boat achieves a state of aero-hydrodynamic equilibrium while sailing in a steady Northerly breeze. During this stage, the yacht sails 'on port' i.e. with the wind hitting the left-hand side of the hull first. After t_1, the automatic navigator takes over and has the possibility of triggering a tack onto starboard (i.e. with the wind hitting the right-hand side of the hull first).

At time t_2= 200s, the True Wind direction shifts towards East by 10° (+10° header). A decision-making problem therefore arises, which can be investigated through decision matrices as pointed out in Section 4.3. Three alternatives (Table 4-1: *m*=3) are considered for the present case: tacking immediately onto starboard (A_1), not tacking unless further windshifts occur (A_2) and delaying the tack by 60 seconds (A_3). Four possible weather scenarios or 'outcomes' are set (Table 4-1: *n*=3): these are referred to as S_1 to S_4 and the respective patterns are highlighted in Table 4-2 below.

Table 4-2: List of outcomes

Scenario 1 S_1	True Wind Speed and True Wind Angle constant from t_2 = 200s onwards;
Scenario 2 S_2	True Wind shifts further right (additional +10°, i.e. a header for port tackers) at t_3 = 320s;
Scenario 3 S_3	True Wind shifts back North (-10°) at t_3 =320s;
Scenario 4 S_4	True Wind shifts back North (-10°), at t_3 =320s, then further left by -10° at t_4 =440s.

As pointed out earlier, setting up a decision matrix requires the calculation of *m*x*n* payoffs $C_{i,j}$. For the present case study, the payoffs can be calculated with the aid of the simulator, according to Eqn. (4.4) below

$$C_{i,j} = \left(1 - \frac{DMG^* - DMG_{i,j}}{DMG^*}\right) * 100 \qquad (4.4)$$

where $DMG_{i,j}$ is the distance sailed towards the upwind mark (i.e. equal to zero if the yacht sailed at right angles to the mark itself) when considering the i-th strategical alternative and the j-th weather scenario. DMG* is the reference distance covered at the equilibrium surge speed $u_1 = u(t_1)$. The calculation of DMG* and $DMG_{i,j}$ refer to an arbitrary time span of 10 minutes. The time span for the analysis is such that, irrespective of the weather scenario, a yacht is not given the possibility to reach the upwind mark. This has been done in order to focus on the upwind leg only, without including actions such as bearing away on the upwind mark.

The formulation of Eqn. (4.4) necessarily yields payoffs within the range [0;1], where higher payoffs correspond to a higher 'benefit' for the decision maker.

Once the initial decision is made (A_1, A_2, or A_3), the yacht is always sailed according to a unique set of strategical rules: for example, the navigator would always call for a tack on 5° headers or more. This propagates to the whole navigation the positive/negative effect of the decision made at t_2.

4.4.2 Results

Let us assume that all weather scenarios are equally likely to occur (P_j= 0.25 for j = 1 to 4). As shown in Table 4-3, higher payoffs are expected when selecting alternative A_1. Alternative A_3 is the 'second-best' choice, despite the gap between $C_{2,j}$ and $C_{3,j}$ varies. When the judgement is made across scenarios rather than across alternatives, i.e. choosing an alternative first and then considering all possible scenarios, it can be observed that higher payoffs are always obtained under scenario S_2.

Table 4-3: DM matrix at t_2 = 200s

	S_1	S_2	S_3	S_4
Probabilities	P_1	P_2	P_3	P_4
A_1 (tack)	*62.47*	*72.94*	*51.77*	*58.77*
A_2 (don't tack)	*34.69*	*66.67*	*47.29*	*55.80*
A_3 (60s delay)	*59.88*	*69.71*	*48.43*	*55.45*

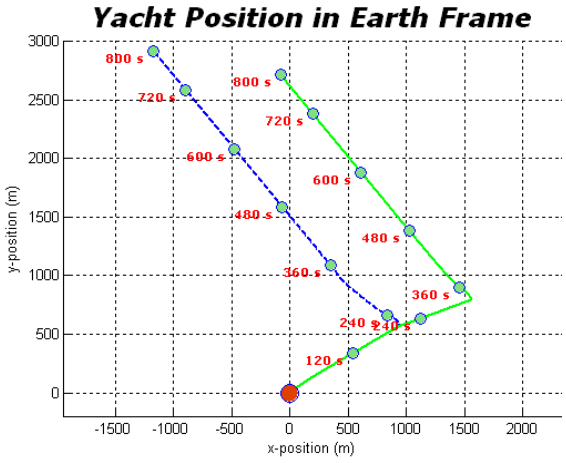

Figure 4-2: Scenario S_2. Dotted line track for choice A_1, solid line track for choice A_2

For example, let us consider scenario S_2 (persistent windshift to East): if alternative A_1 was selected (dotted line track of Figure 4-2), the yacht would tack just once i.e.

onto starboard, at t_2. Any further windshift to the right would indeed be seen as a lift by a starboard boat, yielding therefore higher DMGs. Conversely, if alternative A_2 was chosen (solid line track of Figure 4-2), the yacht would still be sailing on port at t_3 when hit by the subsequent 10° windshift: this would represent a further header for the port-tacker and the navigator would therefore call for a tack onto starboard. In conclusion, the lower payoff ($C_{2,2} < C_{1,2}$) is due to a 120 seconds beat on the disadvantageous tack. These considerations are consistent with widely known principles of race strategy.

4.4.3 Attitude towards risk: from expected payoff to expected utility

According to the considerations of Section 4.3, a closer modelling of decision-making in risky contexts requires two further steps: probability information P_1, P_2, …, P_4 should be associated with outcomes S_1, S_2, ..., S_4, and the decision maker's attitude towards risk should be considered.

Assume a probability distribution with $P_1=P_2$ and $P_3=P_4$; this implies that $P_{perm} = 2*P_1$ is the probability that a permanent windshift occurs and $P_{osc} = 2*P_3$ is the probability to encounter an oscillating wind pattern. Furthermore, let n=2 in Eqns. (4.3.b) and (4.3.c): the expected utility of a choice A_i under the scenario S_j is therefore supposed to be proportional to the square root of the payoff and to the payoff squared respectively. This is a plausible assumption when modeling individuals involved in games of chance (Kelly, 2003). Decision tables expressed in terms of utilities $u(C_{i,j})$ rather than payoffs $C_{i,j}$ were derived from Table 4-3 and several probability distributions were considered. Probabilities were varied at nine levels, with a 10% spacing, such that $P_{perm} = \{0.1, 0.2, ..., 0.9\}$ and simultaneously $P_{osc} = \{0.9, 0.8, ..., 0.1\}$. The purpose of this analysis is to estimate how variations in probability influence the level of expected utility which, in turn, affects the final choice. In Figure 4-3, a risk-averse attitude is considered: expected utilities are plotted vs. the probability (P_{osc}) of encountering oscillatory wind patterns.

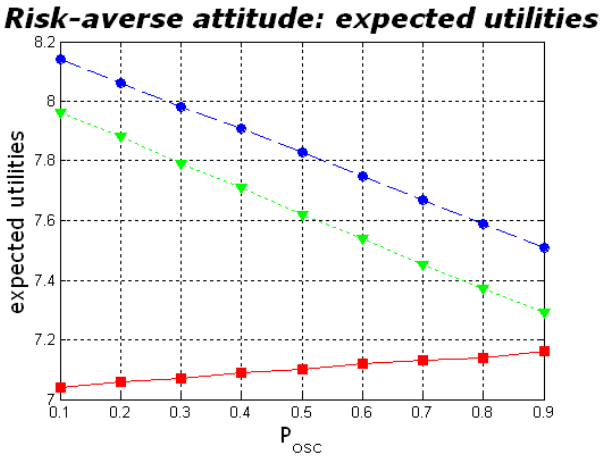

Figure 4-3: Dashed line for choice A_1, solid line for A_2, dotted line for A_3.

It is worth pointing out that choice A_1 (tacking as the first windshift hits the yacht) is the one that yields the largest expected utility: this holds independently on the expected wind pattern. The second-best choice is A_3 (delaying the tack by 60s), whose gap in terms of utility from trend line A_1 is near-constant. This is a consequence of the ground lost because of the delay in decision. In fact, choice A_3 involves sailing the unfavoured (headed) tack for one minute: such a loss cannot be compensated afterwards, since both A_1 and A_2 strategies are alike for t>260s. Both A_1 and A_3 show decreasing utilities as P_{osc} increases, so that higher levels of utility are expected when permanent windshifts are more likely to occur. This is consistent with widely known principles of race strategy.

Figure 4-4 shows expected utilities as perceived by a risk-taking decision-maker: trends for A_1 and A_3 are similar to those of Figure 4-3, but marginal utility (slope of trend line) decreases much faster for risk-takers as P_{osc} increases.

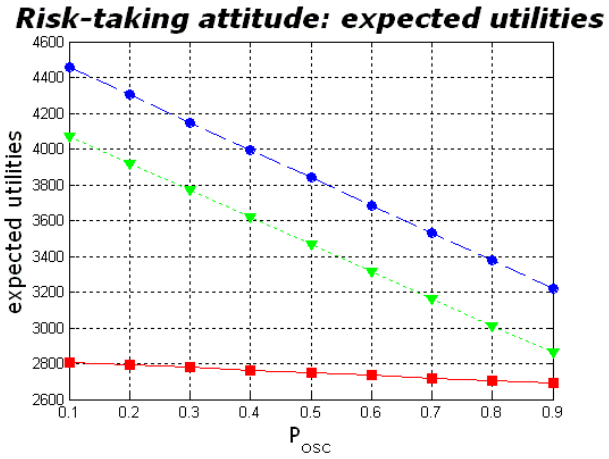

Figure 4-4: Dashed line for choice A_1, solid line for A_2, dotted line for A_3.

4.5 Yacht racing strategy and adaptive decision making: heuristics selection in time constrained environments.

4.5.1 An effort-accuracy framework to investigate decision-making

Investigations of decision making have been carried out in a number of fields: from marketing ('how customers choose a product?') to politics ('how voters choose a candidate?'), from warfare to management sciences, from behavioral finance to criminology ('how people decide to commit a crime?'). As highlighted in Section 4.3, a large part of such models is based on the maximization of expected utility: decision makers are supposed to evaluate an alternative by guessing pay-offs and probabilities for all the possible outcomes, multiplying (weighting) each payoff by the corresponding probability and summing the products over all outcomes. According to 'normative' models, the alternative showing the largest expected value is then selected. The above decision making strategy, usually referred to as WADD, is both the most accurate and the most demanding from a cognitive effort standpoint. In fact, as reported in (Johnson and Payne, 1986), all information processing tasks are known to place a load on the cognitive system, whose capacity and resources are limited (referred to as the 'concept of bounded rationality'). As pointed out in Section 4.5.2 below, the absorption of cognitive resources can be quantified in terms

of elementary information processing operations (EIPs). When operating in time-stress environments, it is unlikely that a careful examination of all alternatives can take place: delaying a decision can result in a loss due to closure of 'windows of opportunity' (Payne *et al.*, 1996) or payoff reductions. Decision makers are therefore known to behave adaptively, partly by accelerating their processing and partly by shifting from more effortful, 'breadth-first' strategies such as WADD, to 'depth-first' techniques for rapidly screening among alternatives. The latter strategies are referred to as *heuristics* and form the basis of the effort-accuracy framework. According to this theory, individuals are supposed to be equipped with their own repertoires of heuristics from which they dynamically pick up the most appropriate; this choice is made by trading off between cognitive effort and accuracy i.e. by selecting the most accurate heuristics within the constraints of limited cognitive resources (Payne *et al.*, 1988).

4.5.2 Effort and accuracy under opportunity-cost time pressure

Several techniques to measure effort and accuracy are reported in (Payne *et al.*, 1988). Effort can be estimated by counting the number of EIPs required to issue a decision. For decision problems formulated as in Table 4-4, examples of EIPs are a) read an alternative's value into short-term memory, b) compare two alternatives on their expected payoffs and c) multiply to weight a payoff with a probability. EIPs are then related to the time spent in deciding, so that the higher the number of EIPs required by a decision-making strategy, the longer the processing and the resultant delay.

Table 4-4: Example of a decision matrix

	Outcome 1	*Outcome 2*	*Outcome 3*	*Outcome 4*
Probabilities	*0.2*	*0.27*	*0.21*	*0.32*
Gamble A	*0.69*	*6.41*	*2.96*	*0.27*
GambleB	*0.37*	*5.14*	*4.38*	*8.94*
Gamble C	*7.53*	*3.13*	*7.62*	*4.28*
Gamble D	*7.84*	*6.07*	*8.70*	*1.28*

Accuracy is measured through expected value calculations. According to a definition reported in (Johnson and Payne, 1985), the Relative Accuracy of a generic heuristic strategy can be expressed by Eqn. (4.5):

$$RA = \frac{EV_{Heuristic} - EV_{RAND}}{EV_{WADD} - EV_{RAND}} \tag{4.5}$$

Opportunity-cost can be defined as the 'cost of something in terms of an opportunity forgone'; such cost is related to the benefits that could have been received from that opportunity. Under opportunity-cost time pressure, the expected payoff EP yielded by an alternative is reduced proportionally to the time spent in deciding. Once again, time delay can be modelled in terms of EIPs, as shown in Eqn. (4.6). The 'Value Loss' or 'Discount' is higher at higher levels of time pressure: levels 0.25, 0.50 and 0.75 correspond to light, moderate and severe time pressure respectively.

$$EP = \frac{1 - (EIP_{Heuristic} * ValueLoss) - EV_{Heuristic}}{EIPs_{WADD}} \tag{4.6}$$

Past research on decision-making under opportunity-cost time constraints, such as that reported in (Payne *et al.*, 1996), show that deciding according to strategies such as WADD may result in poor expected payoffs, owing to the high number of EIPs required. For example, 63 EIPs are needed to issue a decision on the problem in Tab. 4-4 according to WADD. In situations with high levels of time pressure, a random choice (RAND) can yield higher expected payoffs than 'breadth-first' strategies such as WADD.

4.5.3 A toolbox of decision making strategies

Choice rules can be classified according to the amount of information processing required. WADD and RAND can be regarded as the two extremes, since they represent the complete use of information and the complete lack of information respectively. As mentioned earlier, all other strategies are referred to as 'heuristics': potentially useful information is ignored (which saves effort) at the cost of a potentially worst quality of choices (reduction of accuracy). Examples of heuristics are EQW (Gambles are ranked according to the sum of Payoffs across all Outcomes, neglecting Probabilities), LEX (the Outcome whose Probability is higher is selected

first, then the Gamble whose Payoff is higher is chosen), SAT (Satisficing rule), MCD (Majority of Confirming Dimensions rule) and TTB (Take The Best rule). Readers are referred to (Payne *et al.*, 1996) for formal definitions. Strategies such as EQW are referred to as 'alternative-based', since processing is carried out across attributes, while LEX rule belongs to 'attribute-based' choices, since processing is carried out within attributes.

Heuristics' performances at various levels of time pressure were compared in (Payne *et al.*, 1996), where the influence of other factors such as 'dispersion in probability' was also investigated. The latter factor is usually varied at two levels: low and high. An environment featuring a low dispersion in probability is, for example that of Table 4-4, where Probabilities are evenly distributed over Outcomes. The following conclusions were drawn by Payne and co-authors:

- decision-makers faced with opportunity-cost time pressure shift in the direction of less information processing and more attribute-based processing;
- at increased levels of time pressure, attribute-based processing yields higher payoffs than alternative-based processing, such as weighted-added based choices;
- EQW rules perform relatively better in low dispersion environments, while LEX does relatively better when dispersion of probability is high.

4.5.4 A decision making simulation for upwind sailing

The purpose of this study is to check how different heuristics perform under different time-pressure conditions, in order to select the one yielding the best effort-accuracy trade off.

The case study refers to the decision making problem of tacking in a windshift, taken into account in Section 4.3 above. A reduced decision matrix based on Table 4-3 will be referred to: only the alternatives A_1 (to tack) and A_2 (not to tack) will be considered, therefore excluding the possibility of delaying the decision. As suggested in literature, two degrees of dispersion (low and high) were considered for the probability vector $\mathbf{P} = [P_1, P_2, P_3, P_4]$. In fact, $\mathbf{P}_{lo} = [0.2; 0.27; 0.21; 0.32]$ was chosen as the low dispersion condition, while $\mathbf{P}_{hi} = [0.68; 0.12; 0.05; 0.15]$ was

chosen as the high dispersion condition. Sixteen factor combinations were considered, due to a 4 (opportunity-cost time pressure levels, 0, 25, 50 and 75% Value Loss) by 2 (levels of dispersion of probabilities: low and high) by 2 (standard deviations for payoff normal distributions: 10 and 20%) factorial. Monte Carlo simulations were carried out, in order to generate sets of 1000 decision problems for each combination of the above factors. Each decision problem is characterized by a 2-by-4 payoff matrix, generated according to payoff normal distributions described in the previous Section. MS Excel® and Crystal Ball® by Decisioneering Inc. were used to set up Monte Carlo simulations using spreadsheets. Seven decision rules (WADD, EQW, LEX, SAT, MCD, TTB and RAND) were implemented and compared using Visual Basic for Applications (VBA) scripts.

Simulation results for the above decision rules are summarized below, where results are plotted in terms of Relative Accuracy vs. Relative Effort (Figures 4-5 and 4-6) and in terms of Expected Payoff vs. Time Pressure (Figures 4-7 and 4-8).

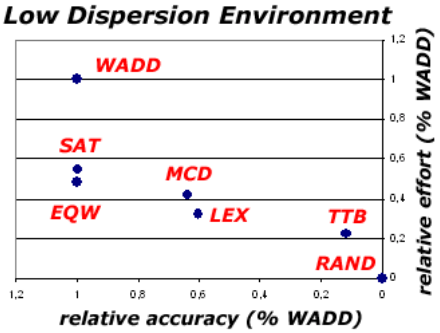

Figure 4-5: Relative effort vs. relative accuracy for the low dispersion environment $\boldsymbol{P}_{lo}$

Low dispersion environments (Figure 4-5) show that alternative-based heuristics (EQW and SAT) yield almost the same relative accuracy as WADD with half the effort. Conversely, all attribute based heuristics perform poorly. At higher levels of dispersion (Figure 4-6), when a given weather scenario is more likely than the others, attribute-based heuristics such as LEX yield the same accuracy as WADD with almost a third of the effort.

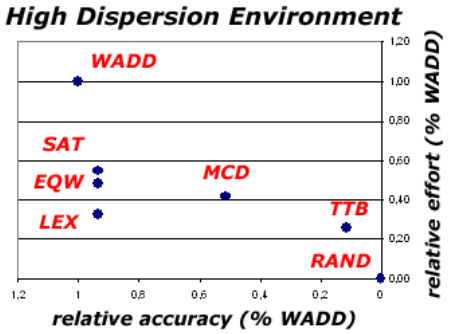

Figure 4-6: Relative effort vs. relative accuracy for the high dispersion environment $\boldsymbol{P}_{hi}$

When dispersion is low and at lower levels of opportunity-cost time pressure (left-hand side of Figure 4-7), EQW proves to yield the highest payoffs. On the other hand, for the high dispersion environments of Figure 4-8, LEX is the strategy that performs best. Further analyses have shown that, given a level of time pressure, strategies are ranked the same way irrespectively of the level of standard deviation considered (10% or 20%). This means that simulator inaccuracies are unlikely to affect the way strategies are ranked.

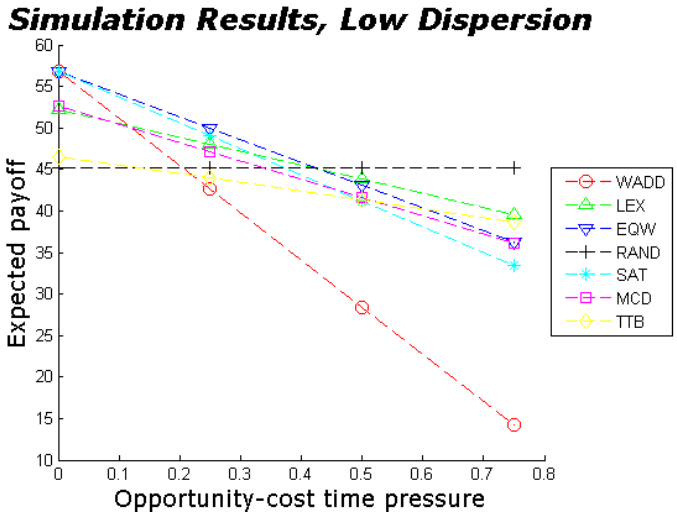

Figure 4-7: Expected Payoff vs. Time Pressure for the low dispersion environment $\boldsymbol{P}_{lo}$

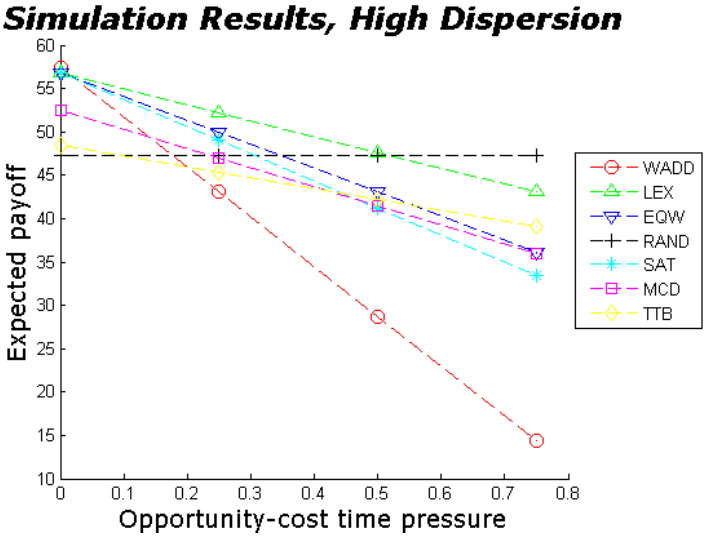

Figure 4-8: Expected Payoff vs. Time Pressure for the high dispersion environment $\boldsymbol{P}_{hi}$

The above results are consistent with those obtained by (Payne *et al.*, 1996): in fact, EQW and LEX did relatively better in low and high dispersion environment respectively. This happens despite some differences in the experimental procedure: in (Payne *et al.*, 1996) the payoff matrices were generated by fully random routines, while in the present study payoffs are obtained from DMG values predicted by the sailing simulator. This is to say that a considerable correlation is present. This also explains the reason why RAND choice does not yield a constant 50% Expected Payoff (Figures 4-7 and 4-8).

4.5.5 Conclusions

In the present Section an investigation on decision making under time-stress is presented. In agreement with past research, individuals are supposed to be 'equipped' with a repertoire of choice rules, from which to choose the most advantageous one by trading off accuracy and effort. Seven rules are taken into account, either alternative-based (WADD, EQW, SAT), attribute-based (LEX,

MCD, TTB), and the random-based choice RAND. A decision matrix consisting of two alternatives and four outcomes is taken into account, which is referred to a dilemma of a strategical nature frequently encountered in yacht racing. The four attributes correspond to four possible weather scenarios: for each of these a set of payoffs expressed in terms of DMG (distance sailed towards the upwind mark) has been evaluated by using Robo-Yacht. The problem is studied in opportunity-cost time pressure environments, where delaying a decision yields a reduction in the expected payoff. Monte Carlo simulations were used to investigate the problem and the influence of three factors (dispersion in probability, payoffs standard deviation and level of time pressure) has been considered as well.

As in past works, it is shown that behaving adaptively (i.e. maximizing accuracy while dealing with limited cognitive resources and time constraints) implies switching to more attribute-based strategies and processing smaller amounts of information. Results of Monte Carlo simulations also show that more effortful, 'breadth-first' strategies such as WADD are likely to perform poorly (i.e. yielding below-random expected values) when severe time constraints are present. In such conditions, particularly for high dispersion contexts, use of less effortful, attribute-based strategies such as LEX is recommended.

4.6 References

Abernethy, B., 'Visual Search Strategies and Decision-Making in Sports'. Int. Journal of Sport Psychology, 22, pp.189-210, 1991.

Araùjo, D., Davids, K., and Serpa, S., 'An ecological approach to expertise effects in decision-making in a simulated regatta', Psychology of Sport and Exercise, 6, pp.671-692, 2005.

Bard, C. *et al.*, 'Relationship Between Perceptual Strategies and Response Adequacy in Sport Situations'. Int. Journal of Sport Psychology, 25, pp. 266-281, 1994.

Johnson, E.J. and Payne, J.W., 'Effort and accuracy in choice'. Management Science, 31(4), pp.395-414, 1985.

Johnson, E.J. and Payne, J.W., 'The decision to commit a crime: an information-procession analysis'. Criminal Decision Making, pp.170-185, 1986.

Kelly, A., ‘Decision making using game theory – An introduction for managers’, Cambridge University Press. (2003)

Mc Garry, T., and Franks, I. M., ‘Modeling Competitive Squash Performance from Quantitative Analysis’. Human Performance, 8(2), pp.113-129, 1995.

McLeod, P., Jenkins, S., ‘Timing Accuracy and Decision Time in High-Speed Ball Games’. Int. Journal of Sport Psychology, 22, pp.279-295, 1991.

Nougier, V., Stein, J.F., Bonnel, A.M., ‘ Information Processing in Sport and Orienting of Attention’. Int. Journal of Sport Psychology, 22, pp.307-327, 1991.

Payne, J.W., Bettman, J.R., and Johnson, E.J., ‘Adaptive strategy selection in decision making’. Journal of Experimental Psychology: Learning, Memory and Cognition, 14(3), pp.534-552, 1988.

Payne, J.W., Bettman, J.R., and Luce, M.F., ‘When time is money: decision behaviour under opportunity-cost time pressure’. Organizational Behavior and Human Decision Processes, 66(2), pp.131-152,1996.

Ripoll, H., ‘The Understanding-Acting Process in Sport: The Relationship Between the Semantic and the Sensorimotor Visual Function’, Int. Journal of Sport Psychology, 22, pp. 221-243, 1991.

Rulence-Paques, P., Fruchart, E., Dru, V., and Mullet, E., ‘Cognitive algebra in sport decision making’, Theory and Decision, 58, pp.387-406, 2005.

Saury, J. And Durand, M., ‘Practical Knowledge in Expert Coaches: On-Site Study of Coaching in Sailing’. Research Quarterly for Exercise and Sport, 69(3), pp.254-266, 1998.

CHAPTER 5

ROBO-RACE: A SIMULINK®-BASED TOOL FOR THE SIMULATION OF INTERACTIVE FLEET RACES

5.1 Generalities and requirements

During the design and development of Robo-Yacht, the run-time shortcomings of MATLAB discussed in Chapter 3 became evident. For example, the high computational costs of interactive races, with one or more sailors controlling the yachts and receiving a visual feedback on the race in real time, would have slowed down the simulation to a rate much slower than real time. Also, it became clear that sensitivity studies with very large test matrices could not be dealt with efficiently in MATLAB. This led to the development of a MATLAB-Simulink-based tool for fleet race simulations that will be referred to as 'Robo-Race'.

Part of the existing MATLAB code was included in Robo-Race as well as a Simulink built-in solver for the yacht equations of motion. To ensure consistency with Robo-Yacht, the equation solver is based on the 4^{th} order Runge-Kutta method. Robo-Race allows users to interact with the fleet by means of joysticks. The joystick-based interaction gives each user the possibility to steer and manoeuvre the yacht, so as to carry out both the strategy and the tactics. Users are also given the possibility to select the most appropriate viewpoint by means of a pointing device, effectively navigating the racing scenario. Also, an improved version of the virtual 3d world was designed and implemented for use in Robo-Race. For example, the graphics and the level of detail were refined with respect of Robo-Race, and real-time visual feedback was provided to the user.

The above issues are known to be of primary importance, since they affect the 'functional fidelity' of the computer simulation. In the Sport Psychology domain, it is claimed that sport simulations should allow users to perform the same functions as those required by the real task (Araùjo *et al.*, 2005). This is to say that, although the

'structure' of the real task and the 'structure' of the simulated task can be different (e.g. an overview on the fleet rather than an onboard view), the 'functions' performed by the user should be consistent. Another issue to be taken into account is the 'ecological validity' of the simulation: this is to say that the judgment of a user is likely to be biased when interacting with an unfamiliar racing context. Ecological constraints are likely to be broken, for example, when the simulation involves an unfamiliar man-machine interface, requires specific computer skills or the visual feedback provided lacks sufficient detail. The lack of detail affects the cue pick-up process and therefore biases the information processed by sailors, so that unrealistic conclusions are likely to be drawn.

Therefore, it is believed that a fairly detailed virtual reality world, a correct positioning of cameras and the availability of onboard instruments can help improving the quality of the simulation results.

5.2 Architecture of Robo-Race

In order to simulate virtual races featuring N yachts, Robo-Race was designed to include M Robo-Yachts (controlled by the simulation engine) and (N-M) human controlled yachts. For each Robo-Yacht, the hull, rig and crew parameters are defined when setting up the simulation, in analogy with the MATLAB-based simulator. This allows a comparison of yacht-crew systems as opposed to comparison of different yacht designs only.

During the design of Robo-Race, the possibility of using entirely Simulink-based modules was evaluated as opposed to including existing pieces of MATLAB code, already implemented for Robo-Yacht. Although the Simulink implementation was preferred for frequently called functions such as the equations of motion (to reduce the computational demand by using built-in equation solvers), MATLAB-based routines were used for the automatic crew models, including those used for routing purposes. In particular, most of the yacht-crew architecture already designed for Robo-Yacht was included in Robo-Race.

With respect to the Robo-Yacht architecture, the scope of the automatic crew was widened. For example, an additional library was implemented, to carry out the race

tactics and to address conflicts between tactics and strategy (e.g. to tack onto an unfavoured beat to sail in 'clean' air, that is outside the bent and turbulent air due to a leading yacht's sails). Other existing modules were included in Robo-Race, such as the race scenario and the weather module.

5.2.1 Embedded MATLAB (EM) and data exchange

EM is essentially a 'low level' version of the conventional MATLAB language that allows to generate efficient embeddable C code. However, many restrictions to the use of MATLAB features apply ('language restrictions') and only a subset of the MATLAB run-time functions is available. Examples are: the impossibility to change class and size of variables after their initial definition and the requirement to define subfunctions within the body of the calling EM function. The language restrictions require a step change in the coding style.

Just as for Robo-Yacht, data structures were used for Robo-Race in order to encapsulate large datasets and facilitate data exchange. However, several constraints to the use of structures exist in EM. For example, structure fields can neither be referenced nor accessed dynamically (i.e. the explicit name of a field must be used when creating, reading from and writing to it). This increased the amount of coding and added verbosity to several Robo-Race routines with respect to their MATLAB-based counterparts.

Another relevant feature of EM consists in the use of 'buses', which are required for routing signals to and from EM Simulink blocks. The 'Ports and Data Manager' tool helps to define the properties of a function's inputs and outputs, such as *name*, *scope* (*input*, *output* or *parameter*), port number and data type mode (e.g. *inherited* or *bus object*). When Simulink models exchange data with EM blocks in the form of a data structure, an appropriate Simulink Bus Object has to be prepared whose name, dimension and field type match those of the structure itself. A 'Bus Types Editor' is also available which allows the definition of name, type and complexity of Bus Objects. It is allowed to use existing Bus Objects as Bus Types.

For the simulation of fleet races, it was decided to simplify the implementation by bundling all data (i.e. 'signals') on the yacht's geometry, physics and dynamics

within the 'YData' Bus Object. This Bus includes elements such as the yacht's displacement (whose type is *double*) and the yacht's sailplan (whose type is the custom bus object 'SailInventory'). The latter bus consists of as many elements as the sails of the inventory, namely mainsail, genoa, jib, spinnaker and asymmetric spinnaker. The individual sails' data are retained in the custom bus object 'GenericSailData', which contains information on the sail geometry (i.e. sail area, luff length, foot length) as well as performance data (i.e. lift and drag coefficients as a function of *awa*).

5.3 Man-in-the-loop

In Robo-Race a user can interact with the software by means of a joystick, in order to control a yacht and to race against one or more Robo-Yachts or other users. As pointed out earlier, this feature was implemented to assess the decision-making process driving a race, to compare the strategies of novices with those of experts and, potentially, to feed the results back in the automatic crew model and build expert systems. To date, only rudder controls were made available to the user, in order to focus the investigation on steering strategies. The following options and controls were implemented:

Tacking: when sailing upwind (*'awa-based'* mode) a tack can be triggered by clicking a joystick button. The software then performs the tack according to a technique previously defined by the user. Examples of available techniques are reported in Chapter 3.

Rudder actions: when sailing at a given heading ('*heading-based*' mode), the yacht's heading can be increased/decreased 0.5 degrees at a time by clicking a joystick button. When in *'awa-based'* mode, the reference apparent wind angle, can be modified in the same way.

Viewpoint location: at each step of the simulation, the viewpoint on the racing area can be changed by selecting an appropriate camera. A list of available cameras is accessed through a drop-down menu in the simulation window.

Viewpoint distance: the extent of the scene displayed in the simulation main window can be changed through the joystick throttle. In particular, the distance between the generic camera and the origin of the yacht-centered reference frame can be adjusted. The minimum and maximum allowed distances can be set prior to the simulation. This feature is used to investigate how the user's performance is affected by limiting the sailors' overview of the race.

5.3.1 Inclusion of a joystick-based control system

A 'joystick block' is available in the Simulink Virtual Reality Toolbox, that allows a user's input to be picked up and made available for control purposes. The controller device used for Robo-Race is a 'Cyborg Evo' (C-E) manufactured by Saitek (www.saitek.com). The device, originally developed for commercial flight simulations, has five buttons and a trigger available at the head of the stick, six base buttons and an eight-way hat switch (see Figure 5-1). The C-E also allows the rotation of the stick around its z-axis (perpendicular to its base) for rudder control purposes.

Figure 5-1:The joystick Saitek Cyborg Evo

The interaction was restricted to the navigation, the steering, and the viewpoint adjustment, whereas the sail trim was carried out automatically. However, the user can be required to select a given sail trimming strategy and to set the parameters concerned (e.g. reef, flat and maximum allowed heel angle), therefore influencing the behaviour of the automatic sail tailing system. The upwind steering is controlled by changing both the sign and the absolute value of awa_{ref}.

A Simulink block (Figure 5-2) was developed to pick-up and transfer the user's input to the sailing simulator. Clicking on the front trigger starts a tack, while clicking on buttons #5 and #6 allows coming up and bearing away by 0.5 degrees per time-step. Therefore, a rudder angle rate of 2.5 degrees/sec can technically be achieved. Moving the stick forwards allows to zoom in to the racing area, while pulling it backwards allows to zoom out. Fixed extents were set for the zoom.

The 'Axes' output port of Figure 5-2 returns a vector of type 'double' whose four elements are in the range [-1,1]. For example, the output corresponding to joystick axis 'y' (channel 2) is +1 when the stick is pushed to the forward end, -1 when pulled to the backward end. The latter signal is used for zooming purposes and is processed as follows: firstly, it is picked up through a 'Selector' block, then filtered through a 'Dead Zone' block to make the control insensitive to stick shaking, amplified and lastly integrated with a saturation to [-1,1].

Each joystick button outputs a '1' when pressed, and a '0' when released. Such signals were used to drive the 'Triggered Subsystems' #1 and #2, that provide the required *awa* correction. A 'Switch' block is used to pass through input 1 (top port, used for awa_{ref} adjustments) when input 2 is non-zero and to pass through input 3 (bottom port, used for tacking) otherwise. Based on the Block of Figure 5-2, tacking does not change the absolute value of awa_{ref} so that the most recent awa_{ref} is retained after the tack.

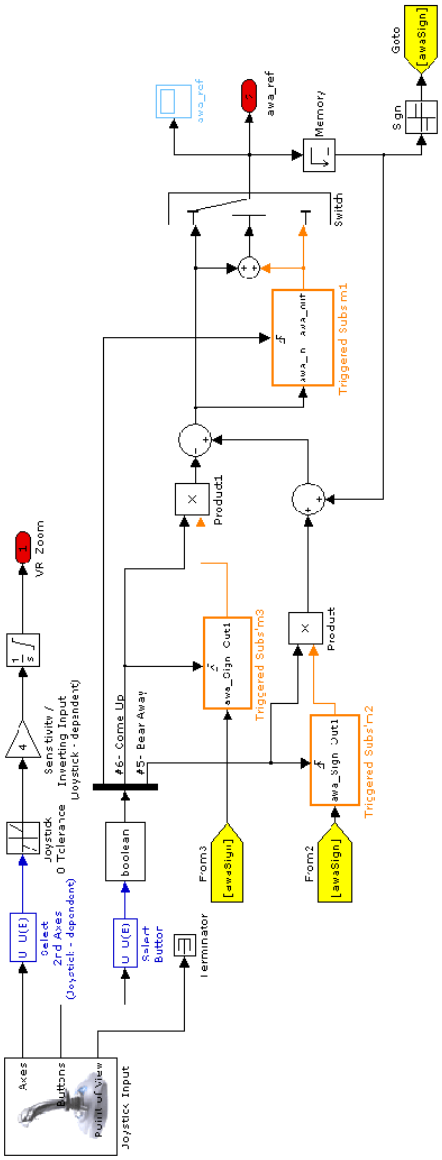

Figure 5-2: Inclusion of a 'joystick' block

5.3.2 Onboard instruments

A number of 'instruments' are available to the user that display information on the yacht state variables (i.e. surge speed, VMG, *awa*, *tws*), conveying therefore an idea on the current performance of the boat. In order to do so, the stepwise values of the state variables were picked up and wired into appropriate ActiveX blocks of the 'Dials and Gauges' Simulink library. The 'onboard instruments' have been collected in a single Simulink window displayed on a separate monitor ('Screen #2', the laptop screen of Figure 5-3). The 'onboard instruments' include the screen of a 'virtual GPS' unit, where the tracks of a predefined number of yachts are displayed, as if each yacht had a GPS transmitter onboard. The tracks are updated and delivered to the user at each simulation time-step. As opposed to the virtual 3d world, the 'virtual GPS' screen shows the tracks as solid lines on a white background. A dashed, black and white grid is superimposed to the background for the sake of clarity. One viewpoint only is made available to the user, i.e. the one perpendicular to the sea surface, positioned such as to span the whole racing area. The main simulation monitor ('Screen #1') displays the animation window as well as the time history of the variables monitored in 'Screen #2'.

Figure 5-3: Interactive session of Robo-Race: screens #1 and #2, joystick and pointing device

5.4 Virtual reality simulations

5.4.1 Virtual 3d world modelling

The design and implementation of VR animations can be performed with the aid of Virtual Reality Modeling Language (VRML) authoring tools, such as 'V-Realm Builder' provided with MATLAB VR Toolbox. The modelling of a 3d virtual world suitable for interactive fleet races presents several obstacles. An issue of major importance was achieving a satisfactory trade-off between the level of detail provided (e.g. hull and cockpit shape, motion of sails) and the simulation speed. Several approaches were explored, such as modelling the entire boat within V-Realm or through a third-part CAD software. For the former case, the quality of the finished product was unsatisfactory when using an 'onboard camera' mode, although acceptable for a far-field view of the race. This may well affect the 'ecological validity' of interactive simulations aiming at the investigation of the cue pick-up process carried out by sailors. As described in Section 5.1, the inclusion of details that sailors are familiar with is crucial to get a reliable response from the user. Therefore, the 3d modelling of the appended hull, the spars and the sails was carried out through the open source 3d modeller 'Blender'. Blender was also used to apply textures on the deck and the sails for identification purposes. The VRML modelling carried out for Robo-Race was composed of eight consecutive stages:

- definition of appropriate yacht frames and world frame;
- modelling of the individual yacht components, i.e. hull, appendages, rig and sails in VRML;
- assembly of components, to obtain a VRML model for the IACC yacht;
- texture drawing and draping over the hull/sails surfaces;
- set up and positioning of cameras;
- scene lighting through ambient lights (global, referred to the world frame) and spotlights (local, yacht frame);
- inclusion of a race scenario;

- inclusion of the N yachts of the fleet in the 3d world. Each member of the fleet is included as a 'Yacht' node. The arbitrary 'Yacht' node is implemented as an instance of the generic VRML model of the IACC yacht.

At the end of the VRML modelling, the whole 3d world is available as a single VRML (.wrl) file composed of a 3d scene, cameras, lights and N 'Yacht' nodes. Each 'Yacht' node shows several sub-nodes, namely 'Hull', 'Rig', 'Mainsail', 'Headsail', 'Rudder' and 'Wheel'. Nodes and sub-nodes have appropriate fields defining for example their position, orientation and scale.
In order to animate the objects of a 3d world, MATLAB's Virtual Reality toolbox can be used as an interface between the VRML environment and the Simulink model. The 3d world must be included in a dedicated Simulink block (or 'VR Sink') where the exposed fields have to be defined and linked to the corresponding simulation variable. Section 5.4.2 below provides further information on this issue.

5.4.2 Inclusion of the 3d world: the Simulink 'VR sink' block.

The Simulink block 'VR sink' allows the inclusion of VRML worlds within Simulink models, so that an animation of the dynamic system can be delivered to users in real-time. In particular, at every time step, the VR sink collects the simulation outputs and updates the state of the dynamic system within the 3d space.
Prior to entering the VR sink, the input signals must be routed into 'VR signal expanders', to be adapted to the VRML format and to fill blank positions with VR placeholders.
The VR sink allows users to control the scene lighting and rendering, capture screenshots and record animations. An interface is also provided to navigate the 3d world using three different systems (walk, examine and fly) and eight directional arrows. More important, the VR sink has an embedded viewer/editor for the VRML tree, where node types and field types are displayed and the exposed fields can be selected as input ports for the simulation. The values of these fields can be updated dynamically by the Robo-Race engine, so that real-time animations can be generated at a frame rate equal to the simulation time step.

As an example, let us consider the rudder angle signal δ_i for the i-th yacht. Based on the stepwise value of δ_i, two animations are generated:

1. a rotation δ_i of the rudder blade about its stock
2. a rotation $k*\delta_i$ of the wheel about its centre, where a gain k=3 is used to amplify the wheel rotations and therefore provide an effective feedback to the user.

Figure 5-4 shows a 'stub' used to verify that rotations (1) and (2) are correctly implemented for the yacht 'Yacht1'.

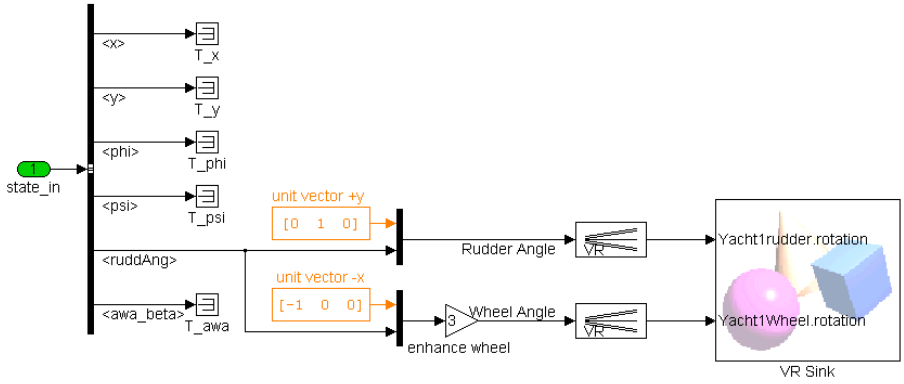

Figure 5-4: The VR sink block: routing example for the 'rudder angle' signal

All the state variables other than δ_1 have been grounded through 'Terminator' blocks, and a VR sink is shown were only the two ports of interest are active. Therefore, if the stub was ran in conjunction with Robo-Race, the blade and wheel motions would be displayed on a still-standing yacht. In order to realize the rudder rotation (1), the 'Rudder' sub-node of the i-th yacht must expose a 'rotation' field to the Robo-Race engine. This is the reason why the field 'Yacht1rudder.rotation' appears among the inputs of the VR sink. According to VRML standards, the signal routed to the 'Yacht1rudder.rotation' input port must be a one-by-four vector, whose field (1,4) is δ_i while the remaining fields must define the direction of rotation, namely [0 1 0]. Similarily, in order to realize the wheel rotation (2), the 'Wheel' sub-node of the i-th yacht must expose a 'rotation' field to the Robo-Race engine.

This is why the VR sink of Figure 5-4 shows the input port 'Yacht1Wheel.rotation'. The signal δ_i (ruddAng) was amplified by the gain k=3, appended to the unit vector [-1 0 0] and routed in the VR sink via a VR signal expander.

5.4.3 Cameras

For the reasons pointed out in Section 5.1, great care was taken in the positioning of the cameras within the 3d world. Several pilot simulations carried out by different users showed the importance of varying both the position and the distance of the camera from the scene. Normally, a far-field viewpoint was used alongside the 'virtual GPS' to get an overview of the race and to check the opponents' positions. Conversely, an onboard viewpoint was preferred for close-quarters racing situations such as port/starboard crossings and mark roundings. A satisfactory solution consisted in using four 'external' cameras (starboard-side fore and aft, plus port-side fore and aft), one onboard camera and a continuous adjustment of the viewpoint location. This proved to be a good solution to navigate the 3d world efficiently i.e. without losing focus on the navigation when changing the active camera.

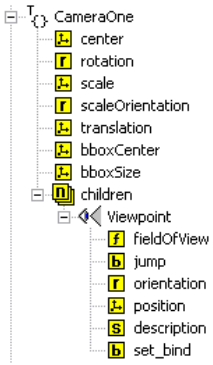

Figure 5-5: 'CameraOne' Transform node and Viewpoint child node

Figure 5-5 shows an excerpt from the V-Realm's tree view pan, which is relative to the 'CameraOne' node. As for any other camera in the model, it was chosen to define Camera One as a 'Transform' node having a 'Viewpoint' node as a child.

'Transform' nodes are used when additional reference frames *O'x'y'z'* are required within the main VRML frame *Oxyz*. The fields CameraOne.Viewpoint.orientation and CameraOne.Viewpoint.position are used to place the camera within *O'x'y'z'*, while the field CameraOne.Viewpoint.description is used to label the camera, for the user's reference.

When a yacht is set in motion, all its cameras should remain fixed in the yacht frame. This was achieved through VRML 'Route' nodes, whose function is that of transmitting (i.e. routing) messages from a source node to a destination node. The term 'message' refers to either scalar values, vectors and strings. In order to keep a camera (e.g. the CameraOne node) fixed within the yacht's reference frame (e.g. the frame for the Yacht1 node), the field Yacht1.translation had to be routed to CameraOne.translation and the field Yacht1.rotation had to be routed to CameraOne.rotation. Each camera, therefore involved the definition of two Route nodes per yacht. Alternatively, the use of Routes could have been avoided by setting up additional input ports for the VR sink, for example a CameraOne.translation port and a CameraOne.rotation port, and setting up those values dynamically, based on the yacht's state. However, this solution would have required further wiring towards the VR sink and would have added unnecessary complication to the model.

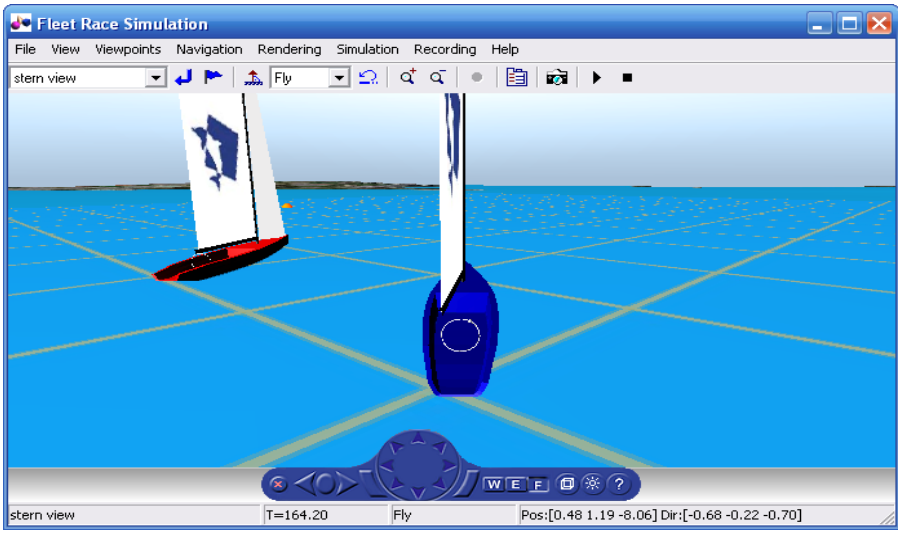

Figure 5-6: Screenshot of Robo-Race, stern camera

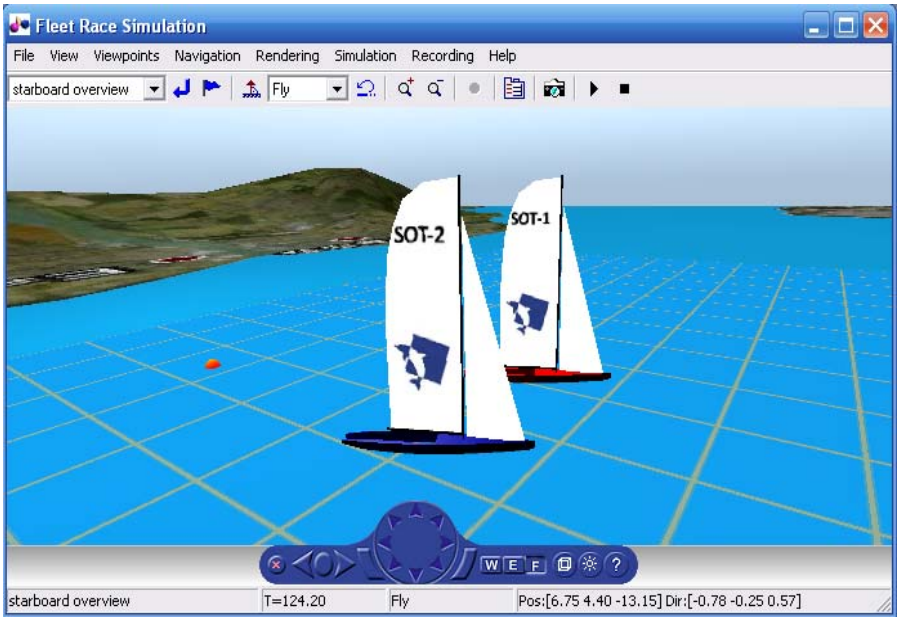

Figure 5-7: Screenshot of Robo-Race, close view of a match-race

5.5 Improvements to the automatic crew: tactician/navigator

An improved version of the navigator was implemented for Robo-Race. As well as race strategy, further issues concerning interactions between two or more boats were addressed. In particular, collision avoidance rules were implemented as well as an elementary model accounting for blanketing effects. Furthermore, a set of parameters regarding the yacht's tactics were monitored and delivered to the user in real time.

5.5.1 Parameters for race tactics

Several parameters were monitored in Robo-Race, which are likely to influence tactical decisions. These can either be delivered to the user in real-time or plotted for post-match analyses. Two examples are the *leverage* of a yacht B on a yacht A or $Lev_{A,B}(t)$ and the *lead* of A on B, or $Lead_{A,B}(t)$.

Let us define $Lev_{A,B}(t)$, as the distance between A's CG and B's centerline at time t, measured at right angles with the true wind vector $\mathbf{W_T}$ (see Figure 5-8). As explained in (Perry, 2000), the larger the leverage, the higher the gain/loss of ground between boats A and B in the event of a windshift. It should be observed that the above formulation yields non-negative values for $Lev_{A,B}(t)$, with the leverage zeroing only in the event of B's centreline intersecting A's CG.

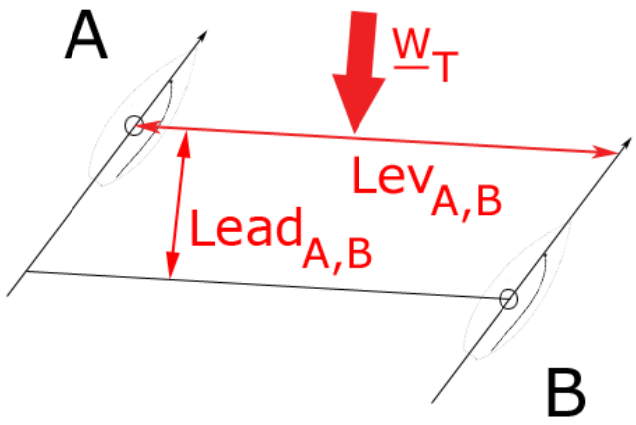

Figure 5-8: Leverage of yacht B on yacht A; lead of yacht A on yacht B

Let us define $Lead_{A,B}(t)$ as the distance between A's CG and B's CG measured parallel to the the true wind vector $\mathbf{W_T}$. Questionnaires and interviews with skilled sailors, carried out for research reported in (Scarponi *et al.*, 2006), (Scarponi *et al.*, 2007) show that both $Lev_{A,B}(t)$ and $Lead_{A,B}(t)$ influence the tactical choices onboard. For example, a large leverage is regarded as a risky situation and a tactician is likely to call for a tack once a given threshold is exceeded. Conversely, when large leads are observed in match-races, the trailing yacht is likely to build up leverage on the leading yacht in order to gain ground when a favourable windshift (i.e. a header) is expected.

5.5.2 Collision avoidance

As far as the 'right of way' rules are concerned, the Racing Rules of Sailing (RRS) should ideally be implemented to ensure 'fair racing'. However, this task goes well beyond the scope of the present Thesis, for which a basic set of collision avoidance rules can yield satisfactory results. It should be borne in mind that even a simple situation like port-starboard crossings leave plenty of room for individual judgement, which is worth addressing when modelling a crew. The latter issue was addressed by tuning the navigator's settings in order to reflect the crew skills (i.e. the likelihood of a collision or the tack location).

Based on the questionnaires mentioned earlier, a decision-making tree (DM tree) was implemented in Embedded MATLAB, within the 'Race Tactics' Simulink block. According to the navigator's settings, the likelihood of a port-starboard collision was estimated by means of the DM tree and, where appropriate, a decision was issued according to Table 5-1. The possible decisions, that is the outputs of the DM tree, are: ignore the crossing, tack to leeward of B or duck B. The automatic navigator makes a judgment based on the assumption of equal speeds and *awa* for yachts A and B and takes action when the starboard yacht enters a circle whose radius is R_{cross}. The information on the crossing are collected within a 'CrossingMatrix', filled in dynamically with B's position in A's frame, the distance between A's CG and B's CG and the angle α between A's centerline and B's CG.

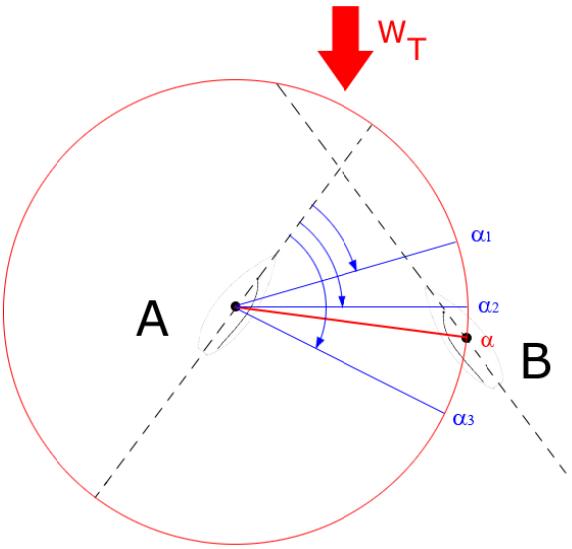

Figure 5-9: Schematic for port-starboard crossings

condition		*Decision*
r > Rcross		ignore crossing
r ≤ Rcross	$0 < \alpha < \alpha_1$	ignore crossing
	$\alpha_1 \leq \alpha < \alpha_2$	duck B
	$\alpha_2 \leq \alpha < \alpha_3$	tack to leeward of B
	$\alpha_3 \leq \alpha < 2\pi$	ignore crossing

Table 5-1: Decisions for port-starboard crossings

5.5.3 Blanketing models

Simulations reported in (Philpott *et al.*, 2004) demonstrate that blanketing models based on weighting factors (rewarding the covering yacht and penalizing the covered yacht) are suitable to model blanketing effects for match race simulation purposes. In the above paper, the physics of covering was modelled in two different fashions, according to the point of sail.

For upwind sailing, the flow region surrounding a yacht is bent with respect to the undisturbed flow, due to the presence of the sailplan. Such a *bent air effect* is known to propagate downstream, affecting any trailing yachts sailing in the vicinity of the leading yacht. Philpott and co-authors identified the bent air region as a truncated circular zone, centered at the end of the boom (i.e. at mid-transom) and extending no further upwind than the bow. Within the *bent air region*, the flow direction is supposed to vary linearly with the distance from the leading yacht, so that the undisturbed direction M_t is restored at a distance R_{bent} from the yacht's transom.

For downwind sailing, when the sails' thrust is mainly due to drag, a region of turbulent flow exists to leeward of the sails. The *turbulent air effect* was modelled in terms of a reduction in wind speed with respect to the undisturbed flow. The speed is supposed to recover linearly, so that the undisturbed speed V_t is restored at a distance R_{turb} from the yacht.

Following (Philpott *et al.*, 2004), Eqns. (5.1) and (5.2) describe the wind direction $\widehat{M}_t$ within the bent air region and the wind speed $\hat{V}_t$ within the turbulent air region respectively.

$$\widehat{M}_t = M_t + (\beta_t - \delta)\left(1 - \frac{r}{R_{bent}}\right) \tag{5.1}$$

$$\hat{V}_t = V_t\left(1 - p_{max}\left(1 - \frac{r}{R_{turb}}\right)\cos^2\left(\frac{\gamma}{\gamma_{turb}}\frac{\pi}{2}\right)\right) \tag{5.2}$$

where δ is the boom angle, β_t is the apparent wind angle, p_{max} is the minimum speed reduction (expressed as a percentage of the undisturbed windspeed) within the turbulent air region and γ is relative to the centerline of the turbulent cone projected by the sailplan.

It is believed that the model described by Eqns. (5.1) and (5.2) meets the accuracy requirements of the interactive race simulations presented herein. More important, it can be easily explained to novice users, who are likely to be unfamiliar with covering issues, prior to a simulation session. Finally, the bent/turbulent regions could easily be implemented as a node of the VRML world and displayed alongside

the yacht motion in order to provide a visual feedback on blanketing and its effects. Further refinements to the above model should be carried out, perhaps with the aid of wind tunnel testing. Experimental investigations would help to clarify the flow recovery process downstream the sails and provide values for R_{bent}, R_{turb}, p_{max} and γ_{turb}. To the author's knowledge, none of these results are in the public domain to date.

5.5.4 Simulink implementation of race tactics

Both the blanketing models and the collision avoidance rules have been implemented in the 'Tactics' block shown in Figure 5-10. Such a block processes yacht, course and weather information, as well as real time data on the opponents. It delivers information of a tactical nature to the navigator, including Lev(t) and Lead(t) relative to all opponents. As an example, let us consider the 'Tactics' block of Figure 5-10, that refers to the Robo-Yacht 'TeamB'. TeamB is involved in three-boat fleet races described in Section 5.6. The inputs required are:

- Port 1: the 'State' bus for TeamB's state variables;
- Ports 2 and 3: two buses of state variables for the opponents (Teams A and C);
- Port 4: the 'Wind' bus, where signals on the wind speed and angle are bundled;
- Port 5: the 'Twa' bus for TeamB's true wind angle;
- Port 6: the 'Battlefield' bus, where all racecourse informations are bundled;
- Port 7: the 'YachtData' for TeamB, relative to the yacht's physics and user's settings.

The outputs are:

- Port 1: BlanketingFactor, a matrix containing $\widehat{M}_t$ or $\widehat{V}_t$, based on TeamB's point of sail and position with respect to a covering opponent. When no blanketing effect is present, $\widehat{M}_t$ and $\widehat{V}_t$ default to M_t and V_t respectively.
- Port 2: paramsTactics, a bus containing $Lev_{B,i}(t)$, $Lead_{B,i}(t)$, $VMG_B(t)$ and the VMG deltas $VMG_{B,i}(t)$, where i = {A, C}.
- Port 3: decTactics _tack, a boolean variable whose value is 1 where the race tactics require a tack or gybe, zero otherwise.

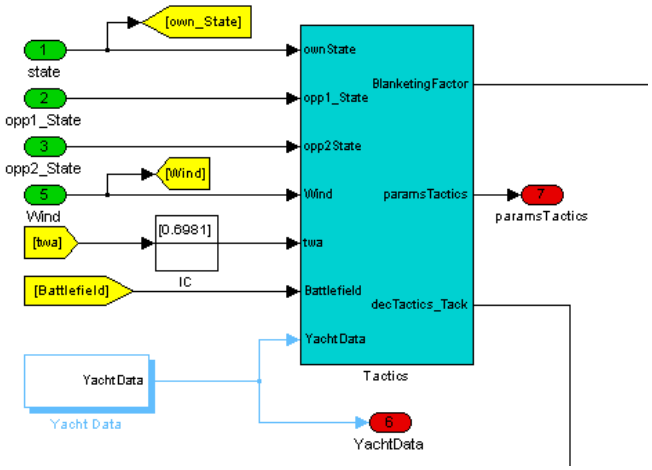

Figure 5-10: Simulink implementation of blanketing models

5.6 Test case: small fleet races

In order to demonstrate the potential of Robo-Race, three test cases are illustrated in this section. In all cases three yachts were involved, whose underlying physical model is that of the IACC 'M566'. The boats, identified with a letter and a colour, were Team A (Blue), Team B (Green) and Team C (Red). Team A was controlled by a user, while Teams B and C were driven by the Robo-Yacht engine. Scope of the simulations is to cross a finishing line upwind of a 400m wide starting line. The two lines are 3.2 Nautical Miles (Nm) apart for Test Cases #1 and #2, and 2.1 Nm apart for Test Case #3. Both lines are perpendicular to the wind direction at time $t_0 = 0$. The x-axis of the earthbound frame is coincident with the starting line, while its y-axis lies on the sea surface and is oriented South to North.

In order to focus on the crew performance only, the yacht physics was kept constant while the crew settings were varied as in Tables 5-2 and 5-3 below. In all cases, a user was given the control of Team A by means of the three axis C-E joystick described in Section 5.3.1 and a pointing device. The user could control the following:

- current awa_{ref}: variations of ± 1° at a time were enabled by clicking two joystick buttons.
- tacking: a tack could be triggered by clicking a joystick button .
- zooming on the race area: by moving the joystick cloche backwards (for zooming out) and forwards (for zooming in) in the longitudinal plane of the cloche.
- camera selection: a camera could be selected at any time on a drop-down list in the simulation main window. Nine cameras are made available.

A rythmically oscillating wind pattern was chosen, with *tws* oscillations in phase with those of *twa*. The conditions were *tws* = (5 ± 0.5) m/s and *twa* ±15°, with the same period of 320s.

5.6.1 Test Case no. 1

Test Case #1	*fleet race, upwind course, two marks 3.2Nm apart, axis North-South*		
Team	*A, Blue*	*B,Green (RY)*	*C,Red (RY)*
Helmsman awa_{ref}	user defined	25°	22°
Main Tailer $[r,f,t]_{main}$	[1.0 1.0 1.0]	[0.9 0.9 0.9]	[1.0 1.0 1.0]
Navigator *tacks on headers*	user defined	≥ 10°	≥ 5°

Table 5-2: Summary for Test Case no.1

In the present test case the user is fully briefed prior to starting about the other Teams and the automatic crew skills. Team B will be sailing with sub-optimal crew settings (as detailed in Table 5-2), while Teams A and C will be sailing with the same sail settings. The user is also informed of the positioning of the fleet at the start. In particular, Team B starts 200m to leeward of A, while Team C starts 200m

to windward of A. Team A starts from the origin of the earth reference frame. The whole fleet starts on starboard.

Tracks from a typical race are shown in Figure 5-11, while the time history of $Lead_{AB}(t)$ is that of Figure 5-12. As shown by the tracks, the race can be divided in two parts: in the first one (t = 0 to 500s circa) the tacks of A and B are in phase, since the only way for A to build up $Lead_{AB}$ is to take advantage of windshifts, while B is losing ground due to the poor crew settings. In the second part of the race, where values of $Lead_{AB}$ in excess of 100m can be observed, A only keeps a loose cover on B (by sailing almost parallel and to windward of B that is, in between the opponent and the finishing line).

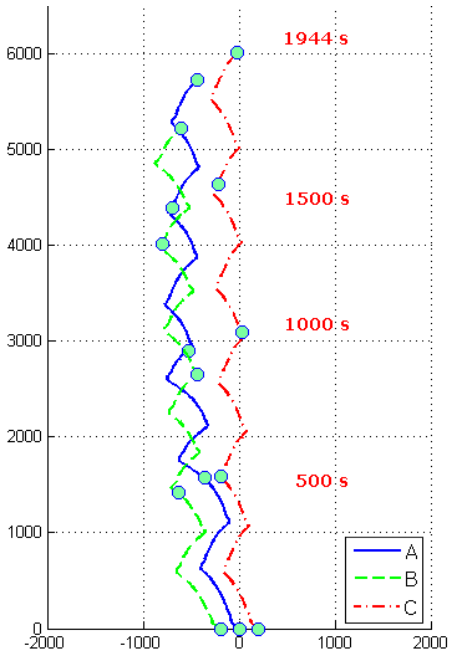

Figure 5-11: Tracks for Test Case no.1

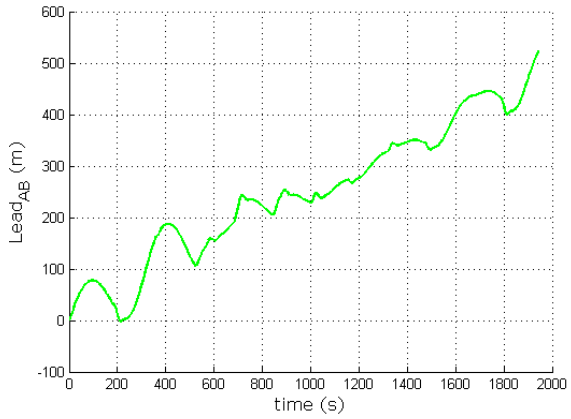

Figure 5-12: $Lead_{AB}(t)$ for Test Case no.1

5.6.2 Test Case no. 2

The settings of Table 5-2 and the oscillating wind profile defined in Section 5.7.1 are used in this test case as well. However, although informed of the positioning of the fleet at the start, the user is unaware of the skills of other Teams. This test case was set up to evaluate the behaviour of users provided with partial information only.

Tracks from a typical race are shown in Figure 5-13, while the time history of $Lead_{AB}(t)$ is shown in Figure 5-14. Just as in the previous case, the race shows a change of the user's behaviour. At the beginning of the race, the decision to get to windward of the fleet is made. However, the two consecutive tacks of Team A yield a substantial loss of ground and the decision to follow the nearest opponent is made (t = 0 to 1000s circa). The user realized that the wind exhibited a rhythmic pattern and caught up on the fleet by taking advantage of the windshifts, placing tacks at every 3° headers circa. Once confident about the strategy, the user aimed at reducing the lateral separation from Team B, skipping one windshift and sailing to the left of the race area. Then, Team A tacked twice (1200s and 1500s) almost in front of Team B, so as to zero the leverage and consolidate the lead. Finally, a conservative, loose cover on B (similarily to Test Case no.1) was chosen, that yielded a slow but steady increase of $Lead_{AB}$ up to 400m, while keeping Lev_{BA} below a 200 m threshold .

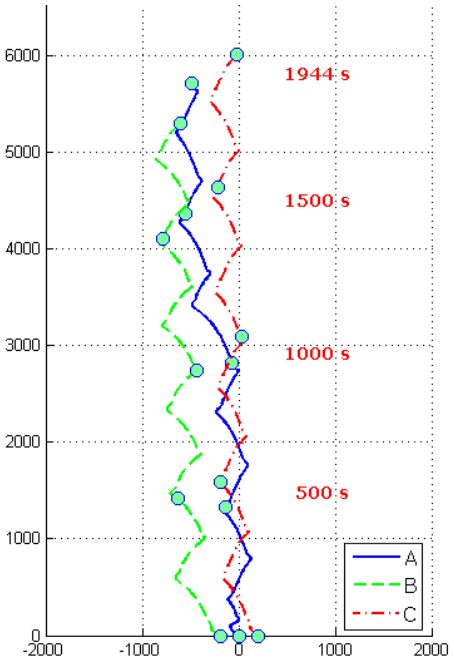

Figure 5-13: Tracks for Test Case no.2

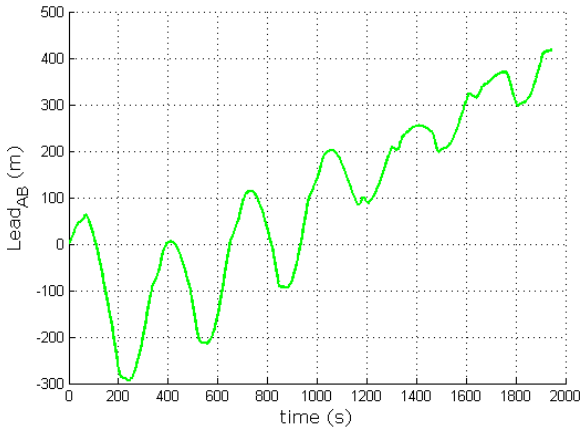

Figure 5-14: Lead$_{AB}$(t) for Test Case no.2

5.6.3 Test Case no. 3

Test Case #3	*fleet race, upwind course, two marks 2.1Nm apart, axis North-South*		
Team	*A, Blue*	*B,Green (RY)*	*C,Red (RY)*
Helmsman awa_{ref}	user defined	22°	22°
Main Tailer $[r,f,t]_{main}$	[1.0 1.0 1.0]	[1.0 1.0 1.0]	[1.0 1.0 1.0]
Jib Tailer $[r,f,t]_{jib}$	[1.0 1.0 1.0]	[1.0 1.0 1.0]	[1.0 1.0 1.0]
Navigator *tacks on headers*	user defined	≥ 5°	≥ 5°

Table 5-3: Summary for Test Case no.3

The settings of Table 5-3 and the oscillating wind profile defined in Section 5.7.1 are used for this Test Case. The length of the upwind leg is 2/3 shorter than in the previous test cases. Team B starts 200m to leeward of C, while Team A starts 200m to windward of A. Team C starts from the origin of the earth reference frame. Both Team B and C are starting on starboard, while Team A starts on port and to windward of the other boats. As opposed to Test Cases #1 and #2, the user was neither informed of the positioning of the fleet on the starting line, nor of the tack the three boats were initially sailing on. This test case was actually centred on the ability of a user to deal with two opponents at a time, both of them with optimal crew settings.

Tracks from a typical race are shown in Figure 5-15. As the wind firstly shifts to the left, Teams B and C automatically react by tacking onto starboard and Team A is therefore given a strategical and tactical advantage. However such an advantage could be used in several ways, for example by tacking immediately and, based on the right of way rules, forcing the opponents to tack or duck. Figure 5-15 shows another option: delaying the tack until the next header. As a consequence, the lead gained by Team A at the start is used between t_1=200s and t_2=450s, when the beat on

starboard is extended and a crossing ahead of Team C can be seen. Then, a tight cover on the latter was used (at t =500s) to increase the lead. Further on in the race, the same pattern was followed in order to cross ahead of Team B: the beat on starboard is extended, then a tight cover on B is used (t_3 = 700s) in order to blanket B and then slow it down. It can be seen (for example at t_4 = 1000) that the chosen technique of covering consisted in tacking ahead of one yacht, while keeping parallel and to windward of the other one. From t_4 on, the race is based on taking advantage of the shifts while keeping in control of the other yachts.

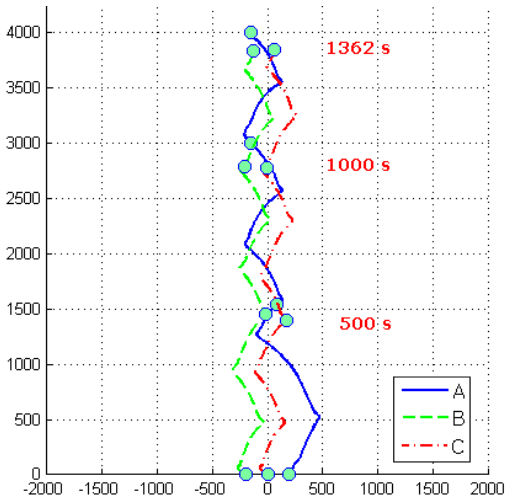

Figure 5-15: Tracks for Test Case no.3

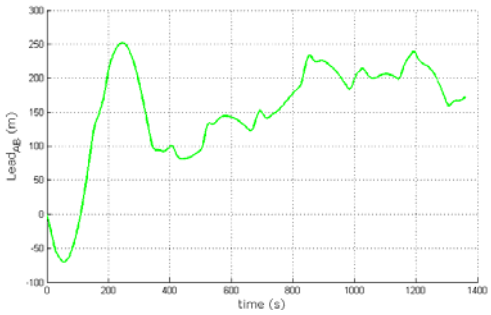

Figure 5-16: $Lead_{AB}(t)$ for Test Case no.3

5.7 Discussion and conclusions

The design and development of 'Robo-Race', a real time sailing simulator based on MATLAB-Simulink® has been described in this Chapter. The simulator can advantageously be used to model small fleet races and has been designed as an interactive tool, where one yacht can be controlled by a real sailor. The user is provided with a visual feedback on the race, showing the position of the fleet within a virtual reality scenario. Mockup 'onboard instruments' are also available to the sailor, for monitoring the performance of the controlled boat as the simulation proceeds on. The 'physics engine' of the simulator is the dynamic model already described in Chapter 2, while the opponents (or 'Robo-Yachts') are based on models for automatic yacht-crew systems addressed in Chapter 3. The skill set of the automatic crew members can be fine-tuned, as well as the decision-making trees upon which the 'navigation engine' is based. These features allowed to model different levels of expertise and to systematically include the effects of tactical decisions made by the crew. This simulation is demonstrated to be capable of capturing such effects through a series of three case studies that race a fleet of three one-design IACC yachts with one yacht controlled by a real sailor. In agreement with published findings presented in Chapter 4, the above case studies show that many 'trademarks of expertise' can be highlighted and, to some extent, measured by using computer simulations. In particular, the use of 'Robo-Race' has shown the ability of expert sailors to trade off risk and benefit, to behave adaptively and to possess a repertoire of decision-making strategies from which the most appropriate ones are consistently selected. For the above reasons, the use of 'Robo-Race' as a coaching aid and a decision-making simulator can be envisaged.

5.8 References

Araùjo, D., Davids, K., and Serpa, S., 'An ecological approach to expertise effects in decision-making in a simulated regatta', Psychology of Sport and Exercise, 6, pp.671-692, 2005.

Perry, D., 'Winning in One-Designs', 3rd ed., US Sailing, ISBN 1-882502-78-7, 2000.

Philpott, A., Henderson S.G., Teirney, D.P., 'A simulation model for predicting yacht match-race outcomes', Operations Research, 52(1), pp. 1-16, 2004.

Scarponi, M., Shenoi, R.A., Turnock, S.R., Conti, P., 'Interactions between yacht-crew systems and racing scenarios combining behavioural models with VPPs', Proc. of The 19th HISWA Symposium on Yacht Design and Yacht Construction, pp.83-97, 2006.

Scarponi, M., Shenoi, R.A., Turnock, S.R., Conti, P., 'A combined ship science-behavioural science approach to create a winning yacht-sailor combination', SNAME, Proc. of The 18th CSYS, pp. 1-10, 2007.

CHAPTER 6

CONCLUSIONS AND FURTHER DEVELOPMENTS

6.1 Summary

The design, development and implementation of a methodology systematically to investigate the behaviour of yacht-crew systems have been described in this Thesis. Firstly, a four DoF dynamic Velocity Prediction Program (VPP) has been developed in order to simulate a yacht racing solo or engaged in 'drag races', where no interactions between yachts are accounted for. The reference yacht for the studies reported in this Thesis is a typical International America's Cup design based on Version 4.0 of the America's Cup Rule. The innovative feature of the VPP consists in the inclusion of behavioural models, shaped as an 'automatic crew'. Such a 'crew' is given tasks and objectives, such as steering the yacht, trimming sails and making decisions of a strategic nature. Both the dynamic VPP and the behavioural models mentioned above were implemented in the form of a sailing simulator, 'Robo-Yacht', developed in the MATLAB® programming environment.

A further step was taken to investigate the role played by human expertise, as opposed to the rule-based skill set of the 'automatic crew'. In order to do so, the dedicated fleet race simulator 'Robo-Race' was developed and the interactive simulation of a fleet race was set up, where a user could control a yacht in real time. Based on MATLAB-Simulink®, the software provided both the 'physics engine' for the dynamic simulations and a visual feedback to the user within a Virtual Reality environment. It has been demonstrated that, based on the above approach, real-time fleet races can be carried out on a standard workstation.

6.2 Conclusions

The steady-state predictions of 'Robo-Yacht' have been compared with those of the well-established VPP 'Win-Design', for validation purposes. The

comparison was satisfactory, particularly for points of sail representative of upwind performance. Differences in boat speed of below 1 knot were observed between 'Robo-Yacht' and 'WinDesign' at true wind angles below 40°.

An approach to crew modelling based on Proportional-Integral-Derivative (PID) controllers proved to be effective. Several crew actions could be modelled, such as steering upwind in a stochastic wind pattern or depowering the boat by easing the mainsail. However, attention should be paid when tuning the PID gains, in order to avoid unrealistic results, e.g. not representative of the reaction time of human beings.

An investigation was carried out with 'Robo-Yacht' systematically to evaluate the influence of the rudder angle on the tacking performance. During the simulated trials, a 'PID-assisted' tacking mode was compared with pre-defined time histories for the rudder angle. It was concluded that PID controllers, having the target apparent wind angle as a setpoint, generally yielded the fastest speed recovery.

'Robo-Yacht' has also been used to investigate decision-making under weather uncertainty. Such a problem was modelled as a game of chance having a set of natural environmental conditions as a second player and involving risk. It has been demonstrated that a formulation in terms of payoff matrices can advantageously be used with risk functions, in order to address matters of a strategical nature.

Building on the above results, further investigations were carried out in opportunity-cost time pressure environments where, as in yacht racing, delaying a decision may yield a reduction in the expected reward. In agreement with decision-making literature, it is shown that behaving adaptively (i.e. maximizing accuracy while dealing with conditions of time-stress) leads to the use of more efficient, 'depth-first' strategies for rapidly screening the available alternatives and selecting the most promising one.

As opposed to the few existing dynamic VPPs, where the role played by the crew has been neglected, 'Robo-Race' has been designed as a detailed yacht race simulator that can systematically include the effects of actions and decisions made

by the crew. Typical simulation results have been illustrated by a series of three case studies that race a fleet of three one-design IACC yachts with one yacht controlled by a real sailor. The test cases demonstrate that, in agreement with recent findings in the Sport Psychology domain, many 'trademarks of expertise' can be highlighted and, to some extent, measured by using computer simulations. In particular, the use of 'Robo-Race' has shown the ability of expert sailors to trade off risk and benefit, to behave adaptively and to possess a repertoire of decision-making strategies from which the most appropriate ones are consistently selected.

6.3 Further Developments

As shown in the Thesis, valuable information on the human factor have been obtained when sailors were given the opportunity of interacting with the simulator. Such feedback has been used both to refine the automatic crew models and to set up meaningful test cases for interactive simulations. However, it should be borne in mind that further efforts are needed to increase the 'ecological validity' of the simulations and minimize the risk of biased results. The use of methodologies developed for flight simulators is recommended, in conjunction with the use of actual sailing equipment (e.g. winches, onboard instruments and a wheel).

As far as the yacht physics is concerned, one possible way forward could be the inclusion of the additional degrees of freedom, i.e. surge and pitch, in the dynamic VPP. However, a careful modeling of tacks and gybes taking into account the skills of the crew (e.g. sail handling, rudder and trim tab time histories) would be equally important to improve the validity of the simulations. In order to do so, the use of data acquired at full scale for both the crew actions and the boat response would be highly beneficial.

The software developed for this Thesis was designed and implemented in order to be strongly cohesive and loosely coupled, so as to maximize its maintainability. As a consequence, the various modules (e.g. blanketing, navigation, decision-making engine) can be improved separately without making the code unstable. If major upgrades were required, for example if the physics engine had to

be extended to six DoF, it is believed that the visual programming environment offered by Simulink would be of help to reduce the time and the effort of coding.

As pointed out throughout the Thesis, the development of the various models was carried out consistently in order to avoid scenarios such as a highly refined model for the yacht physics being coupled with a coarse model for the automatic crew. It is believed that an equally consistent approach should be carried out for the future development of the sailing simulator.

APPENDICES

APPENDIX 1

EVALUATION OF ADDED MASSES AND ADDED MOMENTS OF INERTIA FOR THE IACC YACHT 'M566'

Nomenclature

[Symbol]	[Definition]
Tc	draught of canoe body
$m_{yy,cb}$	added mass in sway, canoe body
$m_{yy,k}$	added mass in sway, keel
$m_{yy,r}$	added mass in sway, rudder
$J_{zz,cb}$	added mass moment of inertia in yaw, canoe body
$J_{zz,k}$	added mass moment of inertia in yaw, keel
$J_{zz,r}$	added mass moment of inertia in yaw, rudder
$c_{yz}(x)$	sectional area coefficient
$h_{\varphi}(x)$	draught of section x at heel angle φ
ρ_w	density of water
b_k [b_r]	wetted area of keel [rudder]
s_k [s_r]	effective span of keel [rudder]
ae_k [ae_r]	effective aspect ratio of keel [rudder]
$cr_{k,e}$ [$cr_{r,e}$]	root chord of extended keel [rudder]
ct_k [ct_r]	tip chord of keel [rudder]
l_k [l_r]	distance between CoG of yacht and CoG of fin [rudder].

A1.1 Overview

Within the framework of a manoeuvering model for sailing yachts, an accurate calculation of added masses and of added moments of inertia should be carried out in order to achieve trustworthy predictions. A general approach to the evaluation of added masses and added moments of inertia for sailing yachts is proposed in (Nomoto and Tatano, 1975), where the sway force and yaw moments are estimated based on strip theory principles. Strip theory methods are fairly accurate, but require a detailed model of the hull in order to integrate the contribution of each cross-sectional strip over the waterline length. When strip theory programmes are not available, empirical formulae often developed for commercial ships can be used. Nomoto's approach is extended by (Keuning and

Vermeulen, 2002) and (Keuning, 2005) based on a large experimental database, the Delft Systematic Yacht Hull Series (DSYHS), spanning over 30 years of expertise in tank testing. In order to trade off accuracy and computational effort, Keuning and co-authors developed a method based on design parameters only, such as sectional areas and breadths at waterline, which are readily available to the yacht designer. Keuning's method and its application to a typical IACC hullform will be considered in the following Sections.

A1.2 Added masses and moments of inertia.

A formula due to Jacobs (A1.1) is of common use for the added mass in surge. Although developed for commercial ship, Jacobs' formula is known to provide a good estimate for m_x and has therefore been adopted for several yacht manoeuvering models, including those devised by Masuyama and by Keuning.

$$m_x = \frac{2 * m * Tc}{LOA} \tag{A1.1}$$

A formulation for the added mass in sway and added mass moment of inertia in yaw for the appended hull can be found in (Keuning and Vermeulen, 2002), based on regression formulae derived from the DSYHS. The integrand in formula (A1.2) is strongly dependent on the sectional area coefficient of the generic section of the underwater hull. Furthermore, a correction coefficient (the 'canoe body draught squared') allows an extension of the formula to the heeled condition. Formulae (A1.2) and (A1.3) have been validated by means of 6 DoF forced oscillation tests carried out through the 'Hexamove' rig at Delft University (Keuning *et al.*, 2005).

$$m_{yy,cb} = \frac{\pi}{2}\rho_w \int_{LWL} h_\varphi(x)^2 \left(3.33 c_{yz}(x)^2 - 3.05 c_{yz}(x) + 1.39\right) dx \tag{A1.2}$$

$$J_{zz,cb} = \frac{\pi}{2}\rho_w \int_{LWL} x^2 h_\varphi(x)^2 \left(3.33 c_{yz}(x)^2 - 3.05 c_{yz}(x) + 1.39\right) dx \tag{A1.3}$$

where the integration variable x is the distance between the canoe body's CoG and the strip of width dx.

Empirical formulae for oscillating flat plates can be used for the appendages (fin keel and rudder) as recommended by Keuning. For example, formulae (A1.3) and (A1.4) refer to the fin keel's contribution to the yacht's added mass in sway and added moment of inertia in yaw respectively.

$$m_{yy,k} = \frac{2\rho_w \pi b_k s_k}{\sqrt{ae_k{}^2 + 1}} \tag{A1.3}$$

$$J_{zz,k} = m_{yy,k} l_k{}^2 \tag{A1.4}$$

where the effective aspect ratio of the fin ae_k is:

$$ae_k = \frac{2(b_k + Tc)}{cr_{k,e} + ct_k} \tag{A1.5}$$

Following Keuning's advice, the distance l_k is measured between the yacht's CoG and a point positioned at 43% of the span of the fin and 0.25 chordlengths from the leading edge. Analogous formulae can be used for the rudder and have therefore been omitted. The added mass in sway for the bulb can be approximated by that of a fully submerged ellipsoid or, even more precisely, by using a strip theory method whose application follows the procedure described above.

The added mass in heave m_z and added moment of inertia in pitch J_{yy} can be calculated based on assumptions by (Masuyama *et al.*, 1995), where a measured pitch-heave natural frequency of 0.53Hz legitimated the assumption of infinite fluid. This, in turn, made it possible to estimate m_z and J_{yy} by means of formulae (A1.6) and (A1.7) respectively.

$$m_z = \frac{\pi}{8}\rho_w \int_{LWL} B^2 C_z(x) dx \tag{A1.6}$$

$$J_{yy} = \frac{\pi}{8}\rho_w \int_{LWL} x^2 B^2 C_z(x) dx \tag{A1.7}$$

where $C_z(x)$ is a function based on the classical Lewis three-parameter conformal mapping (Bishop *et al.*, 1978). In particular, Lewis form coefficients C_1 and C_3 are combined as follows:

$$C_z(x) = \frac{(1 + C_1)^2 + 3{C_3}^2}{(1 + C_1 + C_3)^2} \tag{A1.8}$$

A1.3 Typical results for IACC yachts

Throughout the simulations presented in this Thesis, a reference condition for the M566 is used which is representative of actual sailing conditions with crew and gear onboard. This condition will be referred to as 'loaded trim', the main design parameters for the full scale yacht being summarized in Table A1-1. These are representative of the IACC design trends for the year 2000. For consistency, the 'loaded trim' will be used to derive added masses and moments of inertia.

Dsplt. [Kg]	26448	*LOA [m]*	23.880	b_k *[m]*	2.264
Crew [Kg]	1546	*LWL [m]*	18.894	s_k *[m^2]*	4.429
Gear[Kg]	450	*Tc [m]*	1.046	$cr_{k,e}$ *[m]*	1.378
Volume Dsplt. [m^3]	25.809	*Freeboard[m]*	1.362	ct_k *[m]*	0.771
		BWL [m]	3.324	b_r *[m]*	2.959
		WPA [m^2]	45.223	s_r *[m^2]*	3.400
				$cr_{r,e}$ *[m]*	0.777
				ct_r *[m]*	0.388

Table A1-1: The IACC 'M566' design

The calculations required the use of *Rhinoceros*, a widely used software for Computer Aided Design, and *ShipShape* tool by the Wolfson Unit M.T.I.A.
Firstly, the design draught had to be corrected in order to achieve the 'loaded' draught (i.e. with crew and gear onboard): this process aimed at matching the appropriate Volume Displacement of the 'loaded trim'. Secondly, thirty stations plus bow and transom were exported in the form of point clouds, for further analysis in

ShipShape, such as the calculation of sectional area coefficients (Figure A1-1) or canoe body draught (Figure A1-2). With respect to the latter plot, a gain in waterline length in excess of 1.1% can be observed for the 30° heel case with respect to the upright condition. This is taken into account when evaluating both the added mass in sway (A1-2) and the added moment of inertia in yaw (A1-3), by updating the integration limits. Rhinoceros was used to derive the geometry of the extended fin keel and rudder, so as to calculate the corresponding root chords.

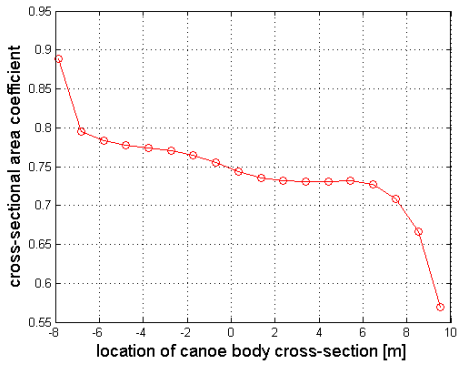

Figure A1-1: Sectional area coefficient $c_{yz}(x)$ over waterline length

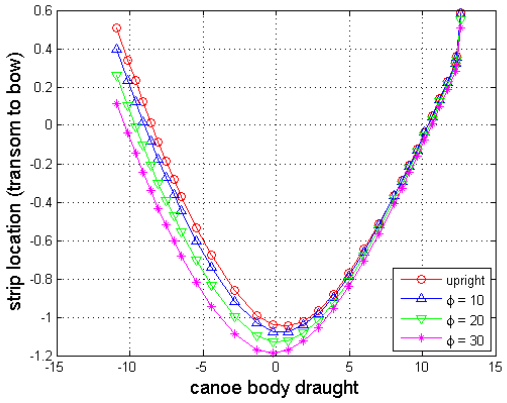

Figure A1-2: Trends of canoe body draught at different heel angles

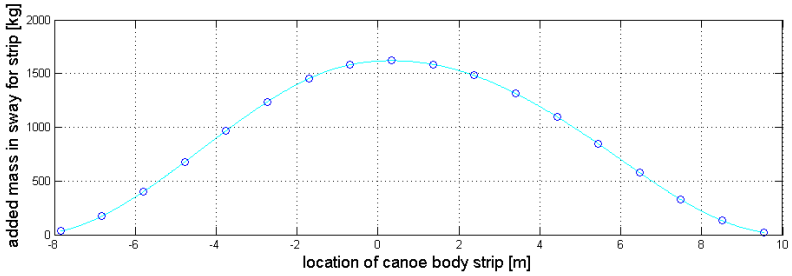

Figure A1-3: Trend of added mass in sway for canoe body strips over WL, upright

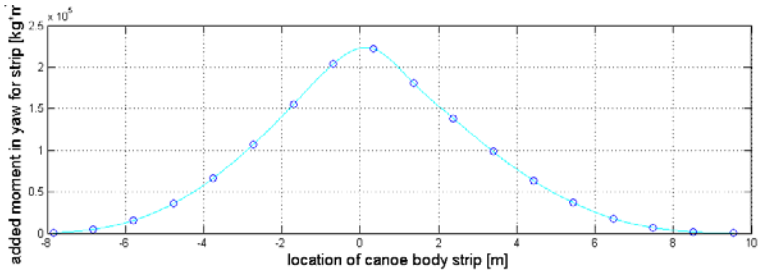

Figure A1-4: Trends of added mass moment of inertia in yaw for canoe body strips over WL, upright

Based on the above calculations, the values of Table A1-2 were derived for use in the simulator. It is worth noting that limited data are available for comparison, those published by Masuyama for a reference 34' cruiser being one example. In the latter case a comparison with the IACC has little meaning, due to the sensible differences between the yachts being investigated. For example, an overestimate can be observed for the m_x/m ratio, equal to 8.7% for the present case as opposed to 3.7% for Masuyama. This may be due to the fact that (A1-1) takes into account the overall length LOA and therefore higher added masses in surge are predicted for yachts with pronounced overhangs such as the IACC M566.

m_m	7.6512E-3	I_{xx}	4.7935E-4	J_{xx}	3.1688E-4
m_x	0.6728E-3	I_{yy}	8.6667E-4	J_{yy}	13.9393E-4
m_y	8.9359E-3	I_{zz}	4.7935E-4	J_{zz}	3.2940E-4
m_z	33.8198E-3				

Table A1-2: Data used for the simulator, non-dimensional form, upright condition

A1.4 References

Bishop, R. E. D., Price, W. G., Tam, P. K. Y., 'Hydrodynamic coefficients of some heaving cylinders of arbitrary shape', International Journal for Numerical Methods in Engineering, Vol.3(1), pp. 17-33, 1978.

Keuning, J.A. and Vermeulen, K.J., 'On the balance of large sailing yachts', 17th HISWA Symposium on Yacht Design and Yacht Construction, Amsterdam, 2005.

Keuning, J.A., Vermeulen, K.J., de Ridder, E.J., 'A generic mathematical model for the manoeuvering and tacking of a sailing yacht', Proc. of The 17th CSYS, pp. 143-163, 2005.

Masuyama, Y., Fukasawa, T., Sasagawa, H., 'Tacking simulations of sailing yachts - numerical integration of equations of motions and application of neural network technique', Proc. of The 12th CSYS, pp. 117-131, 1995.

Nomoto, K., and Tatano, H., 'Balance of helm of sailing yachts', 4th HISWA Symposium on Yacht Design and Yacht Construction, Amsterdam, 1975.

APPENDIX 2

3D MODELLING TECHNIQUES FOR VIRTUAL REALITY ANIMATIONS BASED ON VRML

A2.1 Overview.

As highlighted in Chapters 3 and 5, both Robo-Yacht and Robo-Race provide race animations based on Virtual Reality (VR) environments. These features have been designed in the Virtual Reality Modelling Language (VRML) version 2.0, as implemented in the software V-Realm Builder embedded in MATLAB. The Virtual Reality toolbox was used as an interface between the Simulink model and the VRML world. In the case of Robo-Yacht, an offline, visual postprocessing of the simulation is available: this stage proved to be useful to display drag races i.e. superimpositions of an arbitrary number of Robo-Yacht sessions. Real time animations are available for Robo-Race, to provide users an 'ecological' interaction with the own boat, the rest of the fleet and the race scenario. The offline animations were particularly useful to explore the use of VRML-based 3d worlds in conjunction with MATLAB. In particular, a number of sensitivity studies were carried out for the present Thesis, in order to trade-off computational resources and level of detail (i.e. for the hull model, the race scenario and the landscape) so that 'cost-effective' animations could be delivered. Although the above studies are not reported in this Thesis, details of the final result can be found in this Appendix.

A2.2 The modelling and animation 'toolbox'.

The modeling and the animation of the 3d world required several tools, most of which were used to interpolate the canoe body off existing sections, available in the form of a point cloud. Details on the modeling process are provided in Section A2.3 below.

Once the yacht model was ready, a choice had to be made in terms of animation environment. Many commercial regatta simulators are available that show

outstanding graphics and realism: examples are Virtual Skipper 5® by Nadeo and the web-based AmericasCupAnywhere by Alcatel-Lucent. The former package is a well-known computer game, while the latter provides a virtual environment to follow IACC races in real time. The animations are driven by yachts transmitting data on their position, wind conditions encountered and performance while racing.

Past research at the University of Southampton (Leszczynski *et al.*, 2005) have shown that good results in terms of graphics and level of detail can be achieved through object-oriented software and with the aid of a dedicated workstation. MATLAB can effectively include externally developed code (C++, Java, Fortran), much more suitable for the implementation of high quality graphics. However, it is the Author's opinion that such an emphasis on the animation quality is not necessary for the purpose of this Thesis. In fact, publish evidence exists (Araùjo *et al.*, 2005) that sport simulations should comply with the principle of 'functional fidelity' rather than replicate the context of the task. Therefore, the use of less demanding simulation environments was considered and, among those, VRML was deemed the most appropriate.

VRML was designed as a programming language to model and to animate objects within virtual 3d domains (usually referred to as 'worlds'). VRML specifications were initially designed for web applications: VRML models can therefore be easily transported on the internet and viewed by VRML compatible browsers. Although these features have no direct implications for the present Thesis, it was believed that a 'lightweight', VRML-based approach could be a satisfactory trade-off between simulation speed and visual fidelity. The results were indeed satisfactory, having obtained real-time animations running twice as fast as real-time while being displayed on a 1280x800 pixels screen on commercial dual-core laptops.

A2.3 Relevant VRML nodes.

V-Realm Builder is a VRML authoring tool by Integrated Data Systems Inc. that allows an interactive approach to VRML modelling, as opposed to hand-coding. As far as the present Thesis is concerned, V-Realm Builder was chosen

because it provides an instant visual feedback on the modeling. This was particularly useful when:

- assembling the VRML components (e.g. hull, spars, sails, wheel, rudder blade) within a single 'Yacht' node;
- positioning yacht nodes within the race scenario.

V-Realm Builder features a library of VRML nodes that can be added to the 3d world tree by drag-and-drop. The nodes relevant to the 3d world developed for this Thesis are listed below:

- ***Group:*** can be considered as a folder of nodes. The Group members must be added as children. The Fleet has been implemented as a Group whose children are the Transform nodes Yacht_1, Yacht_2,…, Yacht_N. It should be borne in mind that methods such as 'scale', 'rotation', 'translation' cannot be set globally at Group level, since no such properties exist for a Group node. However, a Group can be included in the VRML tree as a child of a Transform node in order to do so.
- ***Transform:*** is used to set a local reference frame. The methods available include 'scale' (to scale all children nodes in one go), 'rotation' (to rotate all children at once with respect to the global frame) and 'translation' (to translate children nodes). Moreover, the methods of Transform nodes can be set externally, for example with the use of Simulink VR Toolbox. In the virtual simulator, each yacht was modelled as a Transform node, whose 'rotation' and 'translation' methods were accessed by Simulink at each time step and updated according to the yacht state.
- ***Use:*** allows to duplicate existing nodes, therefore avoiding redundancy. For example, the race buoys Mark2 and Mark3 were defined by using Mark1 as a reference. Any changes to methods such as 'scale', 'shape' and 'material' for Mark1 are automatically extended to the other marks.
- ***Viewpoint:*** its methods include 'fieldOfView', 'orientation' and 'position'. It was chosen to keep Viewpoints fixed in the yacht's reference frame. This was achieved by setting up one Transform node (a 'Camera') in the scene, having a

Viewpoint node as child. While the Viewpoint methods were kept constant, the position and orientation of the parent 'Camera' were varied according to the yacht's reference frame (through Route nodes, see Chapter 5)

- ***Shape:*** used to include geometric entities, from primitive geometries to complex shapes. Examples of methods for the Shape node are 'appearance' and 'geometry'. The 'appearance' method is used to specify the object's colour, material, lighting and texture. The 'geometry' method is used to define the object's shape; for this purpose, a library of primitive geometries (box, cone, cylinder, sphere, extrusion) is available. However, VRML objects modelled outside V-Realm Builder can be imported and used as well. In the latter case, the imported geometry is made available as an 'Indexed Face Set' node. When using an external modeller, attention must be paid to a correct definition of the polygon normals, in order to avoid rendering problems.
- ***ElevationGrid:*** used to define a landscape (sea and land) within the 3d world. It was observed by users that adding a textured landscape and a grid on the sea surface, improved the visual feedback for the race. After the addition of a grid the effects of rudder actions became clearer, as well as the feeling for boats' positions and headings.

A2.4 Yacht modelling process

Although the original drawings of the IACC 'M566' were not available, the hull lines were obtained through reverse engineering techniques, namely by digitizing eleven sections of the model canoe body as well as the bow shape, the rudder blade, the fin keel and the bulb. The reverse engineering results were available as IGES files, namely in the form of a point cloud.

Firstly, the Wolfson Unit software ShipShape was used to reduce the size of the cloud and to interpolate the sections with cubic splines. The lines of the canoe body, as obtained through ShipShape, are shown in Figure A2-1 below. Secondly, the open source modelling software 'Blender 2.45' was used, to obtain the canoe body surface off the sections and to optimize the number of polygons. In the same stage, an educated guess was made for the deck and the cockpit shape, based on pictures of

existing IACC yachts. The use of other tools was considered for the M566 modelling, such as the NURBS modelling software ‘Rhinoceros’. In the latter case, the built-in algorithms for surface generation yielded unsatisfactory results: a very large number of polygons was observed aft of station 9 and manual polygon generation was required.

A consistent definition of the local normals to a surface is required by VRML browsers, for rendering purposes. However, due to further shortcomings of Rhinoceros, a manual definition of the normals to the polygons was occasionally required. Figures A2-2 to A2-7 show the yacht components as modelled and rendered in Blender. In the light of the entirely satisfactory results obtained with Blender, either in terms of modelling, meshing and rendering, Blender was chosen as the external 3d modeler. Each part of the yacht was modelled individually, using local reference frames, while V-Realm was used to assemble the yacht in a CG-centered reference frame.

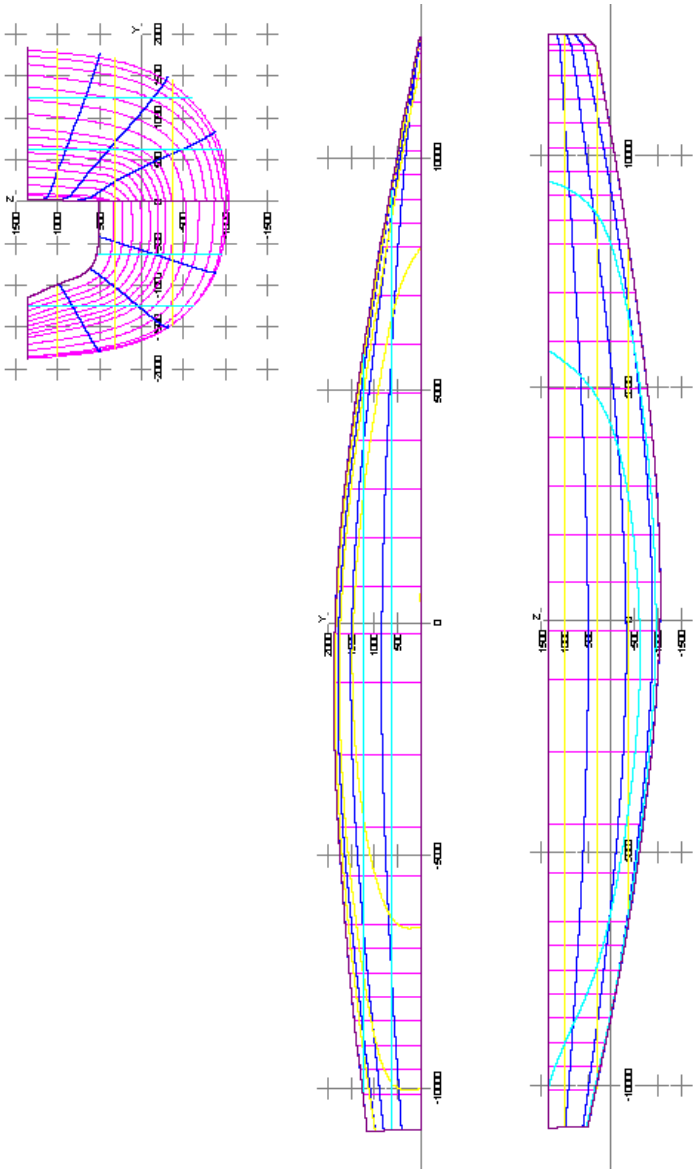

Figure A2-1: Lines for the M566 canoe body, obtained through ShipShape

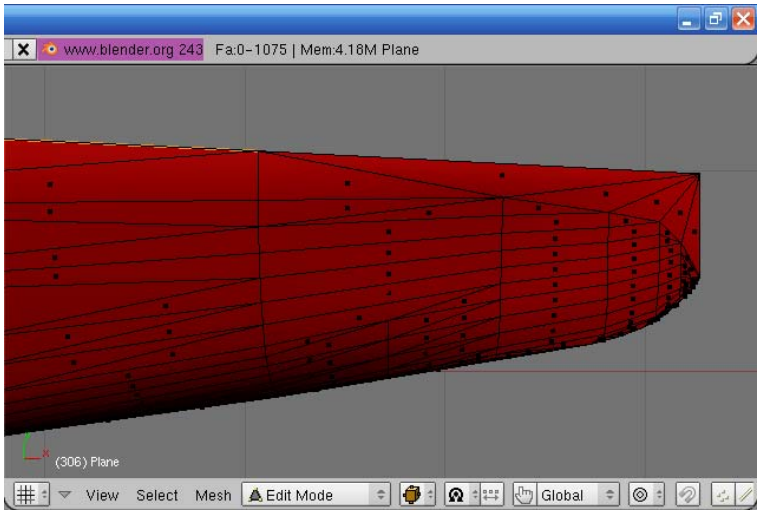

Figure A2-2: Polygons in the bow area (Blender screenshot)

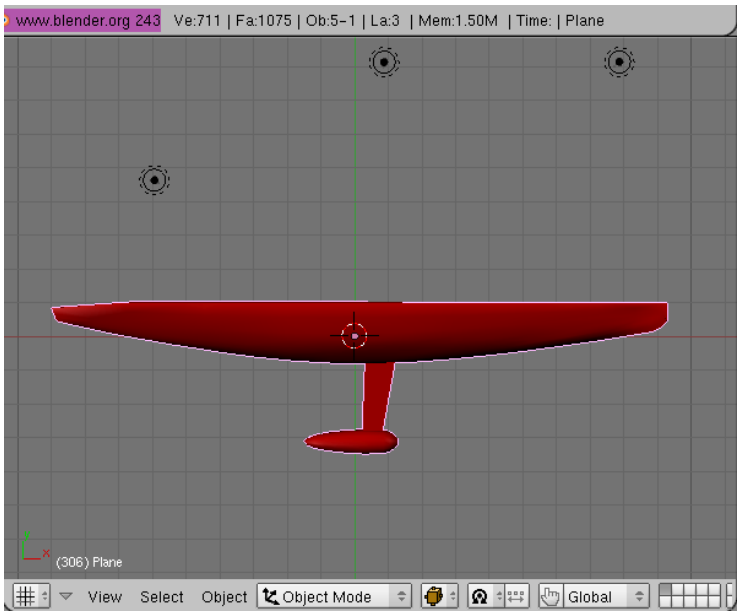

Figure A2-3: 'M566' appended hull (Blender screenshot)

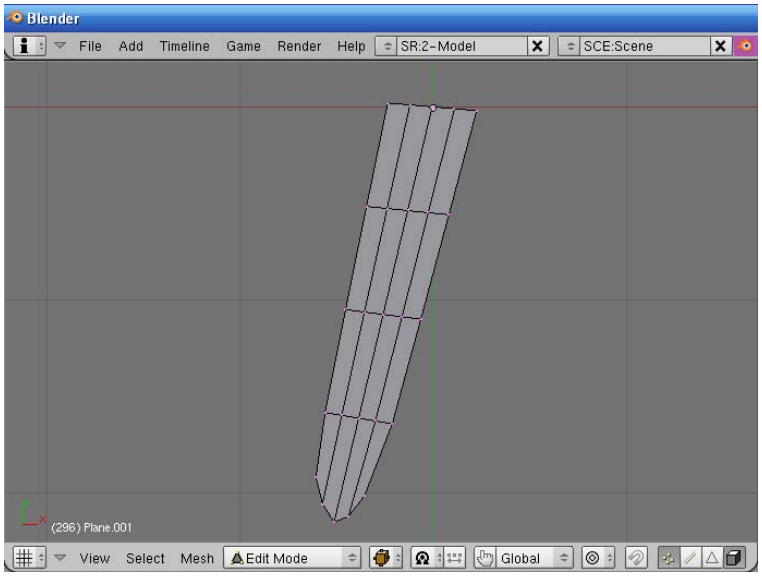

Figure A2-4: Polygon configuration on the rudder blade (Blender screenshot)

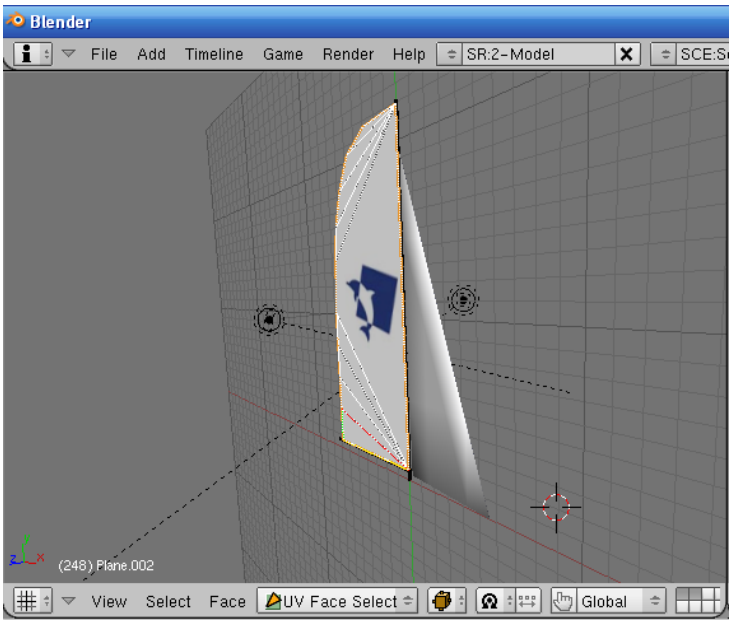

Figure A2-5: Textured sails and position of spotlights (Blender screenshot)

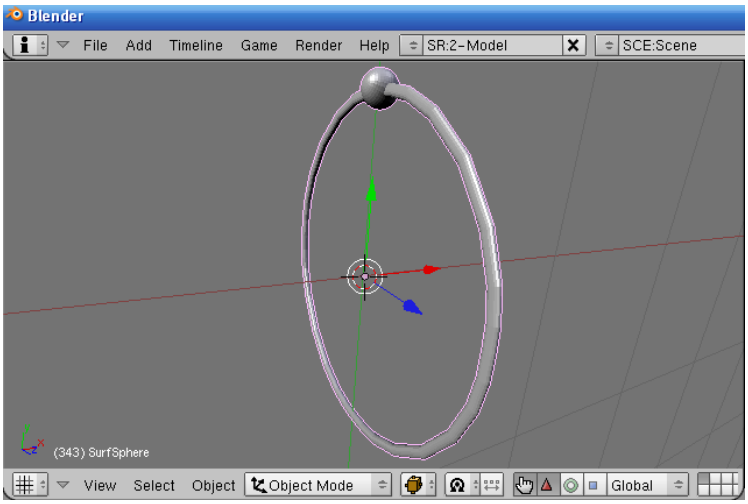

Figure A2-6: Steering wheel (Blender screenshot)

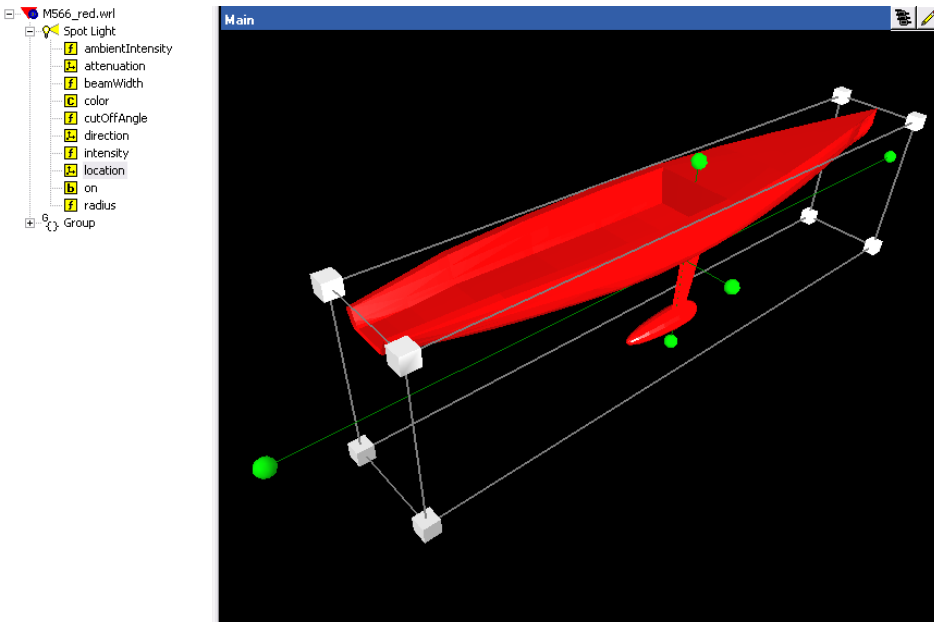

Figure A2-7: Tree-view and render of the 'M566' appended hull (V-Realm screenshot)

A2.5 References

Araùjo, D., Davids, K., and Serpa, S., ‘An ecological approach to expertise effects in decision-making in a simulated regatta’, Psychology of Sport and Exercise, 6, pp.671-692, 2005.

Leszczynski, R., Parker, R., Rock-Evans,M., van Someren, M., Squibb, A., ‘Virtual Trafalgar: Development of a Napoleonic Naval Simulator’, Group Design Project Report, Ship Science, University of Southampton, 2005.

APPENDIX 3

LIST OF PUBLICATIONS

A3.1 Publications

This Appendix summarizes how the present PhD Thesis has contributed towards advancing the state of the art in the modelling and simulation of yacht-crew systems. A list of the most important contributions in journals and conferences is detailed below:

Scarponi, M., Shenoi, R.A., Turnock, S.R., Conti, P., 'Interactions between yacht-crew systems and racing scenarios combining behavioural models with VPPs', Proc. of The 19th HISWA Symposium on Yacht Design and Yacht Construction, pp.83-97, Amsterdam, Holland, 2006.

Shenoi, R.A., Scarponi, M., Turnock, S.R., Conti, P., 'Combining behavioural models with VPPs to derive a winning yacht-sailor combination', Proc. of Small Craft 2006: An International Conference on Small Craft Related Sciences and Engineering, Bodrum, Turkey, 16-18 Nov 2006 (invited paper).

Scarponi, M., Shenoi, R.A., Turnock, S.R., Conti, P., 'A combined ship science-behavioural science approach to create a winning yacht-sailor combination', SNAME, Proc. of The 18th Chesapeake Sailing Yacht Symposium, pp. 1-10, Annapolis (MD), USA, 2007.

Scarponi, M., Shenoi, R.A., Turnock, S.R., Conti, P., 'Interactions between yacht-crew systems and racing scenarios combining behavioural models with VPPs', International Journal of Small Craft Technology – RINA Transactions Part B, 72, Royal Institution of Naval Architects, 2007.

Scarponi, M., Conti, P., Shenoi, R.A., Turnock, S.R., 'Including human performance in the dynamic model of a sailing yacht: a MATLAB-Simulink based tool', Proc. of RINA Conference 'The Modern Yacht', Southampton, UK, 11-12 Oct 2007.

Scarponi, M., McMorris, T., Shenoi, R.A., Turnock, S.R., Conti, P., 'Robo-Yacht: a human behaviour-based tool to predict the performances of yacht-crew systems', Proc. of the 12th European Congress of Sport Psychology, Halkidiki, Greece, 4-9 Sept 2007.

Turnock, S.R., Scarponi, M., Spenkuch, T, Shenoi, R.A., Conti, P., 'Robo-Yacht: a four degree of freedom sailing simulator for assessing crew performance', accepted at: 7th International Conference on the Engineering of Sport, Biarritz, France, 2008.